Ph.D. Dissertation

A study on massive MIMO systems in high mobility environments

고속 이동 환경에서 대규모 다중안테나 시스템에 관한 연구

Hyoung-Keon Kim

August 2020

School of Electrical and Computer Engineering
College of Engineering
Seoul National University

A study on massive MIMO systems in high mobility environments

By

Hyoung-Keon Kim

Submitted to the School of Electrical and Computer Engineering
in partial fulfillment of the requirements for the degree of
Ph.D. in Electrical and Computer Engineering

at

Seoul National University

August 2020

Committee in Charge:

Professor	Saewoong Bahk, Chairman
Professor	Yong-Hwan Lee, Vice-Chairman
Professor	Byonghyo Shim
Professor	Daesik Hong
Professor	Yosan Shin

Abstract

Advanced cellular communication systems may obtain high array gain by employing massive multi-input multi-output (m-MIMO) systems, which may require accurate channel state information (CSI). When users are in high mobility, it may not be easy to get accurate CSI. When we transmit signal to users in high mobility, we may experience serious performance loss due to the inaccuracy of outdated CSI, associated with so-called channel aging effect. This problem may be alleviated by exploiting channel correlation matrix (CCM) in spatial domain. However, it may require an additional process for the estimation of CCM, which may require high signaling overhead in m-MIMO environments. In this dissertation, we consider signal transmission to multiple users in high mobility in m-MIMO environments.

We consider the estimation of CSI with reduced signaling overhead. The signaling overhead for the CSI estimation is a challenging issue in m-MIMO environments. We may reduce the signaling overhead for the CSI estimation by using pilot signal transmitted by means of beamforming with a weight determined by eigenvectors of CCM. To this end, we need to estimate the CCM, which may still require large signaling overhead. We consider the estimation of CCM with antennas in a uniform linear array (ULA). Since pairs of antennas with an equal distance may experience spatial channel correlation similar to each other in ULA antenna environments, we may jointly estimate the spatial channel correlation. We estimate the mean-square error (MSE) of elements of

estimated CCM and then discard the elements whose MSE is higher than a reference value for the improvement of CCM estimation. We may estimate the CSI from the estimated CCM with reduced signaling overhead.

We consider signal transmission robust to the presence of channel aging effect. Users in different mobility may differently experience the channel aging effect. This means that they may differently suffer from transmission performance loss. To alleviate this problem, we transmit signal to maximize the average signal-to-leakage-plus-noise ratio, making it possible to individually handle the channel aging effect. We consider the signal transmission to the eigen-direction of a linear combination of CSI and CCM. Analyzing the transmission performance in terms of signal-to-interference-plus-noise ratio, we control the transmit power by using an iterative water-filling technique.

Finally, we consider the allocation of transmission resource in the presence of channel aging effect. We design a sub-optimal greedy algorithm that allocates the transmission resource to maximize the sum-rate in the presence of channel aging effect. We may estimate the sum-rate from the beam weight and a hypergeometric function (HF) that represents the effect of outdated CSI on the transmission performance. However, it may require very high computational complexity to calculate the beam weight and the HF in m-MIMO environments. To alleviate the complexity problem, we determine the beam weight in dominant eigen-direction of CCM and approximate the HF as a function of temporal channel correlation. Since we may estimate the sum-rate by exploiting spatial and temporal channel correlation, we may need to update the resource allocation only when the change of CCM or temporal channel correlation is large enough to affect the sum-rate. Simulation results show that the proposed scheme provides performance similar

to a greedy algorithm based on accurate sum-rate, while significantly reducing the computational complexity.

Keywords: massive MIMO, mobility, channel aging, outdated CSI, spatial correlation, low complexity.

Student number: 2014-21664

Contents

List of Figures

List of Tables

Chapter 1

Introduction

Demand for mobile data traffic has rapidly been increasing with active deployment of multimedia services [1]. The growth rate of mobile data traffic in high mobility is more than two times that of total mobile data traffic [2]. Advanced wireless communication systems may employ massive multi-input multi-output (m-MIMO) technologies to enhance the transmission capacity and reliability [3-5]. They may achieve m-MIMO capability by employing beamforming and resource allocation techniques with the use of accurate channel state information (CSI) [6, 7].

An m-MIMO system may have difficulty in optimally serving users in high mobility since it may not easily get accurate CSI mainly due to so-called channel aging effect [8-10]. The base station (BS) may significantly suffer from the channel aging effect when it transmits signal by means of spatial multiplexing [4]. Moreover, it needs to consider the effect of CSI inaccuracy to allocate transmission resource to users, which may require very high computational complexity [36]. This problem can somewhat be alleviated by

exploiting channel correlation matrix (CCM)[1] [31-35]. Since the CCM may slowly vary in time [11, 12], the BS may accurately estimate the CCM by using pilot signal. However, it may require high signaling overhead for the transmission of pilot signal [20].

In this dissertation, we consider signal transmission to users in high mobility in m-MIMO environments. We exploit the CSI and the CCM for beamforming and resource allocation. We consider the estimation of CSI and CCM with reduced signaling overhead. We also consider the signal transmission robust to the presence of channel aging effect. Finally, we consider the allocation of transmission resource to users with low computational complexity in the presence of channel aging effect.

It is a challenging issue to estimate the CSI with low signaling overhead in m-MIMO environments, particularly in a frequency-division duplex communication system. A number of previous works considered the estimation of CSI with reduced pilot signaling overhead [14-19]. Most of them exploited the CCM to estimate the CSI, by using pilot signal for the CSI estimation transmitted by means of beamforming with a weight determined by eigenvectors of CCM. A correlated MIMO channel can be represented as a small number of independent channels by means of transforming such as Karhunen-Love transform [15]. Most of previous works assumed that the BS perfectly knows the CCM, since it can estimate the CCM much less frequently than the CSI. However, the CCM estimation may need to transmit orthogonal pilot signals in linear proportion to the number of BS antennas [20, 21]. The estimation of CCM may require signaling overhead much larger than that of CSI in m-MIMO environments.

[1] The CCM may be referred to long-term CSI. In this case, the CSI is referred to short-term CSI. In this dissertation, we refer the former to the CCM, and the latter to the CSI.

Some previous works consider the estimation of covariance matrix of random signal [24-27], which is applicable to the estimation of CCM in m-MIMO environments. We may approximately estimate the CCM by ignoring its elements smaller than a threshold [24], which may be quite valid when the CCM is in a form of a sparse matrix. We can estimate the CCM by means of approximated maximum likelihood estimation in an iterative manner [25]. Some works consider the estimation of CCM of a large size [26, 27], assuming that the number of non-zero eigenvalues of CCM is much less than the number of BS antennas. They minimize a weighted trace norm of CCM that approximately represents the number of non-zero eigenvalues. However, they assume that the pilot signal experiences perfectly independent channel characteristics in time and frequency domain [24-27]. We may need to increase the amount of pilot signal in the presence of channel correlation in practical environments. Moreover, no work has investigated the effect of CCM inaccuracy on the CSI estimation.

In this dissertation, we consider the estimation of CCM with reduced signaling overhead in m-MIMO environments. We may improve the accuracy of CCM estimation by exploiting the antenna array structure. Pairs of antennas in an equal distance may experience spatial channel correlation similar to each other in two-dimensional (2-D) uniform linear array (ULA) environments [23]. This is mainly due to the far-field effect [23]. We assume that pairs of antennas in an equal distance may experience equal spatial channel correlation in an average sense. We may improve the accuracy of CCM estimation by jointly estimating the spatial channel correlation of antenna pairs in an equal distance. We evaluate the estimation accuracy in terms of mean-square error (MSE). For further improvement of estimation accuracy, we neglect spatial channel correlation

terms whose MSE is larger than a reference value. Finally, we estimate the CSI by exploiting the estimated CCM.

When a user is in high mobility, the BS may transmit signal to the user based on outdated CSI, suffering from significant performance loss [10]. It may be desirable to make signal transmission robust to the presence of channel aging effect. We may transmit signal by means of two-stage beamforming, the outer and the inner beamforming [30]. The outer beamforming may suppress the interference among users, while the inner beamforming may maximize the multiplexing gain. The beam weight for the outer beamforming can be determined by a set of eigenvectors of interference channel matrix corresponding to near-zero eigenvalues of interference channel matrix. The beam weight for the inner beamforming can be generated by means of zero-forcing (ZF) or singular value decomposition (SVD) transmission. However, this scheme may not be effective in the presence of channel aging effect since it determines the beam weight based on outdated CSI. We may determine the beam weight by a set of eigenvectors corresponding to dominant eigenvalues of CCM [31, 32]. It may be effective for users in high mobility, but not in low mobility [32]. We may determine the beam weight by using the CCM and the CSI as well, where the outer and the inner beam weight are determined by exploiting the CCM and the CSI, respectively [33-35]. However, it may be less effective than the CSI-based scheme when the CSI is unchanged (*i.e.*, no presence of channel aging effect), and the CCM-based scheme when the CSI is completely outdated (*i.e.*, presence of large channel aging effect) [36].

We may estimate temporal channel variation by using a predictor antenna installed in front of user antennas [37-39]. As a user is moving forward, the location of user antennas

passes through the location of the predictor antenna. This implies that user antennas and the predictor antenna may be correlated with each other [37]. We may predict the CSI of user antennas from that of the predictor antenna [39]. It may be required for all user antennas including the predictor antenna to be installed linearly along with the direction of user mobility [37]. As a consequence, it may not be applicable to practical environments where users may have different mobility. This is mainly because the channel correlation between the predictor and the user antennas may considerably vary according to the user mobility [40].

In this dissertation, we consider the signal transmission robust to the presence of channel aging effect when users are in different mobility. To this end, we determine the beam weight to maximize the average signal-to-leakage-plus-noise ratio (SLNR), enabling to individually take care of user mobility [41]. We determine the beam weight in the eigen-direction of a linear combination of CSI and CCM weighted by temporal channel correlation. With the combined use of CSI and CCM, we may transmit signal in consideration of user mobility. We control the transmit power by means of water-filling so as to provide desired signal-to-interference-plus-noise ratio (SINR) [43].

Previous works for the user scheduling in MIMO environments may be applicable to m-MIMO environments [55]. We may optimally allocate transmission resource to users by means of exhaustive searching, which may require huge computational complexity in m-MIMO environments [55]. We may alleviate the complexity problem by using a sub-optimal greedy algorithm [55-60]. The BS can select users for spatial multiplexing transmission in consideration of achievable sum-rate [58]. However, it may require large computational complexity to estimate the achievable sum-rate of all user sets. The

computational complexity may become even higher in the presence of channel aging effect [36]. We may alleviate the complexity problem by using a metric-based greedy algorithm [61-63]. The BS can select users based on the chordal distance that represents the channel orthogonality [61, 62] or Frobenius norm of channel matrix that represents achievable channel gain [63]. However, we need to estimate the sum-rate at least once for each iteration [61-63]. Moreover, no work considered the channel aging effect.

Some previous works considered the use of a greedy scheduling algorithm with the use of inaccurate CSI [64-68]. The inaccuracy of channel estimation may affect the sum-rate performance as the channel aging effect does [64-66]. However, these works only consider single input single output (SISO) environments, which may not be applicable to m-MIMO environments. Analyzing the block error rate (BLER) analyzed in the presence of CSI inaccuracy, we may perform the user scheduling so that the outage probability of BLER is lower than a threshold [67]. However, it considers a single user for maximum ratio transmission (MRT). We may use a greedy algorithm based on achievable sum-rate for ZF transmission in the presence of channel aging effect [68]. However, it assumes unrealistic operation condition that antennas provide independent channel.

Some other previous works considered the user scheduling in a heuristic manner by exploiting the CCM without consideration of achievable sum-rate [32, 69]. We may allocate a same resource to users having CCM orthogonal to each other [32]. We may determine the orthogonality of CCM by exploiting the maximal eigenvalue of CCM. We may assume that the user channel is orthogonal if the eigenvectors corresponding to the maximal eigenvalue of CCM are orthogonal to each other [32]. We may additionally exploit short-term channel direction to determine the channel orthogonality [69]. These

schemes may considerably reduce the computational complexity since they do not estimate achievable sum-rate for the resource allocation. However, they may provide achievable sum-rate less than the greedy approach since they heuristically determine the channel orthogonality [32, 69].

In this dissertation, we consider the resource allocation in the presence of channel aging effect in m-MIMO environments. We design a greedy algorithm that schedules users to maximize the sum-rate in the presence of channel aging effect. We may estimate the sum-rate by exploiting the beam weight and a hypergeometric function (HF) that represents the effect of outdated CSI. However, it may require very high computational complexity to get the beam weight and the HF. To alleviate the complexity problem, we determine the beam weight in dominant eigen-direction of CCM and approximate the HF as a function of temporal channel correlation. Since we may estimate the sum-rate using spatial and temporal channel correlation, we may need to update the resource allocation only when the change of CCM or temporal channel correlation is large enough to affect the sum-rate. Simulation results show that the proposed scheme provides performance similar to a greedy algorithm based on accurate sum-rate, while significantly reducing the computational complexity.

Following Introduction, Chapter II describes the m-MIMO system in consideration. Chapter III proposes a CCM estimation scheme with reduced signaling overhead in the presence of channel correlation. Chapter IV proposes a mobility-aware signal transmission scheme that exploits the CSI and the CCM, and analyzes the transmission performance of the proposed scheme. Chapter V proposes a mobility-aware resource

allocation scheme with reduced computational complexity. Finally, Chapter VI summarizes conclusions and further research issues.

Notation: Bold upper and lower letters denote matrices and column vectors, respectively. $(\cdot)^T$ and $(\cdot)^H$ denote the transpose and the conjugate transpose (Hermitian), respectively. $E\{\cdot\}$ denotes the expectation operator, $\mathbf{I}_N$ is an $(N \times N)$-dimensional identity matrix, $\mathbf{0}$ is a zero matrix and $\otimes$ denotes the Kronecker product. $[\mathbf{A}]_{i,j}$ denotes the (i,j)-th element of matrix $\mathbf{A}$. $[\mathbf{A}]_{i:j,k:l}$ denotes a submatrix of $\mathbf{A}$ comprising elements from the *i*-th row and the *k*-th column to the *j*-th row and the *l*-th column. $[\mathbf{A}]_{:,i:j}$ denotes a matrix comprising the *i*-th to the *j*-th column vectors of $\mathbf{A}$. $\|\mathbf{A}\|_{p,q}$, $\|\mathbf{A}\|_F$ and $\|\mathbf{A}\|_*$ denote the $L_{p,q}$-norm, the Frobenius norm and the nuclear (trace) norm of $\mathbf{A}$, respectively.

Chapter 2

M-MIMO systems in the presence of channel aging effect

We consider signal transmission by *B* BSs to *K* users, where each BS and user have N_T and N_R antennas, respectively, and $N_T \gg N_R$. We assume that each BS uses antennas of a 2-D ULA structure, where N_{az} and N_{el} antennas are installed in the azimuth and the elevation direction, respectively [22], and $N_T = N_{az}N_{el}$. Let $\mathbf{H}_{b,k} \in \mathbb{C}^{N_R \times N_T}$ be the transmission channel from BS *b* to user *k* and $\mathbf{R}_{b,k,r} \in \mathbb{C}^{N_T \times N_T}$ be the CCM corresponding to the *r*-th antenna of user *k* in spatial domain. We also assume that no correlation exists among the receive antennas (*i.e.*, the CCM is an identity matrix) since users in mobility may experience rich scattering compared to the BS. We also assume that users are located sufficiently far away from the BS, yielding an identical CCM (*i.e.*, $\mathbf{R}_{b,k,r} \approx \mathbf{R}_{b,k}$).

Then, it can be shown that

$$\mathbf{H}_{b,k} = \tilde{\mathbf{H}}_{b,k}\mathbf{R}_{b,k}^{1/2} \tag{2.1}$$

where $\tilde{\mathbf{H}}_{b,k}$ is an uncorrelated channel matrix whose elements are independent and identically distributed (i.i.d.) zero mean complex normal random variables with a unit variance. The spatial channel correlation may slowly change in time [11, 12]. It was reported that the CCM may have a coherence time of a few msec and hundreds of msec in urban environments when users are in a mobility of 60 km/h and 500 km/h [11, 12], respectively. We assume that $\mathbf{R}_{b,k}$ is unchanged during the time interval between the acquisition of CSI and the signal transmission, which is usually less than 10 msec [53].

Let $\hat{\mathbf{H}}_{b,k} \in \mathbb{C}^{N_R \times N_T}$ be the CSI estimated by BS *b*, which has the same statistical characteristics as $\mathbf{H}_{b,k}$. In the presence of channel aging effect, $\mathbf{H}_{b,k}$ can be represented as [13]

$$\mathbf{H}_{b,k} = \rho_k \hat{\mathbf{H}}_{b,k} + \sqrt{1-\rho_k^2}\mathbf{Z}_{b,k} \tag{2.2}$$

where $\mathbf{Z}_{b,k} \in \mathbb{C}^{N_R \times N_T}$ is a temporal channel variation matrix that follows the same distribution as $\hat{\mathbf{H}}_{b,k}$, and ρ_k is the temporal channel correlation between $\hat{\mathbf{H}}_{b,k}$ and $\mathbf{H}_{b,k}$, represented as [13]

$$\rho_k = J_0\left(\frac{2\pi v_k f_c T_k}{c}\right). \tag{2.3}$$

Here, J_0 is the zero-th order Bessel function of the first kind, v_k is the velocity of user *k*, f_c is the carrier frequency, T_k is the time interval between the CSI estimation and the signal transmission to user *k*, and *c* is the light speed. Fig. 2-1 illustrates the channel aging effect.

The received signal of user *k* can be represented as

$$\mathbf{r}_k = \sum_{b \in B_k} \beta_{b,k} \mathbf{H}_{b,k} \mathbf{W}_{T,b,k} \mathbf{s}_k + \sum_c \sum_{l \neq k} \beta_{c,k} \mathbf{H}_{c,k} \mathbf{W}_{T,c,l} \mathbf{s}_l + \mathbf{n}_k \tag{2.4}$$

where B_k is a set of BSs serving user k, $\beta_{b,k}$ is the large-scale fading coefficient, $\mathbf{W}_{T,b,k} \in \mathbb{C}^{N_T \times s_k}$ is the transmit beamforming matrix from BS b to user k, $\mathbf{s}_k \in \mathbb{C}^{s_k \times 1}$ is the data vector, and $\mathbf{n}_k \in \mathbb{C}^{N_R \times 1}$ is the additive noise vector whose elements are i.i.d. zero mean complex normal random variables with variance σ_n^2. Here,

$$\mathbf{W}_{T,b,k} = \mathbf{B}_{b,k} \mathbf{P}_{b,k} \tag{2.5}$$

where $\mathbf{B}_{b,k}$ is the beam weight matrix and $\mathbf{P}_{b,k} \in \mathbb{C}^{s_k \times s_k}$ is the power allocation matrix in a diagonal matrix form.

User k can estimate $\mathbf{H}_{b,k} \mathbf{W}_{T,b,k}$ from a demodulation reference signal (DM-RS) transmitted by BS b and decouple multiple streams of $\mathbf{s}_k$ using a zero-forcing receiver with weight determined by

$$\mathbf{W}_{R,k} = \left(\sum_{b \in B_k} \beta_{b,k} \mathbf{H}_{b,k} \mathbf{W}_{T,b,k} \right)^{\dagger}. \tag{2.6}$$

We may decode the signal by

$$\hat{\mathbf{s}}_k = \mathbf{W}_{R,k} \mathbf{r}_k \,. \tag{2.7}$$

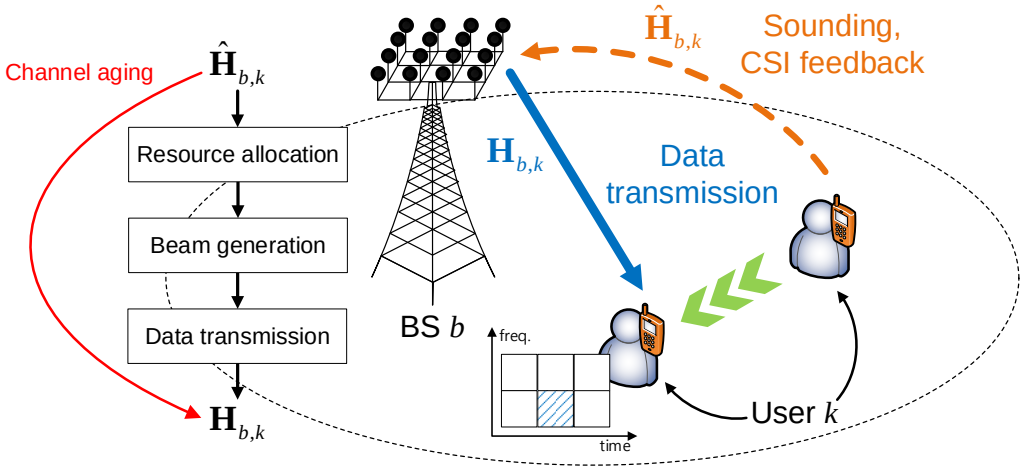

Fig. 2-1. Channel aging effect in signal transmission.

Chapter 3

Estimation of channel correlation matrix

The BS may transmit two types of pilot signal, one for the estimation of CCM and the other for the estimation of CSI. In this chapter, we consider the estimation of CCM with low pilot signaling overhead. The BS may require orthogonal pilot signal linearly proportional to the number of BS antennas for the estimation of CCM. It may require pilot for the estimation of CSI with much reduced signaling overhead by exploiting the CCM [15]. When antennas are installed in a 2-D ULA, pairs of antennas in an equal distance may experience spatial channel correlation similar to each other mainly due to the far-field effect [23]. We jointly estimate the spatial correlation of antenna pairs in an equal distance. We estimate the mean-square error (MSE) of CCM elements and then neglect elements having MSE larger than a reference value for the improvement of CCM estimation. Finally, we verify the estimation performance by computer simulation in various spatial channel correlation environments

3.1. Previous works

The BSs may need to transmit pilot signal to estimate the CCM. They may use resource orthogonal to each other for the transmission of pilot signal without contamination of pilot signal. For ease of description, we consider the estimation of CCM in a single cell environment. After estimating the CCM, the BS transmits pilot signal for the estimation of CSI, as illustrated in Fig. 3-1.

Let $\mathbf{Q} \in \mathbb{C}^{N_T \times N_T}$ be pilot signal for the estimation of CCM. The BS may need N_T resource elements (REs) for the transmission of $\mathbf{Q}$. The received pilot signal of user *k* can be represented as

$$\mathbf{y}_k = \beta_k \mathbf{H}_k \mathbf{Q} + \mathbf{n}_k \tag{3.1}$$

where $\mathbf{y}_k \in \mathbb{C}^{N_R \times N_T}$ and $\mathbf{n}_k \in \mathbb{C}^{N_R \times N_T}$.

We assume that the BS transmits the pilot signal *T* times for accurate estimation of CCM using $N_T T$ REs. Letting $\mathbf{Q}[t]$ be the pilot signal at the time of the *t*-th transmission, we may represent the received pilot signal $\mathbf{y}_k[t]$ as

$$\mathbf{y}_k[t] = \beta_k[t]\mathbf{H}_k[t]\mathbf{Q}[t] + \mathbf{n}_k[t]. \tag{3.2}$$

We may generate $\mathbf{Q}[t]$ by an identity matrix without loss of generality. We can estimate the CCM, denoted by $\hat{\mathbf{R}}_k \in \mathbb{C}^{N_T \times N_T}$, by means of least square (LS) estimation as

$$\hat{\mathbf{R}}_k = \frac{1}{TN_R} \sum_t \mathbf{y}_k^H[t]\mathbf{y}_k[t] \tag{3.3}$$

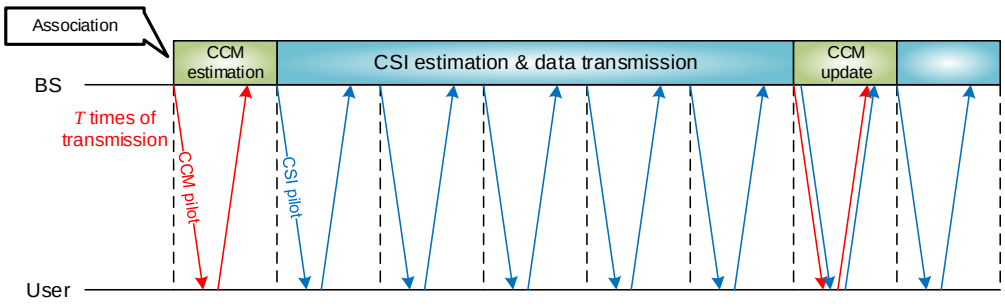

Fig. 3-1. CSI estimation with CCM.

It may require a very large value of T for accurate estimation of CCM, especially when the size of CCM is large [24]. It may not be feasible to allocate such a large resource for the CCM pilot signaling in m-MIMO environments [15]. To alleviate the problem, previous works considered additional refinement of CCM after the CCM estimation by (3.3). For ease of description, we omit the user index and consider the estimation of CCM for a single user in this chapter.

3.1.1. Thresholding and banding

It was shown that when T is very small compared to the size of CCM, denoted by N_T, we may effectively estimate the CCM by neglecting spatial channel correlation terms of small magnitude. It may be very effective when the CCM can be represented in a form of a sparse matrix [24]. We may refine the CCM as

$$\hat{\mathbf{R}}_{th} = T_{s_{th}}\left(\hat{\mathbf{R}}\right) = \left[\left[\hat{\mathbf{R}}\right]_{i,j} \cdot \mathbf{1}\left(\left|\left[\hat{\mathbf{R}}\right]_{i,j}\right| \geq s_{th}\right)\right] \tag{3.4}$$

where $\mathbf{1}(\cdot)$ equals to 1 when the input condition is satisfied and 0 otherwise, and s_{th} is a threshold to be determined.

The spatial channel correlation between two antennas may decrease as the distance between the antennas increases. An CCM element may decrease as it gets away from the diagonal elements [22]. We may refine the CCM by only considering elements near the diagonal elements, referred to banding process [22], as

$$\hat{\mathbf{R}}_{ba} = B_{s_{ba}}\left(\hat{\mathbf{R}}\right) = \left[\left[\hat{\mathbf{R}}\right]_{i,j} \cdot \mathbf{1}\left(|i-j| \le s_{ba}\right)\right] \tag{3.5}$$

where s_{ba} is a threshold to be determined.

The banding scheme may perform better than the thresholding scheme since it considers the relationship between the distance of antennas and the spatial channel correlation as in (3.5) [22]. We may determine s_{ba} through a resampling process [24]. We may randomly partition total T samples (*i.e.*, pilot signal) into two groups comprising T_1 and T_2 samples, respectively, where $T = T_1 + T_2$. We repeat the partitioning process V times. Let $\hat{\mathbf{R}}_1^{(v)}$ and $\hat{\mathbf{R}}_2^{(v)}$ be the CCM of the two groups estimated by (3.3) at the v-th partitioning process, where $1 \le v \le V$.

We may determine s_{ba} by

$$s_{ba} = \arg\min \hat{R}(s) \tag{3.6}$$

where

$$\hat{R}(s) = \frac{1}{V}\sum_{v}\left\| B_s\left(\hat{\mathbf{R}}_1^{(v)}\right) - \hat{\mathbf{R}}_2^{(v)}\right\|_{1,1}. \tag{3.7}$$

Note that we may determine s_{ba} based on the diversity of randomly distributed samples in $\hat{\mathbf{R}}_1^{(v)}$ and $\hat{\mathbf{R}}_2^{(v)}$. Since $\mathbf{H}[t]$ and $\mathbf{H}[u]$ may be correlated with each other for $t \neq u$, the samples may not be independent of each other and may seriously affect the estimation accuracy of (3.7) [22]. Moreover, when $T=1$, s_{ba} cannot be determined.

3.1.2. Tyler estimation

We may represent the probability density function (pdf) of $\mathbf{y}[t]$ in (3.2) as [23]

$$p(\mathbf{y}[t];\mathbf{R}) = \frac{\Gamma(N_T/2)}{2\pi^{N_T/2}}\sqrt{|\mathbf{R}^{-1}|}\left(\mathbf{y}^H[t]\mathbf{R}^{-1}\mathbf{y}[t]\right)^{-N_T/2}. \tag{3.8}$$

Taking the derivative with respect to $\mathbf{y}[t]$ and equating to zero, we may have the maximum likelihood (ML) estimate of $\mathbf{R}$, denoted by $\mathbf{R}_{ty}$, as

$$\mathbf{R}_{ty} = \frac{N_T}{T}\sum_t \frac{\mathbf{y}[t]\mathbf{y}^H[t]}{\mathbf{y}^H[t]\mathbf{R}_{ty}^{-1}\mathbf{y}[t]}. \tag{3.9}$$

It may not be easy to represent $\mathbf{R}_{ty}$ in a closed-form [25]. We consider additional refinement of CCM in an iterative manner as [25]

$$\hat{\mathbf{R}}_{ty}^{(i+1)} = (1-s_{ty})\frac{N_T}{T}\sum_t \frac{\mathbf{y}[t]\mathbf{y}^H[t]}{\mathbf{y}^H[t]\left(\hat{\mathbf{R}}_{ty}^{(i)}\right)^{-1}\mathbf{y}[t]} + s_{ty}\mathbf{I}_{N_T} \tag{3.10}$$

where s_{ty} is a threshold to be determined.

3.1.3. Rank-penalized LS estimation

We may estimate the CCM of a large size by means of rank-penalized LS (RPLS) estimation when the number of non-zero eigenvalues of CCM is much fewer than the size of CCM (*i.e.*, the CCM is not a full-ranked matrix) [26]. We may refine the CCM by

$$\hat{\mathbf{R}}_{RP} = \arg\min_{\mathbf{S}} \left\| \hat{\mathbf{R}} - \mathbf{S} \right\|_F^2 + s_{RP} \left\| \mathbf{S} \right\|_* \tag{3.11}$$

where $\mathbf{S}$ is a Hermitian positive definite matrix and s_{RP} is a threshold to be determined. The larger s_{RP}, the smaller number of non-zero eigenvalues of $\mathbf{S}$. Since the CCM may be rank-limited in practical m-MIMO environments [33], we may effectively estimate the CCM by means of RPLS. We may improve the RPLS by exploiting the structure of antenna array [27]. We may represent the CCM as a Kronecker product of two CCMs in the azimuth and the elevation direction as [22]

$$\mathbf{R} \approx \mathbf{R}_{az} \otimes \mathbf{R}_{el} \tag{3.12}$$

where $\mathbf{R}_{az} \in \mathbb{C}^{N_{az} \times N_{az}}$ and $\mathbf{R}_{el} \in \mathbb{C}^{N_{el} \times N_{el}}$ are the CCM in the azimuth and the elevation direction, respectively. It was shown that permuted $\mathbf{R}$, denoted by $\mathbf{Q}_{\mathbf{R}}$, whose $\left((i-1)N_{az} + j\right)$-th row is equal to $\mathrm{vec}\left([\mathbf{R}]_{(i-1)N_{el}+1:iN_{el},(j-1)N_{el}+1:jN_{el}} \right)^H$, is a non-Hermitian rank 1 matrix (*i.e.*, there exists only a single non-zero eigenvalue) [27]. Here, $\mathrm{vec}(\mathbf{A})$ denotes the vectorized form of $\mathbf{A}$ (*i.e.*, concatenation of columns of $\mathbf{A}$ into a column vector). This implies that the rank-penalized minimization by (3.11) may work effectively to estimate $\mathbf{Q}_{\mathbf{R}}$. In this case, we may have a solution of (3.11), represented as [27]

$$\hat{\mathbf{Q}}_{\mathbf{R}} = \sum_j \left(\hat{\lambda}_j - \frac{s_{RPK}}{2} \right)^+ \hat{\mathbf{u}}_j \hat{\mathbf{v}}_j^H \tag{3.13}$$

where $\hat{\lambda}_j$ is the *j*-th highest singular value of $\mathbf{Q}_{\hat{\mathbf{R}}}$, $\hat{\mathbf{u}}_j$ and $\hat{\mathbf{v}}_j$ are the corresponding left and right singular vectors of $\mathbf{Q}_{\hat{\mathbf{R}}}$, respectively, and s_{RPK} is a threshold to be determined. In (3.13), we neglect singular values smaller than the threshold to estimate the permuted CCM. Finally, we may obtain refined CCM $\hat{\mathbf{R}}_{RPK}$ by de-permuting $\hat{\mathbf{Q}}_{\mathbf{R}}$.

3.2. Proposed scheme

Most of previous works considered the CSI estimation in m-MIMO environments assuming the use of perfect CCM [14-19]. Moreover, they did not investigate the effect of CCM accuracy on the CSI estimation [24-27]. Although the CCM varies slowly even in the presence of user mobility, the signaling overhead for the estimation of CCM may be considerably large when N_T is very large [20]. In practice, we may not transmit pilot signal as much as being required. Moreover, previous works did not consider the presence of channel correlation between $\mathbf{H}[t]$ and $\mathbf{H}[u]$ for $t \neq u$.

We consider the estimation of CCM with reduced signaling overhead in the presence of channel correlation between $\mathbf{H}[t]$ and $\mathbf{H}[u]$ for $t \neq u$. We estimate the CCM in a three-step process. We first estimate the CCM by means of LS estimation exploiting the structure of ULA in m-MIMO environments. Then, we refine the CCM by neglecting CCM element that have estimation error higher than a reference value. Finally, we further refine the CCM by neglecting spatial channel correlation of antenna pairs in a distance larger than a reference value.

3.2.1. LS estimation exploiting the far-field effect

We consider the use of antennas in an ULA, where the distance between two antennas is much smaller than the distance between the BS and a user. Pairs of antennas in an equal distance may experience spatial channel correlation similar to each other mainly due to the far-field effect [23].

We may represent the CCM of a one-dimensional (1-D) antenna array in a form of a Toeplitz Hermitian matrix by exploiting the far-field effect [23]. The spatial channel correlation between antenna *i* and *j* satisfies the following relationship

$$[\mathbf{R}]_{i,j} \approx [\mathbf{R}]_{(i+n),(j+n)} \tag{3.14}$$

where *n* is an integer such that $1 < i+n$ and $j+n < N_T$.

We may easily apply the relationship (3.14) to 2-D ULA environments. Let a_i and e_i be the location of antenna *i*, represented in the azimuth and the elevation direction of antenna array, respectively. Let $\mathbf{d}_{i,j} = (a_i - a_j, e_i - e_j)$ be the distance vector between antenna *i* and *j*, and (i, j) denote a pair of the antennas. Then, for a pair of antennas (a,b), (3.14) can be rewritten as

$$[\mathbf{R}]_{a,b} \approx [\mathbf{R}]_{i,j} \quad \text{for} \quad (a,b) \in S_{\mathbf{d}_{i,j}} \tag{3.15}$$

where $S_{\mathbf{d}_{i,j}}$ is a set of antenna pairs with distance vector $\mathbf{d}_{i,j}$. Fig. 3-2 illustrates that pairs of antennas with a same color may experience spatial channel correlation similar to each other. We may estimate the CCM by means of LS estimation with relationship by (3.15) as

$$\left[\hat{\mathbf{R}}\right]_{i,j} = \frac{1}{TN_R\left|S_{\mathbf{d}_{i,j}}\right|}\sum_{(a,b)\in S_{\mathbf{d}_{i,j}}}\sum_{t}\left(\left[\mathbf{y}[t]\right]_{:,a}\right)^H\left[\mathbf{y}[t]\right]_{:,b}. \tag{3.16}$$

Since the structure of antenna array is unchanged and pre-known to users, users may not have to calculate $S_{\mathbf{d}_{i,j}}$ for all combinations of (i, j) for the estimation of CCM. Note that as $\left|\mathbf{d}_{i,j}\right|$ decreases, $\left|S_{\mathbf{d}_{i,j}}\right|$ increases mainly due to the structure of ULA. This implies that we may accurately estimate the spatial channel correlation by using a pair of antennas with small $\left|\mathbf{d}_{i,j}\right|$ by (3.16). As a result, the CCM elements may be estimated with different accuracy. Fig. 3-2 illustrates some antenna pairs in an equal distance, where antenna pairs in orange-color have a larger number of antenna pairs in an equal distance vector than ones in blue-color. Thus, we may estimate the spatial channel correlation of the former more accurately than that of the latter.

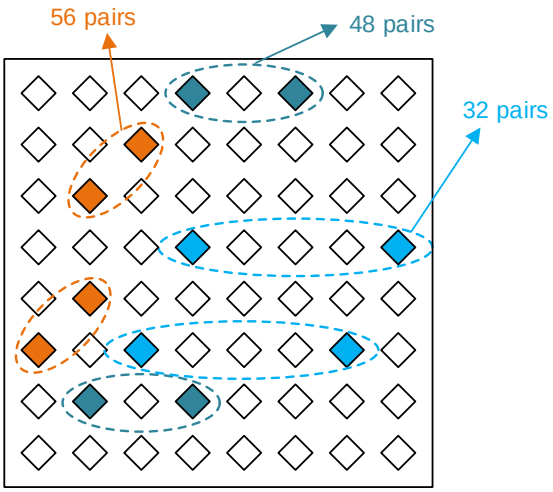

Fig. 3-2. Similarity of spatial channel correlation of antenna pairs in an equal distance.

3.2.2. Refinement of CCM estimation

It may be desirable not to consider CCM elements erroneously estimated for the CCM estimation. Thus, we neglect CCM element $\left[\hat{\mathbf{R}}\right]_{i,j}$ (*i.e.*, set $\left[\hat{\mathbf{R}}\right]_{i,j}$ to zero) when its MSE is larger than a threshold. We may represent the MSE of $\left[\hat{\mathbf{R}}\right]_{i,j}$, denoted by $\sigma^2_{\left[\hat{\mathbf{R}}\right]_{i,j}}$, as

$$\begin{aligned}\sigma^2_{\left[\hat{\mathbf{R}}\right]_{i,j}} &= E\left[\left|\left[\mathbf{R}\right]_{i,j} - \left[\hat{\mathbf{R}}\right]_{i,j}\right|^2\right] \\ &= E\left[\left|\left[\mathbf{R}\right]_{i,j} - \frac{1}{T^2 N_R^2 \left|S_{\mathbf{d}_{i,j}}\right|^2} \sum_{(a,b)\in S_{\mathbf{d}_{i,j}}} \sum_{t} y_{a,b}^{(t,t)}\right|^2\right] \\ &= -\left|\left[\mathbf{R}\right]_{i,j}\right|^2 + E\left[\frac{1}{T^2 N_R^2 \left|S_{\mathbf{d}_{i,j}}\right|^2} \sum_{\substack{(a,b),\\(c,d)\in S_{\mathbf{d}_{i,j}}}} \sum_{t,u} y_{a,b}^{(t,t)} y_{d,c}^{(u,u)}\right]\end{aligned} \tag{3.17}$$

where $y_{a,b}^{(t,u)} \equiv \left(\left[\mathbf{y}[t]\right]_{:,a}\right)^H \left[\mathbf{y}[u]\right]_{:,b}$. It can be shown from Isserlis theorem that (3.17) can be written as [28]

$$\begin{aligned}\sigma^2_{\left[\hat{\mathbf{R}}\right]_{i,j}} &= -\left|\left[\mathbf{R}\right]_{i,j}\right|^2 + \frac{1}{T^2 N_R^2 \left|S_{\mathbf{d}_{i,j}}\right|^2} \sum_{\substack{(a,b),\\(c,d)\in S_{\mathbf{d}_{i,j}}}} \sum_{t,u} \left(E\left[y_{a,b}^{(t,t)}\right] E\left[y_{d,c}^{(u,u)}\right] + E\left[y_{a,c}^{(t,u)}\right] E\left[y_{d,b}^{(u,t)}\right]\right) \\ &= \frac{1}{T^2 N_R^2 \left|S_{\mathbf{d}_{i,j}}\right|^2} \sum_{\substack{(a,b),\\(c,d)\in S_{\mathbf{d}_{i,j}}}} \sum_{t,u} \left\{\left(E\left[h_{a,c}^{(t,u)}\right] + \sigma_n^2 \delta_{a,c}^{(t,u)}\right) \cdot \left(E\left[h_{d,b}^{(u,t)}\right] + \sigma_n^2 \delta_{b,d}^{(t,u)}\right)\right\} \\ &= \frac{1}{T^2 N_R^2 \left|S_{\mathbf{d}_{i,j}}\right|^2} \sum_{\substack{(a,b),\\(c,d)\in S_{\mathbf{d}_{i,j}}}} \sum_{t,u} \left|E\left[h_{a,c}^{(t,u)}\right]\right|^2 + \frac{2\sigma_n^2 + \sigma_n^4}{T N_R \left|S_{\mathbf{d}_{i,j}}\right|}\end{aligned} \tag{3.18}$$

where $h_{a,c}^{(t,u)} = \left(\left[\mathbf{H}[t]\right]_{:,a}\right)^H \left[\mathbf{H}[u]\right]_{:,c}$ and $\delta_{a,c}^{(t,u)}$ is a delta function having a value of 1 when $(a,t) = (c,u)$. It can be seen that $E\left[h_{a,c}^{(t,u)}\right] = E\left[h_{d,b}^{(t,u)}\right]$ since $\mathbf{d}_{a,c} = \mathbf{d}_{b,d}$. It can also be seen that $\sigma^2_{\left[\hat{\mathbf{R}}\right]_{i,j}}$ decreases as $\left|S_{\mathbf{d}_{i,j}}\right|$ increases. The smaller the distance between a pair of antennas, the higher the estimation accuracy of spatial channel correlation. The accuracy of estimation may deteriorate in the presence of channel correlation between $\mathbf{H}[t]$ and $\mathbf{H}[u]$ for $t \neq u$ since non-zero $\left|E\left[h_{a,c}^{(t,u)}\right]\right|$ increases the MSE.

We may require $E\left[h_{a,c}^{(t,u)}\right]$ to calculate the MSE by (3.18), which may not easily be calculated in practice. We may approximate $E\left[h_{a,c}^{(t,u)}\right]$ as

$$\begin{aligned} E\left[h_{a,c}^{(t,u)}\right] &\approx \frac{\hat{\rho}_{t,u}}{TN_R\left|S_{\mathbf{d}_{a,c}}\right|} \sum_{(p,q)\in S_{\mathbf{d}_{a,c}}} \sum_{v} y_{p,q}^{(v,v)} \\ &\equiv \hat{h}_{a,c}^{(t,u)} \end{aligned} \tag{3.19}$$

where $\hat{\rho}_{t,u}$ is the average of correlation between $\mathbf{H}[t]$ and $\mathbf{H}[u]$ for $1 \le t,u \le T$. Since users may know their velocity and temporal interval between $\mathbf{P}[t]$ and $\mathbf{P}[u]$, we may estimate $\hat{\rho}_{t,u}$ using Markov channel variation model by (2.3) [13], or as

$$\hat{\rho}_{t,u} = \frac{1}{N_T N_R} \mathbf{y}[t] \odot \mathbf{y}^*[u] \tag{3.20}$$

where $\odot$ denotes Hadamard product. Note that (3.20) may be valid in m-MIMO environments due to the use of a large N_T. Note also that the approximation by (3.19) is based on the assumption that $\mathbf{R}$ is almost unchanged during the transmission of T pilot signals.

We may approximately represent $\sigma^2_{\left[\hat{\mathbf{R}}\right]_{i,j}}$ as

$$\hat{\sigma}^2_{\left[\hat{\mathbf{R}}\right]_{i,j}} = \frac{1}{T^2 N_R^2 \left|S_{\mathbf{d}_{i,j}}\right|^2} \sum_{\substack{(a,b),\\(c,d)\in S_{\mathbf{d}_{i,j}}}} \sum_{t,u} \left|\hat{h}^{(t,u)}_{a,c}\right|^2 + \frac{2\sigma_n^2 + \sigma_n^4}{TN_R \left|S_{\mathbf{d}_{i,j}}\right|}. \tag{3.21}$$

When the pilot signal is transmitted only once for the estimation of CCM (*i.e.*, $T=1$), (3.21) can be simplified to

$$\hat{\sigma}^2_{\left[\hat{\mathbf{R}}_k\right]_{i,j}} = \frac{1}{N_R^2 \left|S_{\mathbf{d}_{i,j}}\right|^2} \sum_{\substack{(a,b),\\(c,d)\in S_{\mathbf{d}_{i,j}}}} \left|\hat{h}_{a,c}\right|^2 + \frac{2\sigma_n^2 + \sigma_n^4}{N_R \left|S_{\mathbf{d}_{i,j}}\right|} \tag{3.22}$$

where the transmission index of pilot signal is omitted.

Some elements of $\hat{\mathbf{R}}$ may be estimated with some inaccuracy mainly due to small $\left|S_{\mathbf{d}_{i,j}}\right|$ and *T*. $\left|S_{\mathbf{d}_{i,j}}\right|$ and *T* are related to the array structure and the number of transmitted pilot signal, respectively. We may neglect element $\left[\hat{\mathbf{R}}\right]_{i,j}$ if the MSE after neglecting $\left[\hat{\mathbf{R}}\right]_{i,j}$, represented as $E\left[\left[\mathbf{R}\right]_{i,j} - \left[\hat{\mathbf{R}}\right]_{i,j}\right]^2$, is smaller than $\sigma^2_{\left[\hat{\mathbf{R}}\right]_{i,j}}$. This implies that the we may improve the estimation accuracy by neglecting elements estimated with inaccuracy. Let $\sigma^2_{\left[\hat{\mathbf{R}}\right]_{i,j}=0}$ and $\hat{\sigma}^2_{\left[\hat{\mathbf{R}}\right]_{i,j}=0}$ denote the exact and the expected MSE of $\left[\hat{\mathbf{R}}\right]_{i,j}$ after neglecting the element, respectively. It can be shown from $\sigma^2_{\left[\hat{\mathbf{R}}\right]_{i,j}=0} = \left|\left[\mathbf{R}\right]_{i,j}\right|^2$ that

$$\hat{\sigma}^2_{\left[\hat{\mathbf{R}}\right]_{i,j}=0} = \left|\left[\hat{\mathbf{R}}\right]_{i,j}\right|^2. \tag{3.23}$$

Finally, we may refine $\hat{\mathbf{R}}$ as

$$\hat{\mathbf{R}}_{pro} = \left[\left[\hat{\mathbf{R}} \right]_{i,j} \cdot \mathbf{1}\left(\hat{\sigma}^2_{\left[\hat{\mathbf{R}}\right]_{i,j}} < \hat{\sigma}^2_{\left[\hat{\mathbf{R}}\right]_{i,j}=0} \right) \right]. \tag{3.24}$$

It may be desirable to refine the CCM in consideration of the magnitude of CCM elements in addition to the estimation error [20, 24]. The estimation error of $\left[\hat{\mathbf{R}}\right]_{i,j}$ may seriously affect the CSI estimation when $[\mathbf{R}]_{i,j}$ has a very small magnitude [24]. We may accurately estimate $[\mathbf{R}]_{i,j}$, but we may not efficiently use it for the estimation of CSI unless its magnitude is not too small [20]. Thus, we may neglect CCM elements of a very small magnitude regardless of the estimation accuracy.

It can be shown from (3.21) that the expectation of $\sigma^2_{\left[\hat{\mathbf{R}}\right]_{i,j}}$ can be represented as

$$E\left\{ \hat{\sigma}^2_{\left[\hat{\mathbf{R}}\right]_{i,j}} \right\} = \frac{1}{T^2 N_R^2 \left| S_{\mathbf{d}_{i,j}} \right|^2} \sum_{\substack{(a,b),\\ (c,d)\in S_{\mathbf{d}_{i,j}}}} \sum_{t,u} \left| \hat{\rho}_{t,u} [\mathbf{R}]_{a,c} \right|^2 + \frac{2\sigma_n^2 + \sigma_n^4}{TN_R \left| S_{\mathbf{d}_{i,j}} \right|} \tag{3.25}$$

where $\hat{\rho}_{t,u}$ is assumed to be a constant. Assuming that the distance between a pair of antennas (i, j) is sufficiently large (*i.e.*, $[\mathbf{R}]_{i,j}$ has a very small value), (3.25) has a lower bound represented as

$$\begin{aligned} E\left\{ \hat{\sigma}^2_{\left[\hat{\mathbf{R}}\right]_{i,j}} \right\} &\geq \frac{1}{T^2 N_R^2 \left| S_{\mathbf{d}_{i,j}} \right|^2} \sum_{(a,c)\in S_{\mathbf{d}_{i,j}}} \sum_{t,u} \left| \hat{\rho}_{t,u} [\mathbf{R}]_{a,c} \right|^2 + \frac{2\sigma_n^2 + \sigma_n^4}{TN_R \left| S_{\mathbf{d}_{i,j}} \right|} \\ &= \frac{1}{T^2 N_R^2 \left| S_{\mathbf{d}_{i,j}} \right|^2} \sum_{t,u} \left| \hat{\rho}_{t,u} \right|^2 \left| S_{\mathbf{d}_{i,j}} \right|^2 [\mathbf{R}]_{a,c} + \frac{2\sigma_n^2 + \sigma_n^4}{TN_R \left| S_{\mathbf{d}_{i,j}} \right|} \\ &= \frac{\sum_{t,u} \left| \hat{\rho}_{t,u} \right|^2}{T^2 N_R^2} [\mathbf{R}]_{a,c} + \frac{2\sigma_n^2 + \sigma_n^4}{TN_R \left| S_{\mathbf{d}_{i,j}} \right|}. \end{aligned} \tag{3.26}$$

It can be shown that the expectation of $\sigma^2_{\left[\hat{\mathbf{R}}\right]_{i,j}=0}$ can be represented as

$$E\left\{\hat{\sigma}^2_{\left[\hat{\mathbf{R}}\right]_{i,j}=0}\right\}=\left[\mathbf{R}\right]_{a,c}. \tag{3.27}$$

It may be desirable to modify the refinement condition (3.24) to make the lower bound of $E\left\{\hat{\sigma}^2_{\left[\hat{\mathbf{R}}\right]_{i,j}}\right\}$ equal to $E\left\{\sigma^2_{\left[\hat{\mathbf{R}}\right]_{i,j}=0}\right\}$ when $\left[\mathbf{R}\right]_{i,j}$ has a very small magnitude. We can neglect $\left[\mathbf{R}\right]_{i,j}$ of very small magnitude by making the MSE of $\left[\hat{\mathbf{R}}\right]_{i,j}$ higher than a reference value.

Equating (3.26) and (3.27), we may come up with new refinement condition represented as

$$\frac{T^2 N_R^2}{\sum_{t,u}\left|\hat{\rho}_{t,u}\right|^2}\cdot\hat{\sigma}^2_{\left[\hat{\mathbf{R}}\right]_{i,j}}<\hat{\sigma}^2_{\left[\hat{\mathbf{R}}\right]_{i,j}=0}. \tag{3.28}$$

It can be seen that the weighted MSE of the left side in (3.28) does not converge to zero as *T* goes infinite. This mainly because non-zero estimation error always exists. This implies that we may not perfectly estimate the CCM even though we sufficiently transmit pilot signal as much as possible. We may approximately estimate the CCM with tolerable accuracy in practice.

3.2.3. Effective region of CCM

The refined CCM may still include elements inaccurately estimated since the MSE is calculated based on the estimation of spatial channel correlation. It may be desirable to additionally refine the CCM in consideration of the distance between a pair of antennas.

In 1-D antenna array environments, let l_i be the minimum distance between the two antennas (i, j) that does not meet the condition (3.28). We may represent it as

$$l_i = \min_j \left|\mathbf{d}_{i,j}\right| \quad \text{for} \quad \left[\hat{\mathbf{R}}_{pro}\right]_{i,j} = 0 . \tag{3.29}$$

We may additionally refine the CCM as

$$\hat{\mathbf{R}}_{pro}^{eff} = \left[\left[\hat{\mathbf{R}}_{pro}\right]_{i,j} \cdot \mathbf{1}\left(\left|\mathbf{d}_{i,j}\right| < l_i\right)\right]. \tag{3.30}$$

This means that we only consider antennas within a distance of l_i from antenna *i*, referred to effective region of antenna *i*. We may estimate the spatial channel correlation between a pair of antennas in a short distance without large MSE.

In 2-D antenna array environments, it may be desirable to determine the effective region in the azimuth and the elevation direction. We may process the refinement for antenna *i* for each row as in 1-D antenna array environments, as summarized in Table 3-1. For ease of description, we denote the antenna located at the *a*-th row and the *e*-th column of the array by $N_{az}(a-1)+e$ and the index of an antenna in the *a*-th row by j_a.

We determine the effective region of antenna 1, which is located in the corner of the array as illustrated in Fig. 3-3. Note that the first *a* satisfying the condition that $j_a^* = \min j_a$ represents the boundary of effective region in the elevation direction. After the refinement process for antenna 1, we may sequentially determine the effective region of other antennas since it has the same shape as that of antenna 1.

Table 3-1. Additional refinement procedure.

Input: $\hat{\mathbf{R}}_{pro}$

Initialization: $\hat{\mathbf{R}}_{pro}^{eff} = \hat{\mathbf{R}}_{pro}, a = 1$

Do:

1. Obtain $j_a^* = \arg\min_{j_a} \left| \mathbf{d}_{1 j_a} \right|$ satisfying $\left[\hat{\mathbf{R}}_{pro} \right]_{1 j_a} = 0$
2. $\left[\hat{\mathbf{R}}_{pro}^{eff} \right]_{1 j_a} = 0$ for $j_a \geq j_a^*$ and $a \leftarrow a + 1$
3. Repeat 1~2 until $j_a^* = \min j_a$ or $a > N_{el}$
4. Determine the effective region for other antennas and refine $\hat{\mathbf{R}}_{pro}^{eff}$

Output: $\hat{\mathbf{R}}_{pro}^{eff}$

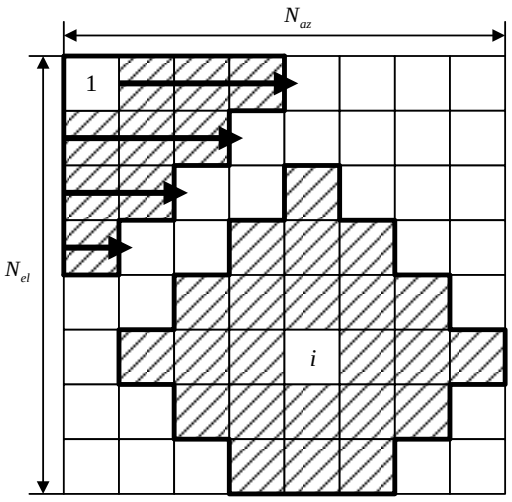

Fig. 3-3. An example of the proposed refinement procedure.

Table 3-2. Evaluation parameters.

Parameters	Values
CCM model	3-D ray-based model [22]
AoD	$-60^\circ \sim 60^\circ$ in azimuth direction
	$40^\circ \sim 80^\circ$ in elevation direction
AS	Moderate and large modes [22]
Carrier frequency $(=1/\lambda)$	2.3 GHz
BS antenna distance	$\lambda/2$
Number of BS antennas (N_T)	64
Number of user antennas (N_R)	1
Number of users	4
CSI estimation	Eigen-space estimation [19]
CSI pilot length	16, 24 (for moderate and large AS, respectively)
Average SNR	20 dB

3.3. Performance evaluation

We evaluate the performance of the proposed scheme by computer simulation. We assume that the BS is equipped with antennas in a 2-D square ULA and the spatial

channel correlation follows non-line-of-sight (NLOS) ray-based model [22]. We consider two angular spread (AS) environments; moderate and large AS modes [22]. We assume that $N_R = 1$ without loss of generality since the increase of N_R is equal to the increase of T for the CCM estimation. We evaluate the estimation performance according to T with a fixed value of N_R. The main simulation parameters are summarized in Table 3-2. We determine the angle of departure (AoD) in consideration of the service coverage of macro cell [22]. We assume that the BS transmits pilot signal for the estimation of CCM and then transmits pilot signal beam-formed by [19] for the estimation of CSI.

In the following figures, "perfect" refers to the case when the CCM is perfectly estimated, "P1" and "P2" refer to the proposed scheme based on the refinement condition (3.24) and (3.28), respectively, "banding" refers to the banding scheme [24], "Tyler" refers to the Tyler scheme [25], and "RPLS" refers to the RPLS scheme with Kronecker structure [26]. We also evaluate the performance when the RPLS scheme is performed after P1 or P2 is applied, which are referred to "P1 + RPLS" and "P2 + RPLS" in the figures. For fair comparison, we apply the proposed LS estimation (3.16) to other schemes except Tyler scheme. Note that Tyler scheme employs an ML estimator based on the estimated CCM by (3.3).

We evaluate the estimation accuracy of CCM based on Frobenius norm of the difference between the original and the estimated CCM [24], represented as

$$e_{\mathrm{CCM}} \equiv \left\| \mathbf{R} - \hat{\mathbf{R}} \right\|_F . \tag{3.31}$$

Fig. 3-4 depicts the average e_{CCM} in two AS environments according to T. The banding scheme is not considered when $T = 1$ since the banding threshold is not defined for

single transmission of pilot signal [24]. It can be seen that all the schemes improve their estimation performance as T increases and that P1 outperforms the other schemes. It can also be seen that P2 is not effective as much as P1 for the estimation of CCM. This is because P2 may neglect more CCM elements than P1, which may yield non-zero estimation error even when T is large. It can also be seen that the RPLS scheme may not be effective when the AS is large. This is because the eigenvalues of CCM may be similar to each other compared to when the AS is not large [22]. The RPLS scheme may not be feasible in large AS environments, since it estimates the CCM based on a few highest eigenvalues of CCM by (3.13). Similarly, combined use of RPLS and the proposed scheme may not also be effective. The Tyler scheme provides the worst performance since it does not employ the proposed LS estimation.

Fig. 3-5 and Fig. 3-6 depict the MSE of CSI (e_{CSI}) and the spectral efficiency of ZF beamforming with the use of estimated CSI, respectively. When the AS is not large, it can be seen that the RPLS outperforms the proposed scheme when $T = 8$, and that P2 outperforms P1. From Fig. 3-4, -5 and -6, we may conjecture that the CCM estimation accuracy may not related to the CSI estimation accuracy. The gap between P1 and P2 may suggest that CCM elements of a very small magnitude are not useful for the CSI estimation [24]. It can also be seen that combined use of RPLS and P1 works better than that of the RPLS and P2. This is because P1 may lose less information of the original CCM than P2, neglecting less elements of the estimated CCM. The RPLS may effectively estimate the CCM after P1 is applied. It can also be seen that the estimation accuracy decreases as the AS increases. It can be seen from Fig. 3-6 that combined use of RPLS and the proposed scheme provides performance similar to the perfect CCM case.

Fig. 3-7 depicts the average extent of effective region. The extent is defined by the number of antennas in the effective region, represented as

$$r_{eff} = \sum_{a} j_a^* . \tag{3.32}$$

It can be seen that as T increases, the average extent increases mainly due to the increase of the LS estimation accuracy. When T is sufficiently large, the effective region of P1 includes more than half of antennas unless the AS is too large. The effective region of P2 is much smaller than that of P1. This is because P2 refines the CCM more strictly than P1.

We evaluate the estimation performance according to the channel correlation between $\mathbf{H}[t]$ and $\mathbf{H}[u]$ for $t \neq u$ when $T = 2$. Fig. 3-8 depicts e_{CCM} in two AS environments. It can be seen that the banding and Tyler scheme are noticeably affected by the presence of channel correlation. The samples of each group in the banding scheme may have statistical characteristics similar to each other in the presence of high channel correlation, yielding inaccurate banding threshold. Tyler scheme estimates the CCM assuming that pilot signal experiences independent channel [25]. The proposed scheme estimates the CCM in consideration of channel correlation, being less affected by the presence of channel correlation.

Fig. 3-9 and Fig. 3-10 depict e_{CSI} and the spectral efficiency with the use of ZF beamforming, respectively. It can be seen that the proposed scheme outperforms the others, being robust to the variation of channel correlation. It can also be seen that P1 works well as the channel correlation increases when the AS is not large, which is contrary to the other schemes. This is because the performance of P1 in Fig. 3-5 (a)

degrades as T increases from 1 to 2. It can also be seen that we may improve the estimation accuracy by using the RPLS and the proposed scheme together.

Fig. 3-11 depicts the average extent of the effective region of the proposed scheme according to the channel correlation. It can be seen that the average extent decreases as the channel correlation increases. This is because the CCM estimation accuracy decreases as the channel correlation increases, as shown in Fig. 3-8. It can also be seen that the variance of average extent of P1 is larger than that of P2.

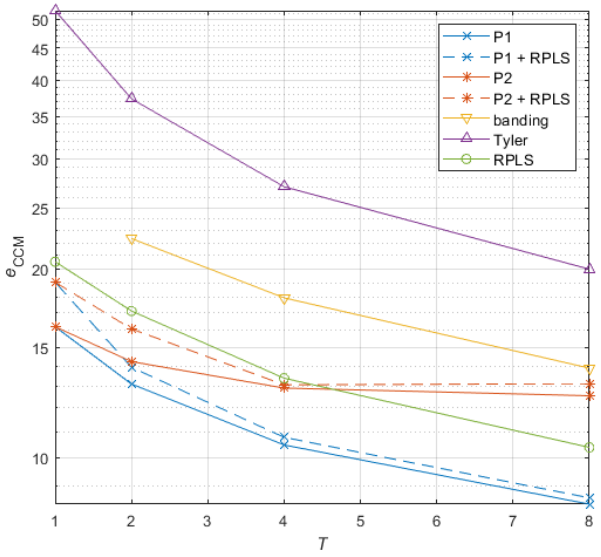

(a) Moderate AS environment.

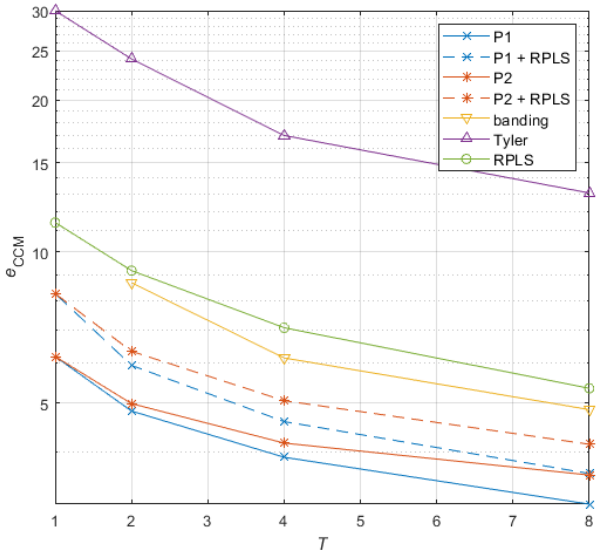

(b) Large AS environment.

Fig. 3-4. Estimation accuracy of CCM according to *T*.

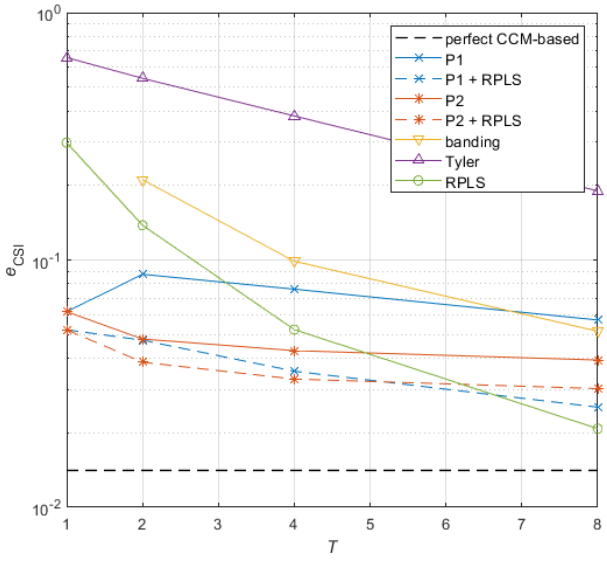

(a) Moderate AS environment.

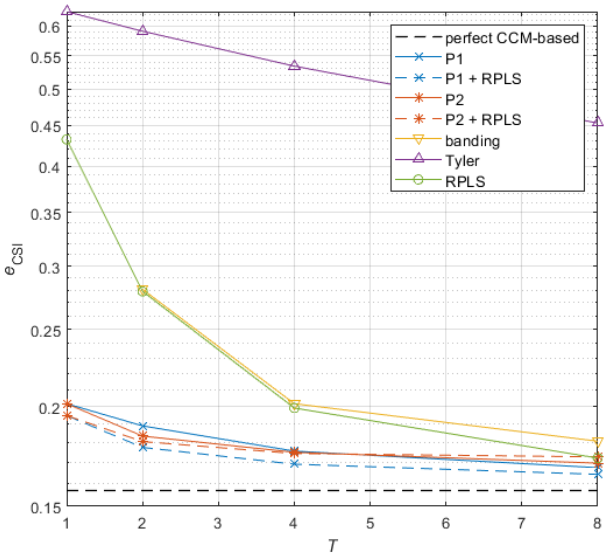

(b) Large AS environment.

Fig. 3-5. Estimation accuracy of CSI according to *T*.

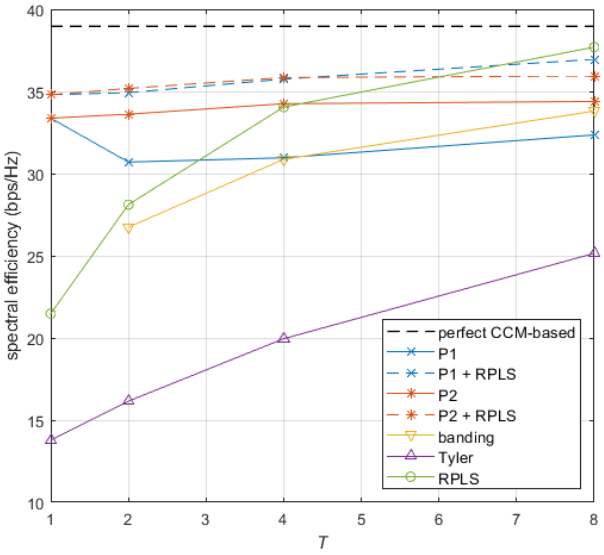

(a) Moderate AS environment.

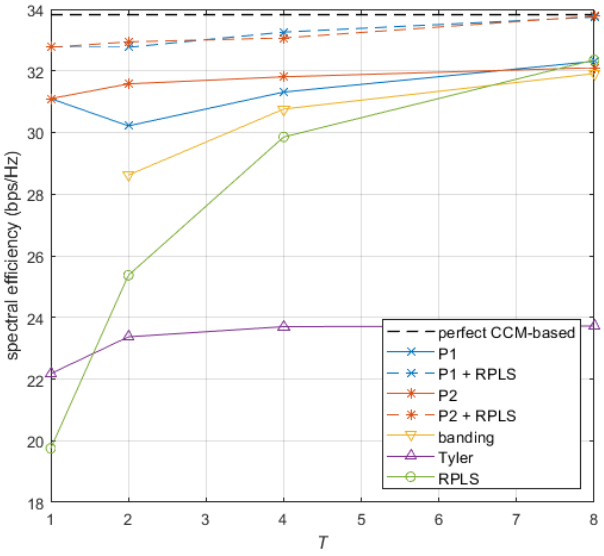

(a) Large AS environment.

Fig. 3-6. Spectral efficiency according to *T*.

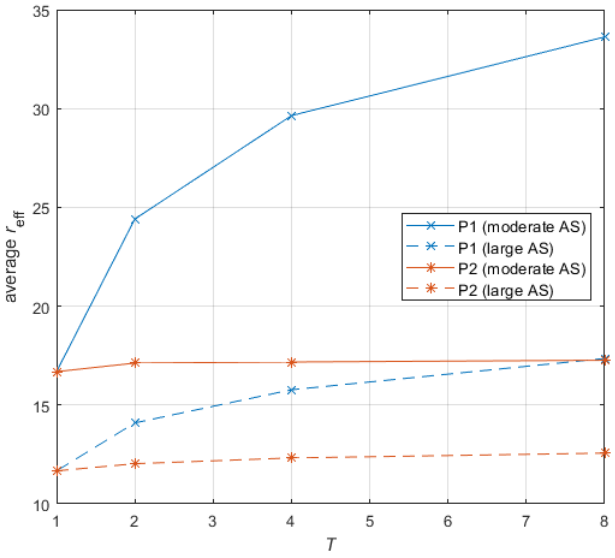

Fig. 3-7. Size of effective region according to *T*.

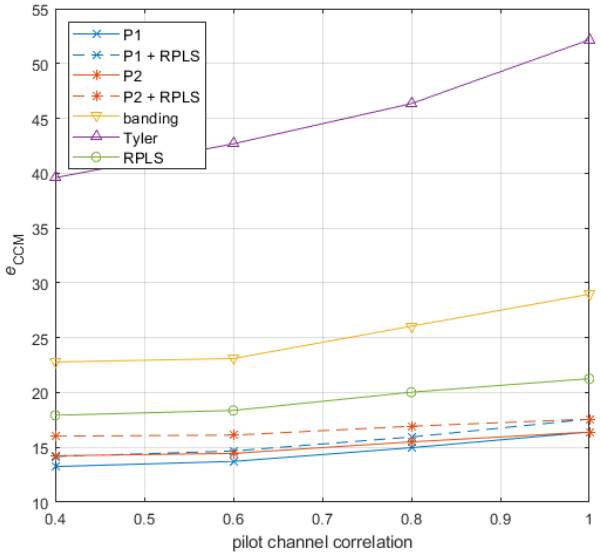

(a) Moderate AS environment.

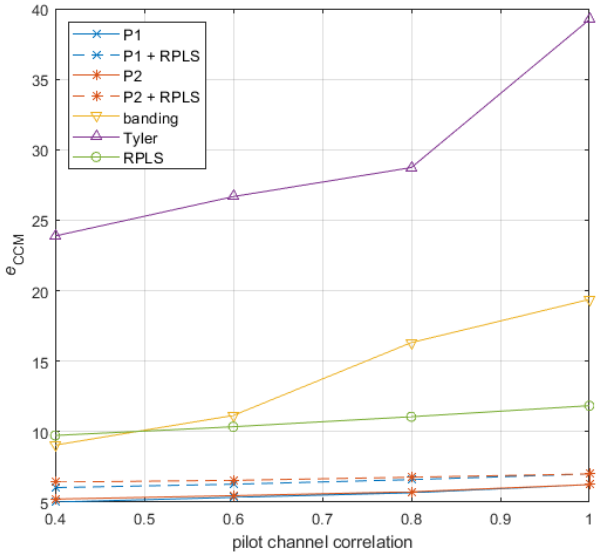

(b) Large AS environment.

Fig. 3-8. Estimation accuracy of CCM according to pilot channel correlation.

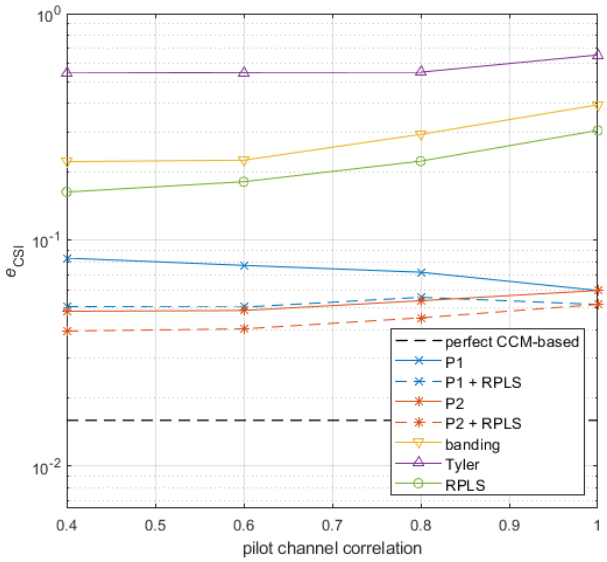

(a) Moderate AS environment.

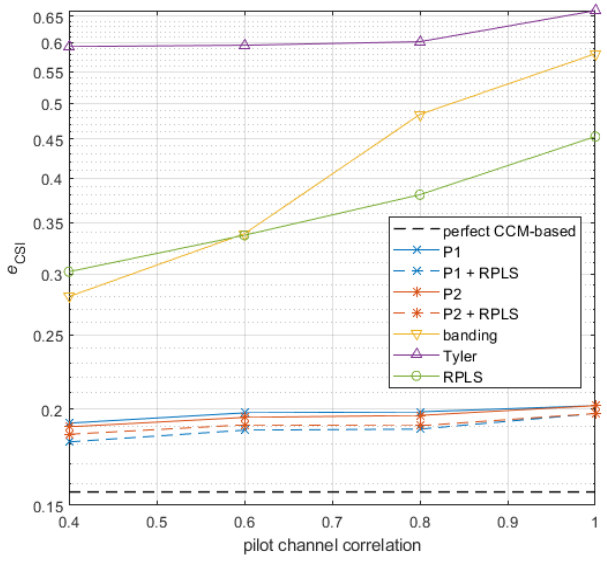

(b) Large AS environment.

Fig. 3-9. Estimation accuracy of CSI according to pilot channel correlation.

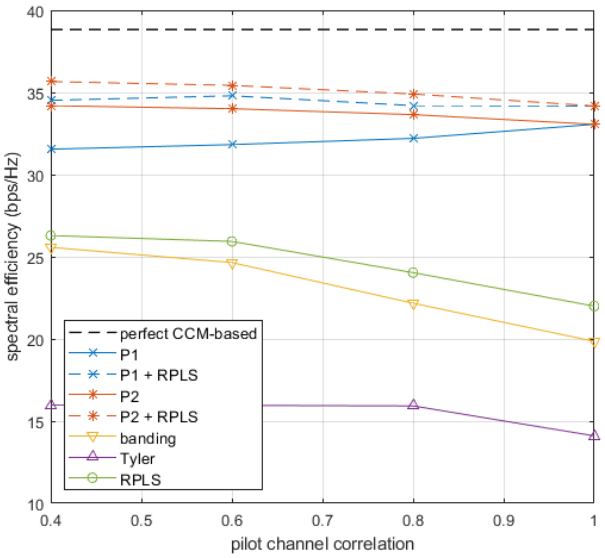

(a) Moderate AS environment.

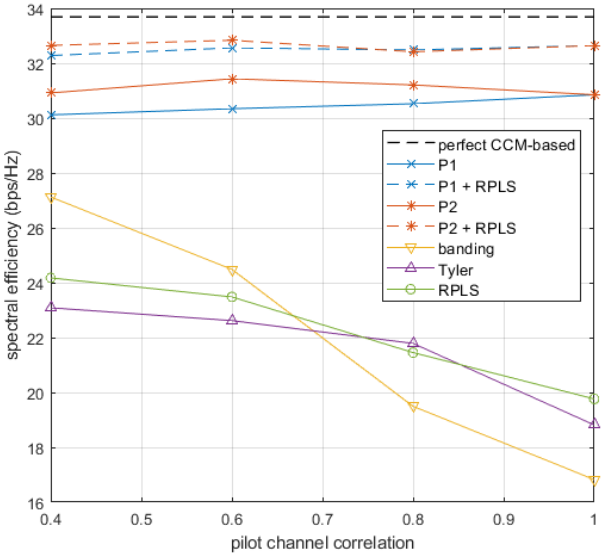

(b) Large AS environment.

Fig. 3-10. Spectral efficiency according to pilot channel correlation.

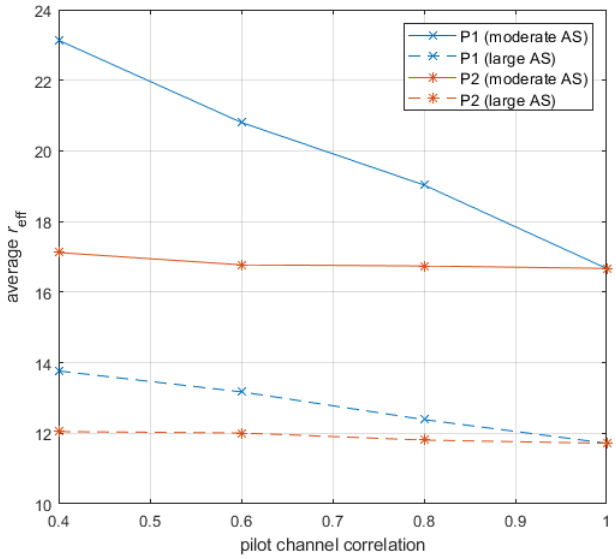

Fig. 3-11. Size of effective region according to pilot channel correlation.

Chapter 4

Mobility-aware signal transmission in m-MIMO environments

In this chapter, we consider the signal transmission to users in the presence of channel aging effect. When a user is in high mobility, the BS may transmit signal to the user based on outdated CSI, suffering from performance degradation [10]. Previous works exploit the CCM to design the beam weight in consideration of channel aging effect [31-35]. However, it may be not efficient to exploit the CCM when users are in low mobility [36]. We may design the beam weight in response to user mobility based on CSI and CCM. We may maximize the average SLNR by transmitting signal in the eigen-direction of a linear combination of CSI and CCM. We analyze the average SINR obtained by the proposed scheme and apply it to the transmit power control by means of iterative water-filling [43].

4.1. Previous works

For ease of description, we briefly review previous works in single-cell environments, where the BS index is omitted.

4.1.1. CSI-based two-stage beamforming

We may determine the beam weight in a two-stage process: suppression of interference from the BS to non-desired users and signal transmission to the desired user [30]. For user *k*, we may represents the interference channel as

$$\bar{\mathbf{H}}_k = \bar{\mathbf{U}}_k \left[\bar{\mathbf{D}}_k \quad \mathbf{0} \right] \left[\bar{\mathbf{V}}_k^{(1)} \quad \bar{\mathbf{V}}_k^{(0)} \right]^H \tag{4.1}$$

where $\bar{\mathbf{H}}_k \equiv \left[\hat{\mathbf{H}}_1^T, ..., \hat{\mathbf{H}}_{k-1}^T, \hat{\mathbf{H}}_{k+1}^T, ..., \hat{\mathbf{H}}_K^T \right]^T$, $\bar{\mathbf{D}}_k$ is a diagonal matrix comprising singular values of $\bar{\mathbf{H}}_k$, $\bar{\mathbf{U}}_k$ is a matrix comprising the left singular vectors, and $\bar{\mathbf{V}}_k^{(1)}$ and $\bar{\mathbf{V}}_k^{(0)}$ are matrices comprising the right singular vectors corresponding to non-zero singular values and zero singular values, respectively.

We may suppress the interference by $\bar{\mathbf{V}}_k^{(0)}$ [30]. We may represent the effective as

$$\hat{\mathbf{H}}_k^{eff} = \hat{\mathbf{H}}_k \bar{\mathbf{V}}_k^{(0)} = \hat{\mathbf{U}}_k^{eff} \hat{\mathbf{D}}_k^{eff} \hat{\mathbf{V}}_k^{eff} \tag{4.2}$$

where $\hat{\mathbf{D}}_k^{eff}$ is a matrix comprising singular values of $\hat{\mathbf{H}}_k^{eff}$, and $\hat{\mathbf{U}}_k^{eff}$ and $\hat{\mathbf{V}}_k^{eff}$ are matrices comprising the left and the right singular vectors of $\hat{\mathbf{H}}_k^{eff}$, respectively. We may determine the beam weight for user *k* by [30]

$$\mathbf{B}_k = \bar{\mathbf{V}}_k^{(0)} \hat{\mathbf{V}}_k^{eff} . \tag{4.3}$$

Since this scheme depends on the estimated CSI, it may not properly mitigate the interference in the presence of channel aging effect, [36].

4.1.2. Statistical beamforming (SBF)

We may utilize the CCM to determine the beam weight since the CCM may vary much slowly in the presence of user mobility. The interference channel (4.1) can be modified as [33]

$$\bar{\mathbf{H}}_k^{LT} \equiv \left[\mathbf{U}_1^{(r)}, ..., \mathbf{U}_{k-1}^{(r)}, \mathbf{U}_{k+1}^{(r)}, ..., \mathbf{U}_K^{(r)} \right]^H \tag{4.4}$$

where $\mathbf{U}_k^{(r)}$ is a matrix comprising the eigenvectors of $\mathbf{R}_k$ corresponding to r dominant eigenvalues of $\mathbf{R}_k$. Here, r is a threshold to be determined by the condition $r(K-1) < N_T$ [33].

We may determine the beam weight by [31-33]

$$\mathbf{B}_k = \bar{\mathbf{V}}_k^{LT} \mathbf{U}_k^{LT} \tag{4.5}$$

where $\bar{\mathbf{V}}_k^{LT}$ is a matrix comprising the right singular vectors of $\bar{\mathbf{H}}_k^{LT}$ corresponding to zero singular values and $\mathbf{U}_k^{LT}$ is a matrix comprising the eigenvectors of $\left(\bar{\mathbf{V}}_k^{LT}\right)^H \mathbf{R}_k \bar{\mathbf{V}}_k^{LT}$. The SBF may work better than the CSI-based scheme with the use of outdated CSI [36]. However, when the CSI is unchanged, the CSI-based scheme may work better than the SBF [36].

4.1.3. Joint spatial division and multiplexing (JSDM)

We consider the use of CSI and CCM by means of two-stage beamforming [33-35]. We may determine the beam weight by

$$\mathbf{B}_k = \bar{\mathbf{V}}_k^{LT} \mathbf{V}_k^{ST} \tag{4.6}$$

where $\mathbf{V}_k^{ST}$ is a singular vector matrix of effective channel $\hat{\mathbf{H}}_k \bar{\mathbf{V}}_k^{LT}$. We utilize the CCM for interference suppression and the CSI for coherent beamforming [33]. The proposed scheme may outperform CSI- and CCM-based schemes when the CSI is partially outdated (*i.e.*, in the presence of moderate channel aging effect) [36]. However, it may be less effective than the CSI-based scheme when the CSI is unchanged, and the CCM-based scheme when the CSI is completely outdated [36].

4.2. Proposed scheme

Previous works mainly considered users in limited mobility. In this dissertation, we consider signal transmission to users in various mobility. We analyze the average SLNR in the presence of channel aging effect and determine the beam weight to maximize the average SLNR. We analyze the performance of the proposed scheme in terms of SINR and optimize the transmit power to maximize the SINR by means of iterative water-filling [43]. We determine the beam weight in single cell environments and then in multi-cell environments.

4.2.1. Proposed beam design

We may represent the SINR of the *i*-th stream of user *k* as

$$\gamma_{k,i} = \left(\left[E\left\{ \mathbf{W}_{R,k} \mathbf{T}_k \mathbf{T}_k^H \mathbf{W}_{R,k}^H \right\} + E\left\{ \mathbf{W}_{R,k} \mathbf{n}_k \mathbf{n}_k^H \mathbf{W}_{R,k}^H \right\} \right]_{i,i} \right)^{-1} \tag{4.7}$$

where $\mathbf{T}_k \equiv \sum_{l \neq k} \beta_k \mathbf{H}_k \mathbf{W}_{T,l} \mathbf{s}_l$ denotes the interference power. We may not easily determine $\mathbf{B}_k$ to maximize the sum-rate $\sum_{k,i} \log_2 \left(1+\gamma_{k,i}\right)$ since $\mathbf{B}_k$ and $\mathbf{B}_l$ should jointly be determined. We may alleviate the problem by means of SLNR-based beamforming that minimizes leakage power instead of interference power $\mathbf{T}_k$ [41]. The leakage is defined by the interference generated by a user signal to other users. The beamforming that maximizes the SLNR is equivalent to one that maximizing the MMSE, which is related to the SINR-maximizing beamforming [30, 42]. Beamforming based on the SLNR may provide near-optimal transmission performance in m-MIMO environments [42].

For ease of design, we assume that each stream is equally powered, *i.e.*, $\mathbf{P}_k = \sqrt{P_k}\mathbf{I}_{s_k}$. We may represent the desired signal power of the *i*-th stream of user *k* by ZF reception as [44]

$$\vartheta_{k,i} = \frac{\beta_k^2 P_k}{\left[\left(\mathbf{B}_k^H \mathbf{H}_k^H \mathbf{H}_k \mathbf{B}_k\right)^{-1}\right]_{i,i}}. \tag{4.8}$$

We may represent the SLNR of user *k* as [41]

$$\begin{aligned}
\varphi_k &= \sum_i \vartheta_{k,i} \cdot E\left[N_R K \sigma_n^2 + P_k E\left\{ \left(\sum_{j \neq k} \beta_j \mathbf{H}_j \mathbf{B}_k \mathbf{s}_k \right)^H \sum_{j \neq k} \beta_j \mathbf{H}_j \mathbf{B}_k \mathbf{s}_k \right\} \right]^{-1} \\
&= \sum_i \frac{1}{\left[\left(\beta_k^2 \mathbf{B}_k^H \mathbf{H}_k^H \mathbf{H}_k \mathbf{B}_k\right)^{-1}\right]_{i,i}} \cdot \left[\frac{N_R K \sigma_n^2}{P_k} + \mathrm{tr}\left(\mathbf{B}_k^H \sum_{j \neq k} \beta_j^2 \mathbf{H}_j^H \mathbf{H}_j \mathbf{B}_k \right) \right]^{-1} \\
&= \sum_i \frac{1}{\left[\left(\beta_k^2 \mathbf{B}_k^H \mathbf{H}_k^H \mathbf{H}_k \mathbf{B}_k\right)^{-1}\right]_{i,i}} \cdot \left[\mathrm{tr}\left(\mathbf{B}_k^H \left\{ \frac{N_R K \sigma_n^2}{P_k} \mathbf{I}_{N_T} + \sum_{j \neq k} \beta_j^2 \mathbf{H}_j^H \mathbf{H}_j \right\} \mathbf{B}_k \right) \right]^{-1} \\
&\equiv \sum_i \frac{1}{\left[\mathbf{S}_k\right]_{ii}} \frac{1}{\mathrm{tr}\left(\mathbf{L}_k\right)}
\end{aligned} \tag{4.9}$$

where $\mathbf{S}_k$ and $\mathbf{L}_k$ in the last line are related to the desired signal and the leakage, respectively.

We consider temporal variation of channel in (2.2). We may represent the average of leakage term $\mathbf{L}_k$ as

$$\begin{aligned} E\{\mathbf{L}_k\} &= \mathbf{B}_k^H \left[\frac{N_R K \sigma_n^2}{P_k} \mathbf{I}_{N_T} + E\left\{ \sum_{j \neq k} \cdot \begin{matrix} \beta_j^2 \left(\rho_j \hat{\mathbf{H}}_j^H + \sqrt{1-\rho_j^2}\, \mathbf{Z}_j^H \right) \\ \left(\rho_j \hat{\mathbf{H}}_j + \sqrt{1-\rho_j^2}\, \mathbf{Z}_j \right) \end{matrix} \right\} \right] \mathbf{B}_k \\ &= \mathbf{B}_k^H \left[\frac{N_R K \sigma_n^2}{P_k} \mathbf{I}_{N_T} + \sum_{j \neq k} \beta_j^2 \left\{ \rho_j^2 \hat{\mathbf{H}}_j^H \hat{\mathbf{H}}_j + N_R \left(1-\rho_j^2\right) \mathbf{R}_j \right\} \right] \mathbf{B}_k \\ &= \mathbf{B}_k^H \left(\frac{N_R K \sigma_n^2}{P_k} \mathbf{I}_{N_T} + \mathbf{U}_k \mathbf{D}_k \mathbf{U}_k^H \right) \mathbf{B}_k \end{aligned} \tag{4.10}$$

where $\mathbf{U}_k$ is a matrix comprising eigenvectors of $\sum_{j \neq k} \beta_j^2 \left\{ \rho_j^2 \hat{\mathbf{H}}_j^H \hat{\mathbf{H}}_j + N_R \left(1-\rho_j^2\right) \mathbf{R}_j \right\}$, and $\mathbf{D}_k$ is a diagonal matrix comprising the corresponding eigenvalues. To remove the term of $\left(N_R K \sigma_n^2 / P_k\right) \mathbf{I}_{N_T} + \mathbf{U}_k \mathbf{D}_k \mathbf{U}_k^H$, we may determine $\mathbf{B}_k$ by

$$\mathbf{B}_k = \mathbf{U}_k \left(\frac{N_R K \sigma_n^2}{P_k} \mathbf{I}_{N_T} + \mathbf{D}_k \right)^{-1/2} \mathbf{B}_{k,2} \equiv \mathbf{B}_{k,1} \mathbf{B}_{k,2} \tag{4.11}$$

where $\mathbf{B}_{k,2} \in \mathbb{C}^{N_T \times s_k}$.

We may represent the leakage power as

$$E\{\mathrm{tr}(\mathbf{L}_k)\} = \mathrm{tr}\left(\mathbf{B}_{k,2}^H \mathbf{B}_{k,2}\right). \tag{4.12}$$

Then, (4.9) can be written as

$$\begin{aligned}\sum_i [\mathbf{S}_k]_{ii}^{-1} &= \sum_i \left[\left(\beta_k^2 \mathbf{B}_{k,2}^H \mathbf{B}_{k,1}^H \mathbf{H}_k^H \mathbf{H}_k \mathbf{B}_{k,1} \mathbf{B}_{k,2} \right)^{-1} \right]_{i,i}^{-1} \\ &= \sum_i \left[\begin{Bmatrix} \beta_k^2 \mathbf{B}_{k,2}^H \left(\rho_k \mathbf{M}_k^H + \sqrt{1-\rho_k^2} \tilde{\mathbf{R}}_k^{1/2} \mathbf{Z}_k^H \right) \\ \cdot \left(\rho_k \mathbf{M}_k + \sqrt{1-\rho_k^2} \mathbf{Z}_k \tilde{\mathbf{R}}_k^{1/2} \right) \mathbf{B}_{k,2} \end{Bmatrix}^{-1} \right]_{i,i}^{-1}\end{aligned} \tag{4.13}$$

where $\tilde{\mathbf{R}}_k = \mathbf{B}_{k,1}^H \mathbf{R}_k \mathbf{B}_{k,1}$ and $\mathbf{M}_k = \hat{\mathbf{H}}_k \mathbf{B}_{k,1}$. We may represent $\mathbf{B}_{k,2}$ in a SVD form as

$$\begin{aligned}\mathbf{B}_{k,2} &= \mathbf{U}_B \begin{bmatrix} \mathbf{D}_B & \mathbf{0} \end{bmatrix}^T \mathbf{V}_B^H \\ &\equiv \mathbf{U}_B \bar{\mathbf{D}}_B \mathbf{V}_B^H\end{aligned} \tag{4.14}$$

where $\mathbf{U}_B \in \mathbb{C}^{N_T \times N_T}$ and $\mathbf{V}_B \in \mathbb{C}^{s_k \times s_k}$ are a left and a right unitary matrix, respectively, $\mathbf{D}_B \in \mathbb{C}^{s_k \times s_k}$ is a diagonal matrix comprising the singular values, and the user index is omitted for simplicity of representation. Then, we may represent the desired signal and the leakage as, respectively,

$$\begin{aligned}\sum_i [\mathbf{S}_k]_{ii}^{-1} &= \sum_i \left[\mathbf{V}_B \begin{Bmatrix} \beta_k^2 \bar{\mathbf{D}}_B^H \mathbf{U}_B^H \left(\rho_k \mathbf{M}_k^H + \sqrt{1-\rho_k^2} \tilde{\mathbf{R}}_k^{1/2} \mathbf{Z}_k^H \right) \\ \cdot \left(\rho_k \mathbf{M}_k + \sqrt{1-\rho_k^2} \mathbf{Z}_k \tilde{\mathbf{R}}_k^{1/2} \right) \mathbf{U}_B \bar{\mathbf{D}}_B \end{Bmatrix}^{-1} \mathbf{V}_B^H \right]_{i,i}^{-1} \\ &\equiv \sum_i \left[\mathbf{V}_B \bar{\mathbf{S}}_k^{-1} \mathbf{V}_B^H \right]_{i,i}^{-1},\end{aligned} \tag{4.15}$$

$$\begin{aligned}E\left\{ \mathrm{tr}\left(\mathbf{L}_k \right) \right\} &= \mathrm{tr}\left(\bar{\mathbf{D}}_B^H \bar{\mathbf{D}}_B \right) \\ &= \mathrm{tr}\left(\mathbf{D}_B^2 \right).\end{aligned} \tag{4.16}$$

It may be desirable to optimize $\mathbf{U}_B$, $\mathbf{V}_B$ and $\mathbf{D}_B$ to maximize the average SLNR which can be represented as

$$\hat{\varphi}_k = \frac{E\left\{\sum_i [\mathbf{S}_k]_{i,i}^{-1}\right\}}{E\left\{\mathrm{tr}\left(\mathbf{L}_k\right)\right\}} = \frac{E\left\{\sum_i \left[\mathbf{V}_B \bar{\mathbf{S}}_k^{-1} \mathbf{V}_B^H\right]_{i,i}^{-1}\right\}}{\mathrm{tr}\left(\mathbf{D}_B^2\right)}. \tag{4.17}$$

However, it may be quite difficult to obtain the mean of the numerator in (4.17) since $\bar{\mathbf{S}}_k^{-1}$ is the inverse of a non-central Wishart distributed matrix with N_R degrees of freedom (DoF), where the expectation of the matrix may not exist due to the lack of DoF [45].

Let $\mathbf{U}_B^*$, $\mathbf{V}_B^*$ and $\mathbf{D}_B^*$ be the solution for the maximization of (4.17). We first consider the case when the BS has perfect information on $\mathbf{Z}_k$, which may be unrealistic in high mobility environments. Note that $\mathbf{Z}_k$ represents temporal channel variation due to the channel aging effect. We may represent $\mathbf{V}_B^*$ as

$$\mathbf{V}_B^* = \arg\max_{\mathbf{V}_B} \sum_i \left[\mathbf{V}_B \bar{\mathbf{S}}_k^{-1} \mathbf{V}_B^H\right]_{i,i}^{-1} \tag{4.18}$$

where we do not consider the denominator of SLNR since $\mathbf{V}_B$ is independent of $\mathbf{D}_B$. It can be shown from the positive definiteness of $\bar{\mathbf{S}}_k$ that $\sum_i \left[\mathbf{V}_B \bar{\mathbf{S}}_k^{-1} \mathbf{V}_B^H\right]_{i,i}^{-1} \le \mathrm{tr}\left(\mathbf{D}_S\right)$, where $\mathbf{D}_S$ is a diagonal matrix with diagonal terms equal to eigenvalues of $\bar{\mathbf{S}}_k$. The equality holds when $\mathbf{V}_B^* = \mathbf{U}_S$ which is a matrix comprising eigenvectors of $\bar{\mathbf{S}}_k$ (refer to Appendix).

We may represent the SLNR as

$$\begin{aligned}\varphi_k &= \frac{\mathrm{tr}\left(\mathbf{D}_S\right)}{\mathrm{tr}\left(\mathbf{D}_B^2\right)} = \frac{\mathrm{tr}\left(\bar{\mathbf{S}}_k\right)}{\mathrm{tr}\left(\mathbf{D}_B^2\right)} \\ &= \frac{\mathrm{tr}\left(\bar{\mathbf{D}}_B^H \mathbf{U}_B^H \left\{\beta_k^2 \mathbf{B}_{k,1}^H \mathbf{H}_k^H \mathbf{H}_k \mathbf{B}_{k,1}\right\} \mathbf{U}_B \bar{\mathbf{D}}_B\right)}{\mathrm{tr}\left(\mathbf{D}_B^2\right)}.\end{aligned} \tag{4.19}$$

Let $\tilde{\mathbf{U}}_k$ be a matrix comprising the eigenvectors of $\beta_k^2 \mathbf{B}_{k,1}^H \mathbf{H}_k^H \mathbf{H}_k \mathbf{B}_{k,1}$ and $\tilde{\mathbf{D}}_k$ be a diagonal matrix with diagonal terms equal to the eigenvalues of $\beta_k^2 \mathbf{B}_{k,1}^H \mathbf{H}_k^H \mathbf{H}_k \mathbf{B}_{k,1}$. Setting $\mathbf{U}_B = \tilde{\mathbf{U}}_k \tilde{\mathbf{U}}_B$ to diagonalize the channel terms in the numerator, we may re-write (4.19) as

$$\begin{aligned}\varphi_k &= \frac{\mathrm{tr}\left(\bar{\mathbf{D}}_B^H \tilde{\mathbf{U}}_B^H \tilde{\mathbf{D}}_k \tilde{\mathbf{U}}_B \bar{\mathbf{D}}_B\right)}{\mathrm{tr}\left(\mathbf{D}_B^2\right)} \\ &\equiv \frac{\mathrm{tr}\left(\mathbf{B}_{k,3}^H \tilde{\mathbf{D}}_k \mathbf{B}_{k,3}\right)}{\mathrm{tr}\left(\mathbf{B}_{k,3}^H \mathbf{B}_{k,3}\right)}.\end{aligned} \tag{4.20}$$

Since φ_k is maximized when $\mathbf{B}_{k,3} = \begin{bmatrix}\mathbf{I}_{s_k} & \mathbf{0}\end{bmatrix}^H$ [41], $\mathbf{U}_B^* = \tilde{\mathbf{U}}_k$ and $\mathbf{D}_B^* = \mathbf{I}_{s_k}$ is a solution.

We consider the case when the BS has no information on $\mathbf{Z}_k$, which may be a more practical case in high mobility environments. It may be difficult for the BS to obtain $\mathbf{U}_B^*$, $\mathbf{V}_B^*$ and $\mathbf{D}_B^*$ by the same procedure described in the previous case. The BS can obtain $\mathbf{U}_B^*$ in an average SLNR manner with an assumption that the exact value of $\mathbf{V}_B^*$ is known to the BS in advance (and it can obtain $\mathbf{V}_B^*$ and $\mathbf{D}_B^*$ by the same way). Assuming that the BS can obtain $\mathbf{V}_B^*$ in advance, the average SLNR can be written as

$$\begin{aligned}\hat{\varphi}_k &= \frac{E\left\{\mathrm{tr}\left(\bar{\mathbf{S}}_k\right)\right\}}{\mathrm{tr}\left(\bar{\mathbf{D}}_B^2\right)} \\ &= \frac{\mathrm{tr}\left(\mathbf{D}_B^H \mathbf{U}_B^H \beta_k^2 \left\{\rho_k^2 \mathbf{M}_k^H \mathbf{M}_k + N_R\left(1-\rho_k^2\right)\tilde{\mathbf{R}}_k\right\}\mathbf{U}_B \mathbf{D}_B\right)}{\mathrm{tr}\left(\bar{\mathbf{D}}_B^2\right)}.\end{aligned} \tag{4.21}$$

By the same approach in (4.20), $\hat{\mathbf{U}}_B^* = \bar{\mathbf{U}}_k$ and $\hat{\mathbf{D}}_B^* = \mathbf{I}_{s_k}$ maximizes (4.21) where $\bar{\mathbf{U}}_k$ is a matrix comprising the eigenvectors of $\rho_k^2 \mathbf{M}_k^H \mathbf{M}_k + N_R\left(1-\rho_k^2\right)\tilde{\mathbf{R}}_k$. When $\mathbf{U}_B^*$ is known to the BS in advance, it can be shown from (4.15) that $\bar{\mathbf{S}}_k^{-1}$ is a diagonal matrix. This implies that $\hat{\mathbf{V}}_B^* = \mathbf{I}_{s_k}$ is a solution of (4.18). We determine the beam weight consisting of $\hat{\mathbf{U}}_B^*$, $\hat{\mathbf{V}}_B^*$ and $\hat{\mathbf{D}}_B^*$, which can be represented as

$$\begin{aligned}\mathbf{B}_k &= \mathbf{B}_{k,1}\mathbf{B}_{k,2} \\ &= \mathbf{B}_{k,1}\hat{\mathbf{U}}_B^* \begin{bmatrix}\hat{\mathbf{D}}_B^* & \mathbf{0}\end{bmatrix}^T \hat{\mathbf{V}}_B^* \\ &= \mathbf{U}_k \left(\frac{N_R K \sigma_n^2}{P_k}\mathbf{I}_{N_T} + \mathbf{D}_k\right)^{-1/2} \left[\bar{\mathbf{U}}_k\right]_{:,1:s_k}.\end{aligned} \tag{4.22}$$

4.2.2. Performance analysis

We consider the allocation of transmit power by using an SINR-based method (*e.g.*, a water-filling scheme). To this end, we analyze the SINR of each beam of the proposed scheme in this part. The average interference term in (4.7) can be represented as

$$\begin{aligned}E_{\mathbf{s}}\left\{\mathbf{W}_{R,k}\mathbf{T}_k\mathbf{T}_k^H\mathbf{W}_{R,k}^H\right\} &= \mathbf{W}_{R,k}E_{\mathbf{s}}\left\{\sum_{l\neq k}\beta_k\mathbf{H}_k\mathbf{W}_{T,l}\mathbf{s}_l\left(\sum_{l\neq k}\beta_k\mathbf{H}_k\mathbf{W}_{T,l}\mathbf{s}_l\right)^H\right\}\mathbf{W}_{R,k}^H \\ &= \mathbf{W}_{R,k}\sum_{\substack{l\neq k\\ m\neq k}}\beta_k^2 E_{\mathbf{s}}\left\{\mathbf{H}_k\mathbf{W}_{T,l}\mathbf{s}_l\mathbf{s}_m^H\mathbf{W}_{T,m}^H\mathbf{H}_k^H\right\}\mathbf{W}_{R,k}^H \\ &= \mathbf{W}_{R,k}\sum_{l\neq k}\beta_k^2\left\{\begin{matrix}\left(\rho_k\hat{\mathbf{H}}_k + \sqrt{1-\rho_k^2}\mathbf{Z}_k\right)\mathbf{W}_{T,l}\cdot \\ \mathbf{W}_{T,l}^H\left(\rho_k\hat{\mathbf{H}}_k^H + \sqrt{1-\rho_k^2}\mathbf{Z}_k^H\right)\end{matrix}\right\}\mathbf{W}_{R,k}^H.\end{aligned} \tag{4.23}$$

Since $\mathbf{W}_k$ and $\mathbf{H}_k\mathbf{W}_{T,l}$ are correlated, it is desirable to split $\mathbf{H}_k\mathbf{W}_{T,l}$ into two terms, where the first term comprises $\mathbf{H}_k\mathbf{W}_{T,l}$ to eliminate $\mathbf{W}_{R,k}\left(=\left(\beta_k\mathbf{H}_k\mathbf{W}_{T,k}\right)^{\dagger}\right)$ and the second term is independent to $\mathbf{W}_{R,k}$. We approximate the term $\mathbf{Z}_k\mathbf{W}_{T,l}$ as a sum of two independent random terms, as

$$\beta_k\sqrt{1-\rho_k^2}\mathbf{Z}_k\mathbf{W}_{T,l} \approx_d \beta_k\sqrt{1-\rho_k^2}\mathbf{Z}_k\mathbf{W}_{T,k}\mathbf{\Psi}_{k,l} + \mathbf{X}_{k,l} \tag{4.24}$$

where $\mathbf{\Psi}_{k,l}$ is a constant matrix and $\mathbf{X}_{k,l}$ is a matrix comprising independent normal random row vectors, while satisfying

$$\begin{cases} \mathbf{\Psi}_{k,l} = \left(\mathbf{W}_{T,k}^H\mathbf{R}_k\mathbf{W}_{T,k}\right)^{-1}\mathbf{W}_{T,k}^H\mathbf{R}_k\mathbf{W}_{T,l} \\ E\left\{\mathbf{X}_{k,l}\right\} = \mathbf{0} \\ E\left\{\mathbf{X}_{k,l}^H\mathbf{X}_{k,l}/N_R\right\} = \beta_k^2\left(1-\rho_k^2\right)\left\{\mathbf{W}_{T,l}^H\mathbf{R}_k\mathbf{W}_{T,l} - \mathbf{\Psi}_{k,l}^H\left(\mathbf{W}_{T,k}^H\mathbf{R}_k\mathbf{W}_{T,k}\right)\mathbf{\Psi}_{k,l}\right\} \\ \qquad\qquad \equiv \mathbf{Y}_{k,l} \end{cases}. \tag{4.25}$$

Then it can be shown that

$$\begin{aligned} E_{\mathbf{Z},\mathbf{X}}\left\{\mathbf{W}_{R,k}\mathbf{T}_k\mathbf{T}_k^H\mathbf{W}_{R,k}^H\right\} &= E_{\mathbf{Z},\mathbf{X}}\left\{\mathbf{W}_{R,k}\sum_{l\neq k}\left[\begin{matrix}\left(\beta_k\mathbf{H}_k\mathbf{W}_{T,k}\mathbf{\Psi}_{k,l}+\mathbf{X}_{k,l}+\mathbf{Q}_{k,l}\right)\\ \cdot\left(\beta_k\mathbf{H}_k\mathbf{W}_{T,k}\mathbf{\Psi}_{k,l}+\mathbf{X}_{k,l}+\mathbf{Q}_{k,l}\right)^H\end{matrix}\right]\mathbf{W}_{R,k}^H\right\} \\ &= \sum_{l\neq k}E_{\mathbf{Z},\mathbf{X}}\left\{\begin{matrix}\mathbf{\Psi}_{k,l}\mathbf{\Psi}_{k,l}^H \\ +\mathbf{W}_{R,k}\mathbf{X}_{k,l}\mathbf{X}_{k,l}^H\mathbf{W}_{R,k}^H \\ +\left(\mathbf{\Psi}_{k,l}\mathbf{Q}_{k,l}^H\mathbf{W}_{R,k}^H+\mathbf{W}_{R,k}\mathbf{Q}_{k,l}\mathbf{\Psi}_{k,l}^H\right) \\ +\mathbf{W}_{R,k}\mathbf{Q}_{k,l}\mathbf{Q}_{k,l}^H\mathbf{W}_{R,k}^H\end{matrix}\right\} \\ &\equiv \sum_{l\neq k}\left(\mathbf{\Psi}_{k,l}\mathbf{\Psi}_{k,l}^H+\mathbf{C}_{k,l}^{(1)}+\mathbf{C}_{k,l}^{(2)}+\mathbf{C}_{k,l}^{(3)}\right) \end{aligned} \tag{4.26}$$

where $\mathbf{Q}_{k,l} \equiv \beta_k\rho_k\left(\hat{\mathbf{H}}_k\mathbf{W}_{T,l} - \hat{\mathbf{H}}_k\mathbf{W}_{T,k}\mathbf{\Psi}_{k,l}\right)$. Note that $\mathbf{\Psi}_{k,l}$ and $\mathbf{Q}_{k,l}$ are perfectly known to the BS. Since $\mathbf{X}_{k,l}$ and $\mathbf{Z}_k$ are independent of each other, we can represent $\mathbf{C}_{k,l}^{(1)}$ as

$$\begin{aligned}\mathbf{C}_{k,l}^{(1)} &= E\left\{\mathbf{W}_{R,k}\boldsymbol{\Gamma}_{k,l}\mathbf{W}_{R,k}^{H}\right\} \\ &= \mathrm{tr}\left(\mathbf{Y}_{k,l}\right)E\left\{\mathbf{W}_{R,k}\mathbf{W}_{R,k}^{H}\right\}\end{aligned} \tag{4.27}$$

where

$$\begin{aligned}\boldsymbol{\Gamma}_{k,l} &= E\left\{\mathbf{X}_{k,l}\mathbf{X}_{k,l}^{H}\right\} \\ &= \mathrm{tr}\left(\mathbf{Y}_{k,l}\right)\mathbf{I}.\end{aligned} \tag{4.28}$$

It may be quite difficult to obtain the expectation of $\mathbf{W}_{R,k}\mathbf{W}_{R,k}^{H}$ due to lack of its DoF [45]. We consider asymptotic SINR when $\rho_k \to 0$ and $\rho_k \to 1$. When $\rho_k \to 0$, we may ignore $\mathbf{C}_{k,l}^{(2)}$ and $\mathbf{C}_{k,l}^{(3)}$, and represent the SINR of the *i*-th stream of user *k* as

$$\gamma_{k,i} = \left[\sum_{l\neq k}\left(\boldsymbol{\Psi}_{k,l}\boldsymbol{\Psi}_{k,l}^{H} + \mathbf{C}_{k,l}^{(1)}\right) + \sigma_n^2 E\left\{\mathbf{W}_{R,k}\mathbf{W}_{R,k}^{H}\right\}\right]_{i,i}^{-1}. \tag{4.29}$$

We can represent the *i*-th diagonal element of $\mathbf{W}_{R,k}\mathbf{W}_{R,k}^{H}$ as [48]

$$\begin{aligned}\left[E\left\{\mathbf{W}_{R,k}\mathbf{W}_{R,k}^{H}\right\}\right]_{i,i} &= \left[E\left\{\left(\beta_k^2\mathbf{W}_{T,k}^{H}\mathbf{H}_k^{H}\mathbf{H}_k\mathbf{W}_{T,k}\right)^{-1}\right\}\right]_{i,i} \\ &= E\left\{\frac{\left|\left(\mathbf{G}_k^{(i-)}\right)^{H}\mathbf{G}_k^{(i-)}\right|}{\left|\mathbf{G}_k^{H}\mathbf{G}_k\right|}\right\} \\ &\approx \frac{E\left\{\left|\left(\mathbf{G}_k^{(i-)}\right)^{H}\mathbf{G}_k^{(i-)}\right|\right\}}{E\left\{\left|\mathbf{G}_k^{H}\mathbf{G}_k\right|\right\}}\end{aligned} \tag{4.30}$$

where $\mathbf{G}_k \equiv \beta_k\mathbf{H}_k\mathbf{W}_{T,k}$, and $\mathbf{G}_k^{(i-)}$ denotes $\mathbf{G}_k$ without the *i*-th column. It was shown that [49]

$$E\left\{\left|\mathbf{G}_k^H\mathbf{G}_k\right|\right\} = \left|\bar{\mathbf{R}}_k\right|2^{s_k}\frac{\Gamma_{s_k}\left(\frac{N_R}{2}+1\right)}{\Gamma_{s_k}\left(\frac{N_R}{2}\right)}{}_1F_1\left(-1;\frac{N_R}{2};-\frac{\boldsymbol{\Omega}_k}{2}\right) \equiv \zeta_k \tag{4.31}$$

where $\bar{\mathbf{R}}_k = \beta_k^2\left(1-\rho_k^2\right)\mathbf{W}_{T,k}^H\mathbf{R}_k\mathbf{W}_{T,k}$, $\boldsymbol{\Omega}_k = \bar{\mathbf{R}}_k^{-1}\hat{\mathbf{G}}_k^H\hat{\mathbf{G}}_k$ for $\hat{\mathbf{G}}_k \equiv \beta_k\rho_k\hat{\mathbf{H}}_k\mathbf{W}_{T,k}$, $\Gamma_{s_k}(\cdot)$ denotes the multivariate gamma function, and ${}_1F_1(\cdot)$ denotes the HF. Similarly, it can be shown that

$$E\left\{\left\|\left(\mathbf{G}_k^{(i-)}\right)^H\mathbf{G}_k^{(i-)}\right\|\right\} = \left|\left(1-\rho_k^2\right)\bar{\mathbf{R}}_k^{(i-)}\right|2^{s_k-1}\frac{\Gamma_{s_k-1}\left(\frac{N_R}{2}+1\right)}{\Gamma_{s_k-1}\left(\frac{N_R}{2}\right)}{}_1F_1\left(-1;\frac{N_R}{2};\frac{\boldsymbol{\Omega}_k^{(i-)}}{2}\right) \equiv \zeta_k^{(i-)} \tag{4.32}$$

where $\bar{\mathbf{R}}_k^{(i-)} \equiv \beta_k^2\left(1-\rho_k^2\right)\left(\mathbf{W}_{T,k}^{(i-)}\right)^H\mathbf{R}_k\mathbf{W}_{T,k}^{(i-)}$ and $\boldsymbol{\Omega}_k^{(i-)} \equiv \beta_k^2\rho_k^2\left(\bar{\mathbf{R}}_k^{(i-)}\right)^{-1}\left(\hat{\mathbf{G}}_k^{(i-)}\right)^H\hat{\mathbf{G}}_k^{(i-)}$. We can approximate the SINR as

$$\hat{\gamma}_{k,i}^{(0)} = \left(\sum_{l\neq k}\left\{\left[\boldsymbol{\Psi}_{k,l}\boldsymbol{\Psi}_{k,l}^H\right]_{i,i} + \mathrm{tr}\left(\mathbf{Y}_{k,l}\right)\frac{\zeta_k^{(i-)}}{\zeta_k}\right\} + \sigma_n^2\frac{\zeta_k^{(i-)}}{\zeta_k}\right)^{-1} \tag{4.33}$$

When $\rho_k \to 1$, we can approximate $\mathbf{C}_{k,l}^{(2)}$ and $\mathbf{C}_{k,l}^{(3)}$ as, respectively,

$$\mathbf{C}_{k,l}^{(2)} \approx \boldsymbol{\Psi}_{k,l}\mathbf{Q}_{k,l}^H\left(\hat{\mathbf{G}}_k^{\dagger}\right)^H + \hat{\mathbf{G}}_k^{\dagger}\mathbf{Q}_{k,l}\boldsymbol{\Psi}_{k,l}^H \equiv \hat{\mathbf{C}}_{k,l}^{(2)}, \tag{4.34}$$

$$\mathbf{C}_{k,l}^{(3)} \approx \hat{\mathbf{G}}_k^{\dagger}\mathbf{Q}_{k,l}\mathbf{Q}_{k,l}^H\left(\hat{\mathbf{G}}_k^{\dagger}\right)^{\dagger} \equiv \hat{\mathbf{C}}_{k,l}^{(3)}. \tag{4.35}$$

Table 4-1. Proposed power allocation scheme.

Input: $\hat{\mathbf{H}}_k, \mathbf{R}_k, \rho_k$
Initialization: Obtain $\mathbf{B}_k$ according to (4.22) and initialize $\mathbf{P}_k$
Do: 1. Update $\hat{\gamma}_{k,i}$ according to (4.37) 2. Update $p_{k,i}$ using the water-filling algorithm 3. Normalize $\mathbf{P}_k$ for power constraints 4. Repeat 1~3 N_p times
Output: $\mathbf{P}_k$

It can be shown that $\mathbf{C}_{k,l}^{(1)}$ is the same as that when $\rho_k \to 0$. Thus, we can approximate the SINR as

$$\hat{\gamma}_{k,i}^{(1)} = \left(\sum_{l \neq k} \left\{ \left[\mathbf{A}_{k,l} \right]_{i,i} + \mathrm{tr}\left(\mathbf{Y}_{k,l} \right) \frac{\zeta_k^{(i-)}}{\zeta_k} \right\} + \sigma_n^2 \frac{\zeta_k^{(i-)}}{\zeta_k} \right)^{-1} \tag{4.36}$$

where $\mathbf{A}_{k,l} \equiv \mathbf{\Psi}_{k,l} \mathbf{\Psi}_{k,l}^H + \hat{\mathbf{C}}_{k,l}^{(2)} + \hat{\mathbf{C}}_{k,l}^{(3)}$.

When $0 < \rho_k < 1$, the approximation in (4.30) may not be valid since the numerator and the denominator are not independent of each other. However, simulation results show that $\hat{\gamma}_{k,i}^{(0)}$ and $\hat{\gamma}_{k,i}^{(1)}$ are still show the accurate analysis for $0 < \rho_k < 1$. Considering that $\rho_k = \sqrt{1-\rho_k^2}$ when $\rho_k = 0.5$, we can approximately represent the SINR when $0 \le \rho_k \le 1$ as

$$\hat{\gamma}_{k,i} = \begin{cases} \hat{\gamma}_{k,i}^{(1)}, & \rho_k \geq \sqrt{0.5} \\ \hat{\gamma}_{k,i}^{(0)}, & \rho_k < \sqrt{0.5} \end{cases}. \tag{4.37}$$

The proposed scheme employs an iterative water-filling algorithm [43] with the average SINR estimated by (4.37). The detailed procedure is described in Table 4-1. In the table, $p_{k,i}$ denotes the *i*-th diagonal element of $\mathbf{P}_k$, and N_p denotes the number of iterations for the water-filling.

4.2.3. Extension to multi-cell environments

We extend the proposed beam weight in consideration of coordinated and joint transmission modes [50, 60]. We also extend the SINR analysis in the previous section.

In the coordinated transmission mode, each BS transmits data considering the interference to users served by other adjacent BSs [60]. Let $\mathbf{B}_{b_k,k}^{(1)}$ and $\mathbf{B}_{b_k,k}^{(2)}$ be the outer and inner beam weights for user *k*, transmitted by serving BS b_k. The BS can suppress the intra-cell and inter-cell interference by modifying the beam weight by (4.22) as

$$\mathbf{B}_{b_k,k}^{(1)} = \mathbf{U}_{b_k,k} \left(\frac{N_R K \sigma_n^2}{P_k} \mathbf{I}_{N_T} + \mathbf{D}_{b_k,k} \right)^{-1/2} \tag{4.38}$$

where $\mathbf{U}_{b_k,k}$ is a matrix comprising the eigenvectors of $\sum_{l \neq k} \left\{ \rho_l^2 \hat{\mathbf{H}}_{b_k,l}^H \hat{\mathbf{H}}_{b_k,l} + N_R \left(1 - \rho_l^2\right) \mathbf{R}_{b_k,l} \right\}$, and $\mathbf{D}_{b_k,k}$ is a diagonal matrix with diagonal terms equal to the eigenvalues of $\sum_{l \neq k} \left\{ \rho_l^2 \hat{\mathbf{H}}_{b_k,l}^H \hat{\mathbf{H}}_{b_k,l} + N_R \left(1 - \rho_l^2\right) \mathbf{R}_{b_k,l} \right\}$. $\mathbf{B}_{b_k,k}^{(2)}$ can be determined as same as (4.22).

In the joint transmission mode, the transmission performance may significantly degrade in terms of SINR, because a phase of each received signal from different BS does

not match each other, may resulting destructively combined signal at the user side [50]. We may alleviate the problem by means of QR decomposition-based transmission, where each BS controls a phase of the beam weight to make a coherent combining of the signal at the user side [50]. We modify the inner beam weight by (4.22) in consideration of the phase matching. We should be remined that B_k denotes a set of BSs jointly transmitting data to user k as described in chapter 2. For $b \in B_k$, the QR decomposition of the effective channel, $\bar{\mathbf{H}}_{b,k} \equiv \hat{\mathbf{H}}_{b,k}\mathbf{B}_{b,k}^{(1)}$, is represented as

$$\bar{\mathbf{H}}_{b,k} = \mathbf{L}_{b,k}\mathbf{Q}_{b,k} \tag{4.39}$$

where $\mathbf{L}_{b,k}$ is a lower triangular matrix and $\mathbf{Q}_{b,k}$ is an orthogonal matrix. The phase adjustment matrix is defined as [50]

$$\mathbf{J}_{b,k} = \mathrm{diag}\left(\left[\frac{\left[\mathbf{L}_{b,k}\right]_{1,1}}{\left|\left[\mathbf{L}_{b,k}\right]_{1,1}\right|},...,\frac{\left[\mathbf{L}_{b,k}\right]_{N_T,N_T}}{\left|\left[\mathbf{L}_{b,k}\right]_{N_T,N_T}\right|}\right]\right). \tag{4.40}$$

Then, we may determine the phase-matched beam weight as

$$\mathbf{B}_{b,k}^{(2)} = \mathbf{Q}_{b,k}\mathbf{J}_{b,k}\left[\mathbf{U}_{b,k}^{QR}\right]_{:,1:s_k} \tag{4.41}$$

where $\mathbf{U}_{b,k}^{QR}$ is a right unitary matrix of SVD of $\sum_{b\in B_k}\mathbf{L}_{b,k}\mathbf{J}_{b,k}$. Note that we exploit only CSI to design the inner beam weight by (4.41), since the CCM does not contain any information about a phase of signal [50].

We now analyze the SINR of the proposed scheme in multi-cell environments. The interference term in (4.7) can be rewritten as

$$
\begin{aligned}
E_{\mathbf{s}}\left\{\mathbf{W}_{R,k}\mathbf{T}_k\mathbf{T}_k^H\mathbf{W}_{R,k}^H\right\} &= \mathbf{W}_{R,k}\sum_{\substack{l\neq k,\\ m\neq k}}\left(\sum_{b\in B_l}\beta_{b,k}\mathbf{H}_{b,k}\mathbf{W}_{T,b,l}E_{\mathbf{s}}\left\{\mathbf{s}_l\mathbf{s}_m^H\right\}\sum_{b\in B_m}\beta_{b,k}\mathbf{W}_{b,m}^H\mathbf{H}_{b,k}^H\right)\mathbf{W}_{R,k}^H \\
&= \mathbf{W}_{R,k}\sum_{\substack{l\neq k,\\ m\neq k}}\left(\sum_{b\in B_l}\beta_{b,k}\mathbf{H}_{b,k}\mathbf{W}_{T,b,l}\sum_{b\in B_l}\beta_{b,k}\mathbf{W}_{b,l}^H\mathbf{H}_{b,k}^H\right)\mathbf{W}_{R,k}^H.
\end{aligned}
\tag{4.42}
$$

By the same approach in (4.24), we approximate $\sum_{b\in B_l}\beta_{b,k}\sqrt{1-\rho_k^2}\mathbf{Z}_{b,k}\mathbf{W}_{T,b,l}$ as

$$
\sum_{b\in B_l}\beta_{b,k}\sqrt{1-\rho_k^2}\mathbf{Z}_{b,k}\mathbf{W}_{T,b,l} \approx_d \sum_{b\in B_k}\beta_{b,k}\sqrt{1-\rho_k^2}\mathbf{Z}_{b,k}\mathbf{W}_{T,b,k}\boldsymbol{\Psi}_{k,l}+\mathbf{X}_{k,l} \tag{4.43}
$$

where $\boldsymbol{\Psi}_{k,l}$ and $\mathbf{X}_{k,l}$ are satisfying

$$
\begin{cases}
\boldsymbol{\Psi}_{k,l} = \left(\sum_{b\in B_k}\beta_{b,k}^2\mathbf{W}_{T,b,k}^H\mathbf{R}_{b,k}\mathbf{W}_{T,b,k}\right)^{-1}\sum_{b\in B_k}\beta_{b,k}^2\mathbf{W}_{T,b,k}^H\mathbf{R}_{b,k}\mathbf{W}_{T,b,l} \\
E\left\{\mathbf{X}_{k,l}\right\} = \mathbf{0} \\
E\left\{\dfrac{\mathbf{X}_{k,l}^H\mathbf{X}_{k,l}}{N_R}\right\} = \left(1-\rho_k^2\right)\left(\sum_{b\in B_l}\beta_{b,k}^2\mathbf{W}_{T,b,l}^H\mathbf{R}_{b,k}\mathbf{W}_{T,b,l}-\boldsymbol{\Psi}_{k,l}^H\sum_{b\in B_k}\beta_{b,k}^2\mathbf{W}_{T,b,k}^H\mathbf{R}_{b,k}\mathbf{W}_{T,b,k}\boldsymbol{\Psi}_{k,l}\right) \\
\qquad\qquad \equiv \mathbf{Y}_{k,l}
\end{cases}. \tag{4.44}
$$

Then we can represent the interference as

$$
\begin{aligned}
E_{\mathbf{Z},\mathbf{X}}\left\{\mathbf{W}_{R,k}\mathbf{T}_k\mathbf{T}_k^H\mathbf{W}_{R,k}^H\right\} &= \sum_{l\neq k}\left\{\begin{array}{c}\boldsymbol{\Psi}_{k,l}\boldsymbol{\Psi}_{k,l}^H \\ +\mathbf{W}_{R,k}E_{\mathbf{X}}\left\{\mathbf{X}_{k,l}\mathbf{X}_{k,l}^H\right\}\mathbf{W}_{R,k}^H \\ +\left(\boldsymbol{\Psi}_{k,l}\mathbf{Q}_{k,l}^H\mathbf{W}_{R,k}^H+\mathbf{W}_{R,k}\mathbf{Q}_{k,l}\boldsymbol{\Psi}_{k,l}\right) \\ +\mathbf{W}_{R,k}\mathbf{Q}_{k,l}\mathbf{Q}_{k,l}^H\mathbf{W}_{R,k}^H\end{array}\right\}. \\
&\equiv \sum_{l\neq k}\left(\boldsymbol{\Psi}_{k,l}\boldsymbol{\Psi}_{k,l}^H+\mathbf{C}_{k,l}^{(1)}+\mathbf{C}_{k,l}^{(2)}+\mathbf{C}_{k,l}^{(3)}\right)
\end{aligned}
\tag{4.45}
$$

where $\mathbf{Q}_{k,l} \equiv \rho_k \left(\sum_{b \in B_l} \beta_{b,k} \hat{\mathbf{H}}_{b,k} \mathbf{W}_{T,b,l} - \sum_{b \in B_k} \beta_{b,k} \hat{\mathbf{H}}_{b,k} \mathbf{W}_{T,b,k} \mathbf{\Psi}_{k,l} \right)$. The result in (4.45) has the same form with (4.26). By the same procedure in the previous section, we can approximate the SINR into the same form with (4.37).

4.2.4. Computational complexity

We consider computational complexity of the proposed scheme which can be represented by the required number of arithmetic operations [51]. For example, the matrix multiplication for square matrices comprising n columns require n^3 scalar multiplications and $n^3 - n^2$ scalar additions. In this case, we represent the computational complexity as $O\left(n^3\right)$ [51].

For the beam weight generation by (4.22), the eigen-decomposition may require computational complexity of $O\left(N_T^3\right)$. This complexity is similar to that of the CSI-based scheme [30]. The only difference comes from the linear combination of CSI and CCM, which may require computational complexity of $O\left(N_T^2\right)$ for each addition.

In the power allocation procedure, the BS repeatedly calculates $\hat{\gamma}_{k,i}^{(1)}$ and the number of beams for each user is $s_k = N_R$ in the worst case. The initialization of SINR has computational complexity of $O\left(N_T N_R^2\right)$. The estimation of $\hat{\gamma}_{k,i}^{(1)}$ may require computational complexity of $O\left(N_T^2 N_R\right)$ without computation of the HF. The calculation of HF requires computational complexity of $O\left(P_{N_h N_R}^2 N_R\right)$, where $P_{N_h N_R}^2 \sim O\left(e^{2\pi\sqrt{2N_h/3}}\right)$ and N_h is the number of iterations in the HF [52]. When N_h is large, the computational complexity of the HF may be much expensive since the computational complexity is sub-exponential in N_h. In each update step, the BS updates power matrices (*i.e.*, $\mathbf{P}_k$) only

and there is no need to calculate the beam weight and the HF repeatedly. The procedure has computational complexity of $O\left(N_R^2\right)$ in each iteration, which is relatively small.

Table 4-2. Evaluation parameters.

Parameters	Values
CCM model	3-D ray-based model [22]
AS	Moderate mode [22]
Carrier frequency $\left(=1/\lambda\right)$	2.3 GHz
BS antenna distance	$\lambda/2$
Macro cell radius	200 m
Number of BS antennas $\left(N_T\right)$	64
Number of BS antennas $\left(N_R\right)$	4 (if not specified)
Number of users $\left(K\right)$	4
Number of iterations for power allocation $\left(N_p\right)$	3
Number of iterations in the approximated HF $\left(N_h\right)$	20 [52]

4.3. Performance evaluation

We evaluate the performance of the proposed scheme by computer simulation. Since the proposed scheme in a single cell scenario is a special case of the coordinated transmission mode, we verify the performance in multi-cell environments only. We consider two adjacent macro cells where each BS is equipped with antennas in a 2-D square ULA, and the spatial channel correlation follows the NLOS ray-based model in moderate AS environments [22]. The main simulation parameters are summarized in Table 4-2.

We compare the proposed scheme with the generalized two-stage beamforming [30], the JSDM [33], and the SBF [31], referred to "GTSBF," "JSDM," and "SBF" respectively. For fair comparison, we apply the power allocation described in Table 4-1 to the conventional schemes.

We first verify the performance analysis of the proposed scheme according to temporal channel correlation in fixed SNR environments. Fig. 4-1 depicts the spectral efficiency of the proposed scheme and the analysis results in coordinated and joint transmission modes. It can be seen that the analysis matches quite well with the simulation result in various environments. There exists a slight gap between them when ρ_k is near $\sqrt{0.5} \approx 0.7$, which comes from the approximation in (4.37). It can also be seen that the performance of the joint transmission decreases faster than that of the coordinated one when ρ_k is small. This is because we exploit the CSI to design the inner beam weight by (4.41) considering the phase matching problem. When ρ_k is large, it can be seen that the joint transmission works better than the coordinated one.

Fig. 4-2 depicts the spectral efficiency according to the temporal channel correlation, where the SNR is set to 20 dB. In the case of the coordinated transmission, it can be seen that the proposed scheme outperforms the other schemes. When $\rho_k \to 1$, the GTSBF seems to be very effective because it can fully take advantage of high coherent beamforming gain from accurate CSI. When $\rho_k \to 0$, the SBF outperforms the GTSBF since it does not utilize the outdated CSI. Although the JSDM utilizes both of CSI and CCM, the scheme does not design a beam weight in consideration of user mobility. As a result, the JSDM provides poor performance when $\rho_k \to 0$ and $\rho_k \to 1$. In the case of joint transmission, it can be seen that the proposed scheme outperforms the other schemes except when $\rho_k \to 0$.

Fig. 4-3 depicts the spectral efficiency according to N_R, where $\rho_k = 0.7$ for all the users. It can be seen that the proposed scheme outperforms the other schemes. The GTSBF provides poor performance when N_R is small, but provides much improved performance when N_R is large. This is because the GTSBF can generate orthogonal beams most effectively exploiting diversity of CSI, whereas the other schemes exploiting CCM may have limited number of orthogonal beams when users are located nearby each other [31]. Also, since users obtain the CSI using DM-RS transmitted from the BSs, the channel aging effect may be alleviated more effectively by the ZF receiver when N_R is large.

We verify the performance of the schemes in more practical environments, where users have various mobility conditions. We assume that each user is moving at a speed of uniformly randomly distributed in a range of (0, 60) km/h, and the delay between the channel estimation and the signal transmission is 5 ms [53]. Users are uniformly

randomly distributed in an edge area of the macro cells where the minimum distance between a user and a serving BS is set to half of the macro cell radius [60]. We verify the performance according to the edge SNR, which is defined as the received SNR of a user located at the macro cell radius [54]. Fig. 4-4 depicts spectral efficiency according to the edge SNR. It can be seen that the proposed scheme outperforms the other schemes in every edge SNR level. It can also be seen that the GTSBF provides poor performance even when the edge SNR is high, suffering from the channel aging effect. The SBF provides the worst performance since the scheme does not utilize the CSI even when users are moving at low speeds.

Fig. 4-5 depicts empirical cumulative density function (CDF) of spectral efficiency of each user. We consider two SNR environments for each transmission mode where the edge SNR is set to 0 dB, and the SNR of every user is fixed to 20 dB. It can be seen that the proposed scheme improves overall spectral efficiency of users regardless of mobility. It can also be seen that the spectral efficiency of the GTSBF is most widely distributed, especially when the SNR is fixed. This means that some portion of users in low mobility may benefit from the coherent beamforming, but other users in high mobility may suffer from the interference in the presence of channel aging effect. It can also be seen that both of the JSDM and the SBF have lower peak of spectral efficiency than the proposed scheme and the GTSBF, which comes from the loss of coherent beamforming gain.

We also consider an environment where each user is moving at a speed of uniformly randomly distributed in a range of (0, 120) km/h. Fig. 4-6 and Fig. 4-7 depict spectral efficiency and empirical CDF of spectral efficiency, respectively. It can be seen that the proposed scheme outperforms the other schemes in a wide range of the edge SNR. It can

also be seen that the performance of the GTSBF significantly degrades in comparison with the previous result, due to large channel aging effect. In the case of the coordinated transmission, the SBF is quite effective among the conventional schemes considering that the scheme does not require the acquisition of CSI. However, there exist a large performance gap between the proposed scheme and the SBF which comes from the adaptive utilization of CSI and CCM in consideration of user mobility.

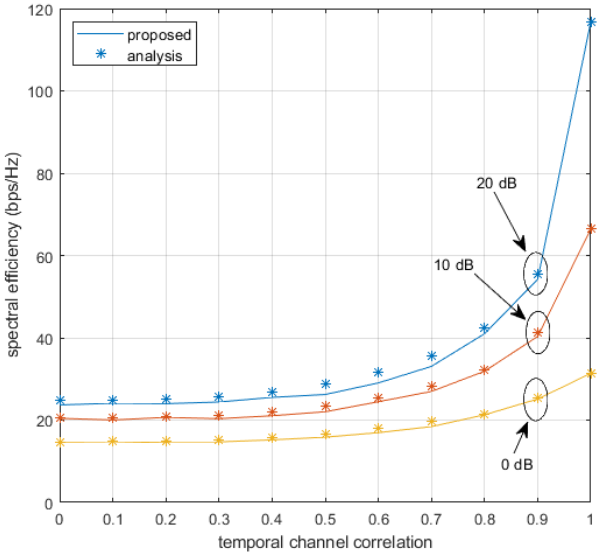

(a) Coordinated transmission mode.

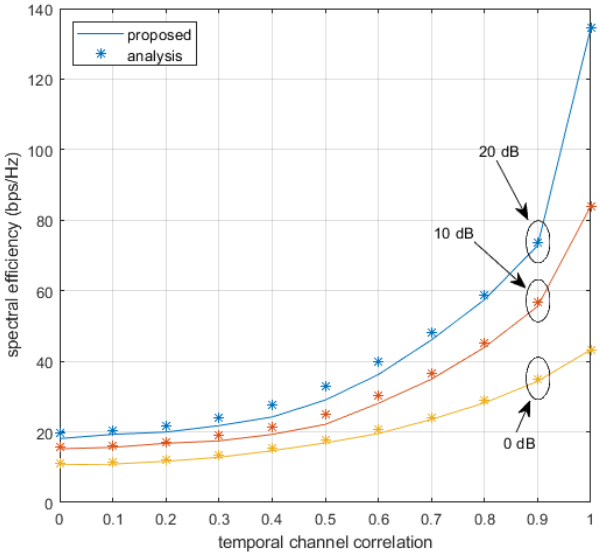

(b) Joint transmission mode.

Fig. 4-1. Performance analysis of the proposed scheme.

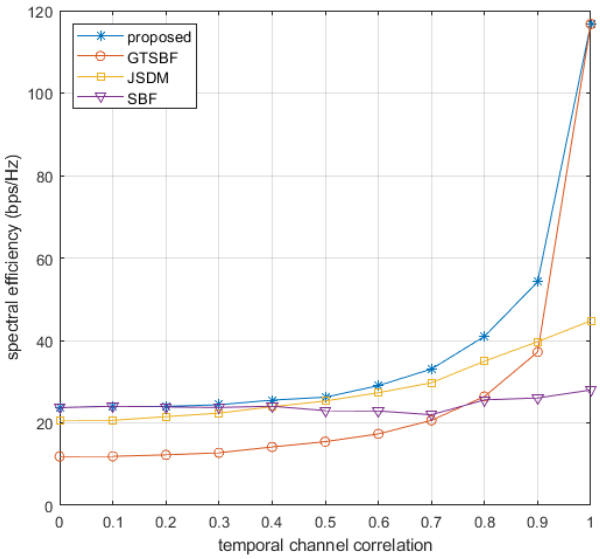

(a) Coordinated transmission mode.

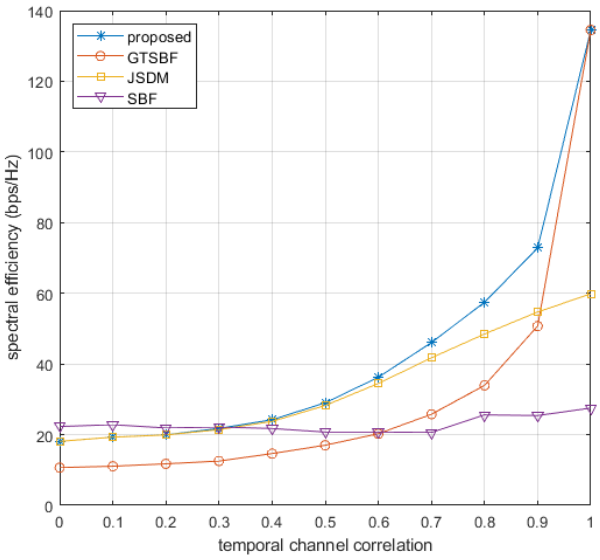

(b) Joint transmission mode.

Fig. 4-2. Spectral efficiency according to temporal channel correlation.

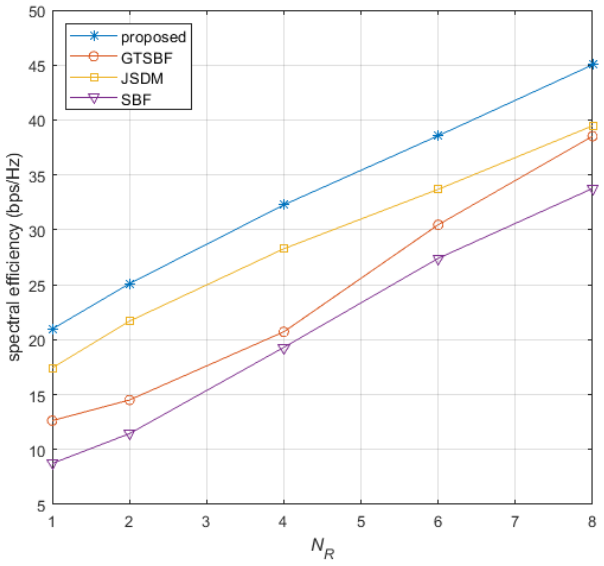

(a) Coordinated transmission mode.

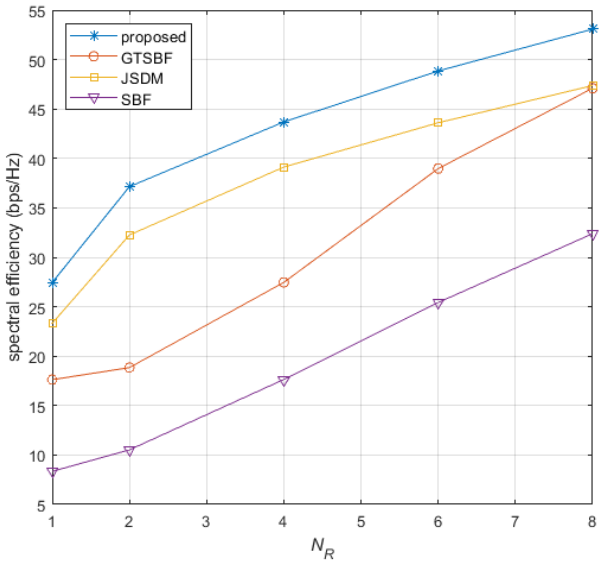

(b) Joint transmission mode.

Fig. 4-3. Spectral efficiency according to the number of user antennas.

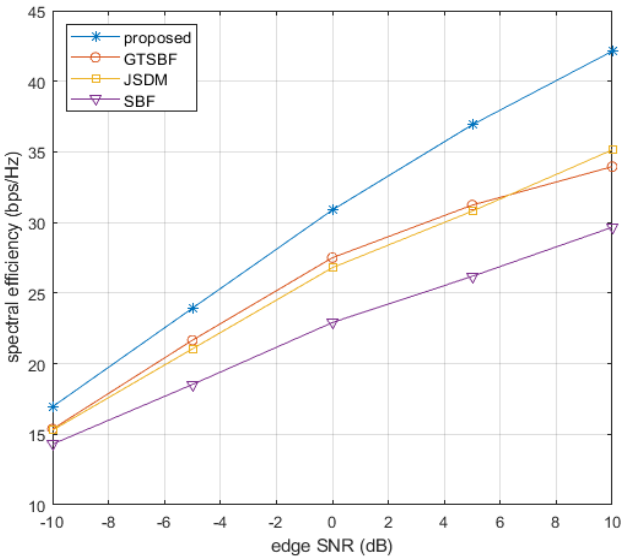

(a) Coordinated transmission mode.

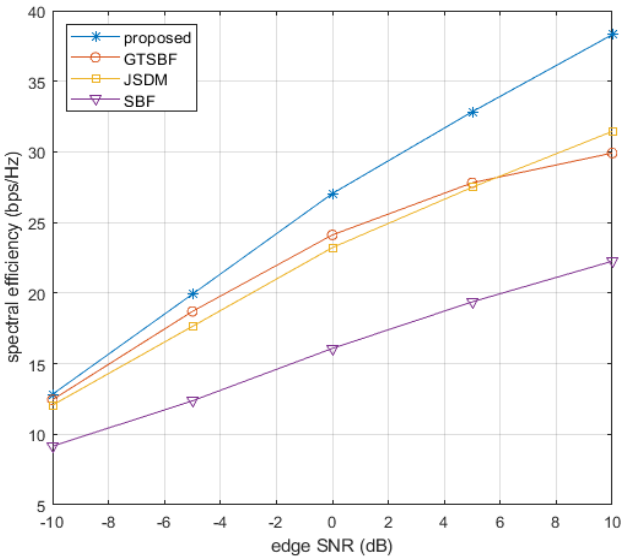

(b) Joint transmission mode.

Fig. 4-4. Spectral efficiency in mobility of (0, 60) km/h.

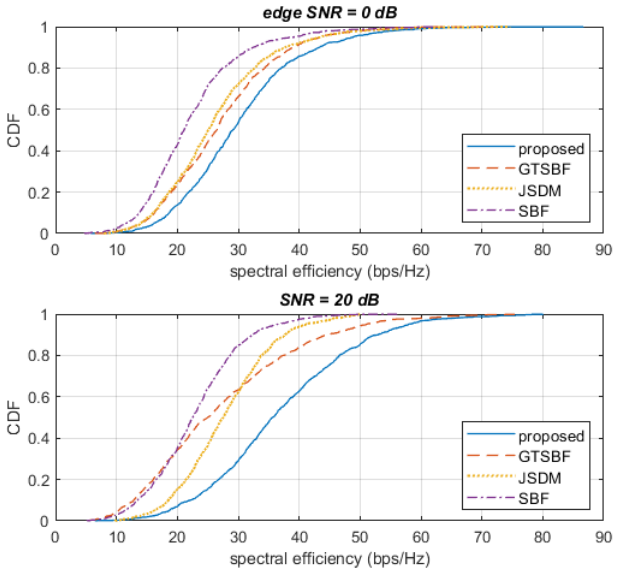

(a) Coordinated transmission mode.

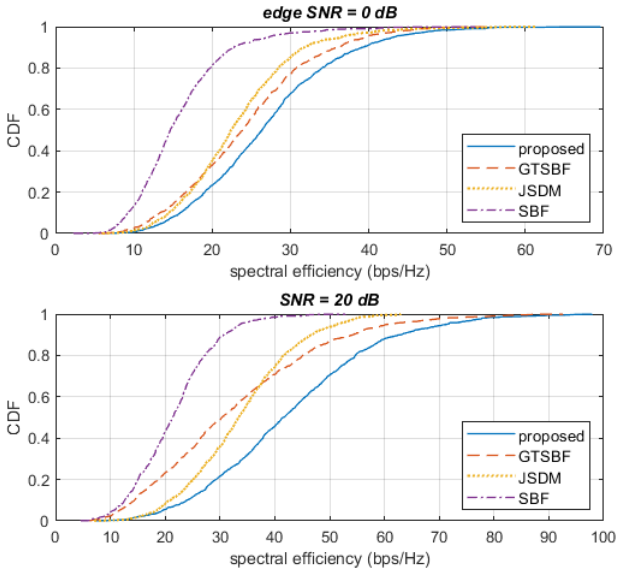

(b) Joint transmission mode.

Fig. 4-5. Empirical CDF of spectral efficiency in mobility of (0, 60) km/h.

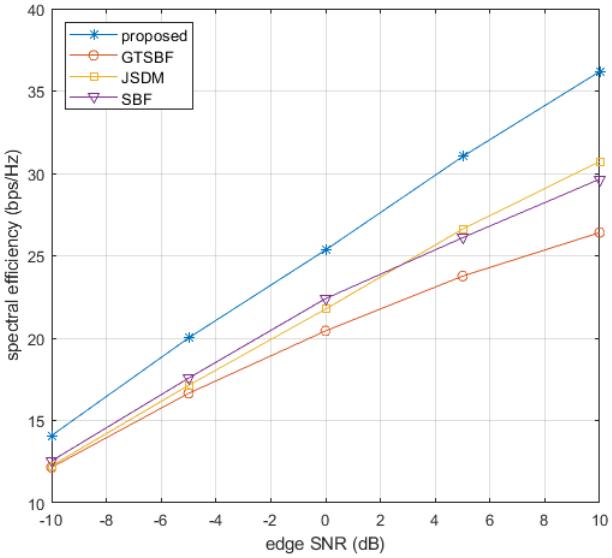

(a) Coordinated transmission mode.

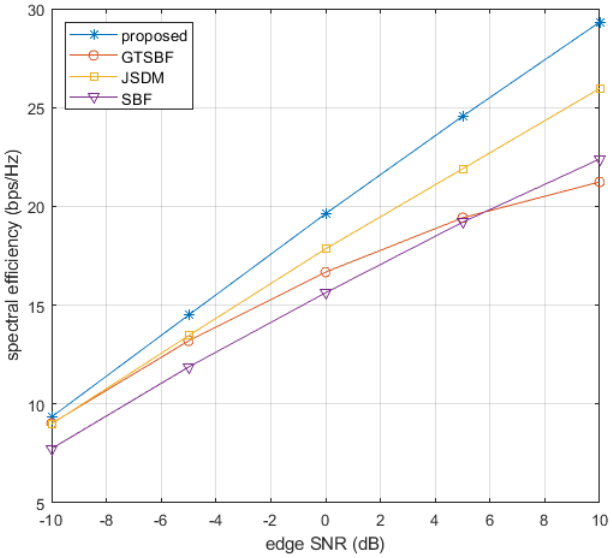

(b) Joint transmission mode.

Fig. 4-6. Spectral efficiency in mobility of (0, 120) km/h.

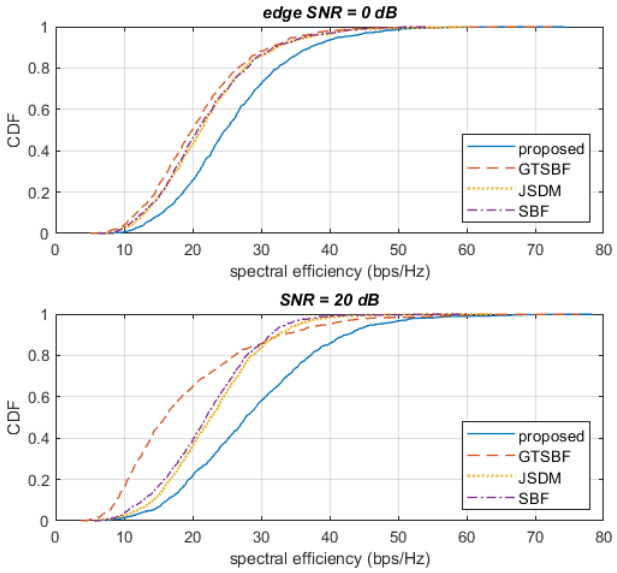

(a) Coordinated transmission mode.

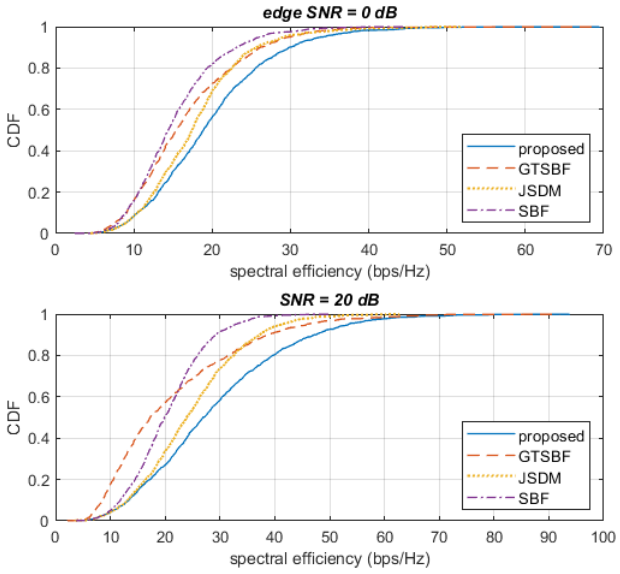

(b) Joint transmission mode.

Fig. 4-7. Empirical CDF of spectral efficiency in mobility of (0, 120) km/h.

Chapter 5

Mobility-aware resource allocation in m-MIMO systems

In this chapter, we consider mobility-aware resource allocation in m-MIMO environments. We design a sub-optimal greedy algorithm that allocates the transmission resources to maximize achievable sum-rate in the presence of channel aging effect. We may estimate the sum-rate from the beam weight and the HF, which may require high computation complexity in m-MIMO environments. To reduce the complexity, we determine the beam weight in the dominant eigen-direction of CCM and approximate the HF as a function of temporal channel correlation. Since we may estimate the approximated sum-rate by exploiting spatial and temporal channel correlation, we may need to update the resource allocation only when the change of CCM or temporal channel correlation of any user is large enough to affect the sum-rate.

5.1. Sum-rate-based greedy algorithm

For ease of description, we consider a transmission frame structure in the time-division duplex system as illustrated in Fig. 5-1. We assume that the transmission frame comprises N_{SF} downlink subframes, where we may estimate the CSI during the uplink period. We assume that the CCM does not change during a single frame interval as described in chapter 2, where the subframe refers to the minimum size of transmission resource to be allocated to users.

Let $\hat{\gamma}_{k,i}[t,n]$ be the approximated SINR of user k at the n-th subframe of the t-th frame. We may represent the achievable sum-rate of user k as

$$\hat{C}_k[t,n] = \sum_i \log_2\left(1+\hat{\gamma}_{k,i}[t,n]\right). \tag{5.1}$$

It may be desirable to allocate transmission resource to users so as to maximize the achievable sum-rate by (5.1). We may allocate transmission resource to users as [55-58]

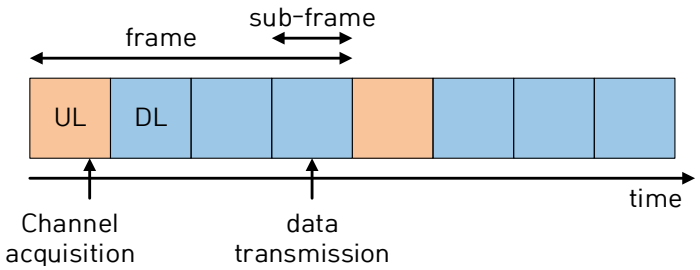

Fig. 5-1. Transmission frame structure.

Table 5-1. Greedy resource allocation at current frame *t*.

Input: $\hat{\mathbf{H}}_{b,k}[t], \mathbf{R}_{b,k}[t], \rho_k[t,n]$

Initialization: $S[t,n]=\varnothing, S_{rem}[t,n]=\{1,2,...,K\}$

In every subframe do:

1. For $k \in S_{rem}[t,n]$, compute $\hat{C}_{S[t,n]\cup\{k\}}[t,n]$
2. If $\hat{C}_{S[t,n]}[t,n] < \hat{C}_{S[t,n]\cup\{k^*\}}[t,n]$ where $k^* = \arg\max_k \hat{C}_{S[t,n]\cup\{k^*\}}[t,n]$, $S[t,n] = S[t,n]\cup\{k^*\}$, $S_{rem}[t,n] = S_{rem}[t,n]\setminus\{k^*\}$
3. Repeat 1~2 until $\hat{C}_{S[t,n]}[t,n] \geq \hat{C}_{S[t,n]\cup\{k^*\}}[t,n]$ or $S_{rem}[t,n]=\varnothing$

Output: $S[t,n]$

$$\begin{aligned} S^*[t,n] &= \arg\max_{S[t,n]} \sum_{k\in S[t,n]} \hat{C}_k[t,n] \\ &\equiv \arg\max_{S[t,n]} \hat{C}_{S[t,n]}[t,n] \end{aligned} \tag{5.2}$$

where $S[t,n]$ is a set of scheduled users to the *n*-th subframe of the *t*-th frame. We may treat (5.2) as a user scheduling problem for given resource [55]. We may obtain the optimal solution $S^*[t,n]$ by means of exhaustive searching which may require unaffordable computational complexity [55].

We may employ a sub-optimal greedy algorithm to reduce the complexity, which searches a set of users in an iterative manner as summarized in Table 5-1 [58]. We select a user that mostly increases the achievable sum-rate at each iteration. However, it may still require high computational complexity to estimate the sum-rate for all candidate user sets, involving complex matrix operations (*e.g.*, the eigen-decomposition of CSI) for the

generation of beam weight by (4.22). The computational complexity may become even higher in the presence of channel aging effect, as described in the previous chapter.

5.2. Proposed scheme

We consider the resource allocation with reduced computational complexity in this chapter. We avoid the calculation of beam weight and HF by approximating the achievable sum-rate in the presence of channel aging effect. We consider the update of resource allocation in a long-term basis. We may update the resource allocation only when the change of CCM or temporal channel correlation is large enough to affect the sum-rate. We only newly allocate resource to users affected by the change of CCM or temporal channel correlation.

5.2.1. Simplification of the beam weight

We simplify the SINR analysis in (4.37) by approximating CSI-dependent terms in (4.22) as CCM-dependent terms [32]. In this case, $\mathbf{U}_{b,k}$ and $\mathbf{D}_{b,k}$ in (4.22) are replaced by the eigenvectors and the eigenvalues of $\sum_{l \neq k} N_R \mathbf{R}_{b,l}$, and $\tilde{\mathbf{U}}_{b,k}$ is replaced by eigenvectors of $N_R \tilde{\mathbf{R}}_{b,k}$. For simplicity of representation, we omit the indices of frames and subframes. Although we may determine the beam weight without CSI, we may still need to handle the multiplication of matrices of a large size (*e.g.*, approximated beam weight and CCM).

In 2-D ULA environments, we may represent $\mathbf{R}_{b,k}$ as a Kronecker product of two CCMs in the azimuth and the elevation direction of the antenna array, as [22]

$$\mathbf{R}_{b,k} \approx \mathbf{R}_{az,b,k} \otimes \mathbf{R}_{el,b,k} \tag{5.3}$$

where $\mathbf{R}_{az,b,k} \in \mathbb{C}^{N_{az} \times N_{az}}$ and $\mathbf{R}_{el,b,k} \in \mathbb{C}^{N_{el} \times N_{el}}$ are CCMs in the azimuth and the elevation direction, respectively. We may approximate the eigenvectors of CCM as a discrete Fourier transform (DFT) matrix in m-MIMO environments [32]. In this case, the eigenvectors of CCM are not dependent of users (*i.e.*, the eigenvectors of CCM are identical for every user). We can obtain a similar result by employing AJD algorithm to get a common unitary matrix that diagonalizes $\mathbf{R}_{az,b,k}$ (or $\mathbf{R}_{el,b,k}$) for every user even when N_{az} and N_{el} are not sufficiently large [46]. We may approximate the CCM as

$$\begin{cases} \mathbf{R}_{az,b,k} \approx \mathbf{F}_{az,b} \hat{\mathbf{\Lambda}}_{az,b,k} \mathbf{F}_{az,b}^{H} \\ \mathbf{R}_{el,b,k} \approx \mathbf{F}_{el,b} \hat{\mathbf{\Lambda}}_{el,b,k} \mathbf{F}_{el,b}^{H} \\ \mathbf{R}_{b,k} \approx \mathbf{F}_{b} \hat{\mathbf{\Lambda}}_{b,k} \mathbf{F}_{b}^{H} \end{cases} \tag{5.4}$$

where $\mathbf{F}_{az,b}$, $\mathbf{F}_{el,b}$ and $\mathbf{F}_b = \mathbf{F}_{az,b} \otimes \mathbf{F}_{el,b}$ are the approximated eigenvectors of $\mathbf{R}_{az,k}$, $\mathbf{R}_{el,k}$ and $\mathbf{R}_k$, respectively, and $\hat{\mathbf{\Lambda}}_{az,b,k}$, $\hat{\mathbf{\Lambda}}_{el,b,k}$ and $\hat{\mathbf{\Lambda}}_{b,k}$ are diagonal matrices comprising the corresponding eigenvalues of $\mathbf{R}_{az,k}$, $\mathbf{R}_{el,k}$ and $\mathbf{R}_k$, respectively.

We may approximate the beam weight by (4.22) as

$$\begin{aligned} \mathbf{W}_{T,b,k} &= \alpha_{b,k} \mathbf{B}_{b,k}^{(1)} \mathbf{B}_{b,k}^{(2)} \mathbf{P}_{b,k} \\ &= \alpha_{b,k} \mathbf{F}_b \left(\frac{N_R K \sigma_n^2}{P_k} \mathbf{I}_{N_T} + N_R \sum_{l \neq k} \beta_{b,l}^2 \hat{\mathbf{\Lambda}}_{b,l} \right)^{-1/2} \mathbf{E}_{b,k} \mathbf{P}_{b,k} \\ &\equiv \alpha_{b,k} \mathbf{F}_b \tilde{\mathbf{\Lambda}}_{b,k}^{-1/2} \mathbf{E}_{b,k} \mathbf{P}_{b,k} \end{aligned} \tag{5.5}$$

where $\alpha_{b,k}$ is a normalization factor for the power allocation [30], and $\mathbf{E}_{b,k}$ is a matrix comprising eigenvectors of $\tilde{\mathbf{R}}_{b,k} \equiv \hat{\mathbf{\Lambda}}_{b,k} \tilde{\mathbf{\Lambda}}_{b,k}^{-1}$ corresponding to s_k number of highest eigenvalues of $\tilde{\mathbf{R}}_{b,k}$.

For simplicity of analysis, we assume that no power allocation and $s_k = N_R$ which is quite reasonable when $N_T \gg N_R$ [30]. It can be seen that $\mathbf{P}_{b,k}$ is an identity matrix and the normalization factor can be represented as [30]

$$\alpha_{b,k} = P_T \left\{ K_b \mathrm{tr}\left(\mathbf{E}_{b,k}^H \tilde{\mathbf{\Lambda}}_{b,k}^{-1} \mathbf{E}_{b,k} \right) \right\}^{-1} \tag{5.6}$$

where K_b is the number of users to which BS *b* transmits data. We assume that diagonal values of $\tilde{\mathbf{R}}_{b,k}$ are arranged in a descending order. From (4.44), we may approximate $\mathbf{\Psi}_{k,l}$ as

$$\begin{aligned}
\mathbf{\Psi}_{k,l} &= \left(\sum_{b \in B_k} \mathbf{W}_{T,b,k}^H \mathbf{R}_{b,k} \mathbf{W}_{T,b,k} \right)^{-1} \sum_{b \in B_k} \mathbf{W}_{T,b,k}^H \mathbf{R}_{b,k} \mathbf{W}_{T,b,l} \\
&\approx \left(\sum_{b \in B_k} \alpha_{b,k}^2 \mathbf{E}_{b,k}^H \tilde{\mathbf{\Lambda}}_{b,k}^{-1/2} \hat{\mathbf{\Lambda}}_{b,k} \tilde{\mathbf{\Lambda}}_{b,k}^{-1/2} \mathbf{E}_{b,k} \right)^{-1} \sum_{b \in B_k} \alpha_{b,k} \alpha_{b,l} \mathbf{E}_{b,k}^H \tilde{\mathbf{\Lambda}}_{b,k}^{-1/2} \hat{\mathbf{\Lambda}}_{b,k} \tilde{\mathbf{\Lambda}}_{b,l}^{-1/2} \mathbf{E}_{b,l} \\
&\equiv \left(\sum_{b \in B_k} \alpha_{b,k}^2 \mathbf{\Delta}_{b,k,k}^{(k)} \right)^{-1} \sum_{b \in B_k} \alpha_{b,k} \alpha_{b,l} \mathbf{\Delta}_{b,k,l}^{(k)} \\
&\equiv \hat{\mathbf{\Psi}}_{k,l}
\end{aligned} \tag{5.7}$$

where $\mathbf{\Delta}_{b,k,l}^{(k)}$ is a diagonal matrix whose *i*-th elements are non-zero only when the *i*-th column vectors of $\mathbf{E}_{b,k}$ and $\mathbf{E}_{b,l}$ are identical. We may approximate $\mathbf{Y}_{k,l}$ as

$$\begin{aligned}
\mathbf{Y}_{k,l} &= \left(1 - \rho_k^2\right) \left\{ \sum_{b \in B_l} \mathbf{W}_{T,b,l}^H \mathbf{R}_{b,k} \mathbf{W}_{T,b,l} - \mathbf{\Psi}_{k,l}^H \left(\sum_{c \in B_k} \mathbf{W}_{T,c,k}^H \mathbf{R}_{c,k} \mathbf{W}_{T,c,k} \right) \mathbf{\Psi}_{k,l} \right\} \\
&\approx \left(1 - \rho_k^2\right) \left\{ \sum_{b \in B_l} \alpha_{b,l}^2 \mathbf{\Delta}_{b,l,l}^{(k)} - \hat{\mathbf{\Psi}}_{k,l}^H \left(\sum_{c \in B_k} \alpha_{c,k}^2 \mathbf{\Delta}_{c,k,k}^{(k)} \right) \hat{\mathbf{\Psi}}_{k,l} \right\} \\
&\equiv \hat{\mathbf{Y}}_{k,l}
\end{aligned} \tag{5.8}$$

where $\hat{\mathbf{\Psi}}_{k,l}$ and $\hat{\mathbf{Y}}_{k,l}$ are diagonal matrices, and can be obtained by multiplication of diagonal matrices with reduced computational complexity.

5.2.2. Quantization of the HF

We can approximate the input matrix of HF in (4.31) as

$$\begin{aligned}\hat{\mathbf{\Omega}}_k &= \eta_k E\{\mathbf{\Omega}_k\} \\ &= \eta_k \rho_k^2 \bar{\mathbf{R}}_k^{-1} \sum_{b,c} \beta_{b,k}\beta_{c,k} \mathbf{W}_{T,b,k}^H E\left\{\hat{\mathbf{H}}_{b,k}^H \hat{\mathbf{H}}_{c,k}\right\} \mathbf{W}_{T,c,k} \\ &= \eta_k \rho_k^2 N_R \bar{\mathbf{R}}_k^{-1} \sum_{b} \beta_{b,k}^2 \mathbf{W}_{T,b,k}^H \mathbf{R}_{b,k} \mathbf{W}_{T,b,k} \\ &= \frac{\eta_k \rho_k^2 N_R}{\left(1-\rho_k^2\right)} \mathbf{I}_{s_k}\end{aligned} \tag{5.9}$$

where η_k is a calibration value to reflect the effect of CSI on $\mathbf{\Omega}_k$, defined as [36]

$$\eta_k \equiv \frac{1}{B} \sum_{b} \frac{\mathrm{tr}\left(\mathbf{W}_{T,b,k}^H \hat{\mathbf{H}}_{b,k}^H \hat{\mathbf{H}}_{b,k} \mathbf{W}_{T,b,k}\right)}{N_R \cdot \mathrm{tr}\left(\mathbf{W}_{T,b,k}^H \mathbf{R}_{b,k} \mathbf{W}_{T,b,k}\right)}. \tag{5.10}$$

Note that the HF is a function of temporal channel correlation ρ_k, since the approximated input matrix depends on ρ_k. We may avoid the calculation of HF for sum-rate estimation by quantizing ρ_k. We pre-calculate the HF-dependent terms in (4.31) and (4.32) for given quantization levels of ρ_k, and form a look-up table of the HF-dependent terms. We quantize the temporal channel correlation of each user, and utilize the pre-calculated HF-dependent terms to estimate the sum-rate, using the look-up table. Let $S_\rho = \{\bar{\rho}_1, ..., \bar{\rho}_i, ..., \bar{\rho}_N\}$ be a set of quantization levels of ρ_k. From (5.9), ρ_k can be approximated as

$$\hat{\rho}_k = \arg\min_{\bar{\rho}_i \in S_\rho} \left| \bar{\rho}_i - \sqrt{\frac{\eta_k \rho_k^2}{1-\rho_k^2}\left(\frac{\eta_k \rho_k^2}{1-\rho_k^2}+1\right)^{-1}} \right|. \tag{5.11}$$

It can be shown that $\hat{\mathbf{\Omega}}_k = \left\{\hat{\rho}_k^2 N_R \big/ \left(1-\hat{\rho}_k^2\right)\right\}\mathbf{I}_{s_k}$ only depends upon $\hat{\rho}_k$. However, we may need to utilize the CSI to calculate η_k for the quantization of ρ_k. We may further approximate the input matrix of HF by averaging the numerator in (5.10) over $\hat{\mathbf{H}}_{b,k}$. Then, it can be shown that $\eta_k = 1$. We may quantize ρ_k as

$$\hat{\rho}_k = \arg\min_{\bar{\rho}_i \in S_\rho} \left|\bar{\rho}_i - \rho_k\right|. \tag{5.12}$$

We may need HF terms corresponding to elements in S_ρ, which can be pre-calculated. We may represent the quantized HF-dependent terms in (4.31) and (4.32) corresponding to $\bar{\rho}_i \in S_\rho$ as

$$\begin{cases} \Upsilon_1\left(\bar{\rho}_i\right) = 2^{N_R} \dfrac{\Gamma_{N_R}\left(\dfrac{N_R}{2}+1\right)}{\Gamma_{N_R}\left(\dfrac{N_R}{2}\right)} {}_1F_1\left(-1; \dfrac{N_R}{2}; -\dfrac{\bar{\rho}_i^2 N_R}{2\left(1-\bar{\rho}_i^2\right)}\mathbf{I}_{N_R}\right) \\ \Upsilon_2\left(\bar{\rho}_i\right) = 2^{N_R-1} \dfrac{\Gamma_{N_R-1}\left(\dfrac{N_R}{2}+1\right)}{\Gamma_{N_R-1}\left(\dfrac{N_R}{2}\right)} {}_1F_1\left(-1; \dfrac{N_R}{2}; -\dfrac{\bar{\rho}_i^2 N_R}{2\left(1-\bar{\rho}_i^2\right)}\mathbf{I}_{N_R-1}\right) \end{cases}. \tag{5.13}$$

Then, we can approximate (4.31) and (4.32) as

$$\begin{cases} \hat{\zeta}_k = \left|\left(1-\rho_k^2\right)\sum\limits_{b\in B_k} \alpha_{b,k}^2 \beta_{b,k}^2 \mathbf{\Delta}_{b,k,k}^{(k)}\right| \Upsilon_1\left(\hat{\rho}_k\right) \\ \hat{\zeta}_k^{(i-)} = \left|\left(1-\rho_k^2\right)\sum\limits_{b\in B_k} \alpha_{b,k}^2 \beta_{b,k}^2 \left(\mathbf{\Delta}_{b,k,k}^{(k)}\right)^{(i-)}\right| \Upsilon_2\left(\hat{\rho}_k\right) \end{cases} \tag{5.14}$$

where $\left(\mathbf{\Delta}_{b,k,k}^{(k)}\right)^{(i-)}$ denotes $\mathbf{\Delta}_{b,k,k}^{(k)}$ without the *i*-th row and column.

We may approximate the achievable sum-rate of a given set of users, denoted by *S*, as

$$M_S \equiv \sum_{k\in S}\sum_i \log_2\left(1+\left\{\sum_{l\neq k}\left\{\left[\hat{\mathbf{\Psi}}_{k,l}\hat{\mathbf{\Psi}}_{k,l}^H\right]_{i,i}+\mathrm{tr}\left(\hat{\mathbf{Y}}_{k,l}\right)\frac{\hat{\varsigma}_k^{(i-)}}{\hat{\varsigma}_k}\right\}+\sigma_n^2\frac{\hat{\varsigma}_k^{(i-)}}{\hat{\varsigma}_k}\right\}^{-1}\right). \quad (5.15)$$

We do not need to calculate the beam weight and the HF to estimate the proposed metric, but only need to handle multiplications of diagonal matrices whose elements are dependent of the CCM, significantly reducing the computational complexity. The greedy algorithm based on the proposed metric is summarized in Table 5-2. Here, $M_{S[t,n]}[t,n]$ denotes the proposed metric for users in $S[t,n]$ at the *n*-th subframe of the *t*-th frame.

Table 5-2. Proposed resource allocation at current frame *t*.

Input: $\mathbf{R}_{b,k}[t], \rho_k[t,n]$

Initialization: $S[t,n]=\varnothing, S_{rem}[t,n]=\{1,2,...,K\}$

In every subframe do:

1. For $k\in S_{rem}[t,n]$, compute $M_{S[t,n]\cup\{k\}}[t,n]$
2. If $M_{S[t,n]}[t,n] < M_{S[t,n]\cup\{k^*\}}[t,n]$ where $k^* = \arg\max_k M_{S[t,n]\cup\{k\}}[t,n]$,
   $S[t,n]=S[t,n]\cup\{k^*\}$, $S_{rem}[t,n]=S_{rem}[t,n]\setminus\{k^*\}$
3. Repeat 1~2 until $M_{S[t,n]}[t,n] \geq M_{S[t,n]\cup\{k^*\}}[t,n]$ or $S_{rem}[t,n]=\varnothing$

Output: $S[t,n]$

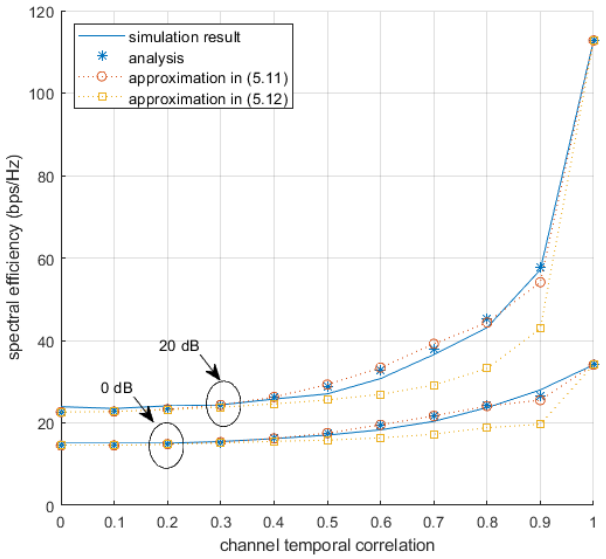

Fig. 5-2. Estimation of achievable sum-rate.

Fig. 5-2 depicts the sum-rate estimations based on (5.11) and (5.12) for the SNR of 0 and 20 dB, where $N_T = 64$, $N_R = 4$, $B = 2$, $K = 4$ and $S_\rho = \{0, 0.1, 0.2, ..., 1\}$. To evaluate the effect of the calibration by (5.10) on the estimation of sum-rate, we do not consider the approximation of the beam weight by (5.5) here. It can be seen that the approximation based on (5.12) provides underestimated sum-rate, whereas the approximation based on (5.11) provides quite accurate sum-rate.

5.2.3. Resource allocation update algorithm

Since the proposed scheme depends on the CCM and the temporal channel correlation, it may be desirable to update the resource allocation only when any of the

both parameters have changed considerably. We define two conditions to trigger the update for resource allocation.

First, at the current frame *t*, we update the user set $S[t,n]$ through the greedy algorithm in Table 5-2, when there exists a user whose eigenvectors of the CCM have changed. Let $A_{b,k,n_A}[t]$ and $E_{b,k,n_E}[t]$ be sets of indices of eigenvectors of $\mathbf{R}_{az,b,k}[t]$ and $\mathbf{R}_{el,b,k}[t]$ corresponding to n_A and n_E number of highest eigenvalues of the CCMs, respectively. Also, let $A^{(up)}_{b,k,n_A}$ and $E^{(up)}_{b,k,n_E}$ be sets of indices of the dominant eigenvectors of the CCMs, at the time when the resource allocation was updated most recently due to the change of CCM of user *k*. We update the resource allocation at the current frame only when any user *k* exists satisfying $A_{b,k,n_A}[t] \bigcap A^{(up)}_{b,k,n_A} = \varnothing$ or $E_{b,k,n_E}[t] \bigcap E^{(up)}_{b,k,n_E} = \varnothing$. The condition implies that the dominant eigenvectors of CCM in the azimuth or the elevation direction have changed from the last update time. For larger n_A (or n_E), the more dominant eigenvectors of CCM need to be changed to trigger the update, resulting in less frequent updates for resource allocation. We may determine n_A and n_E in consideration of the average number of data streams transmitted to each user at the previous frame, since the number of data streams is strongly related with the number of dominant eigenvectors of CCM [31]. We may determine the both parameters as [31]

$$n_A = n_E = \frac{1}{\left|S[t-1,n]\right|} \sum_{k \in S[t-1,n]} \sqrt{s_k[t-1,n]} \tag{5.16}$$

where $s_k[t-1,n]$ denotes the number of data streams transmitted to user *k* at the *n*-th subframe of the previous frame. In this case, $A_{b,k,n_A}[t,n]$, $E_{b,k,n_E}[t,n]$, $A^{(up)}_{b,k,n_A}[n]$ and $E^{(up)}_{b,k,n_E}[n]$ depend on the subframe index *n*.

Second, we update $S[t,n]$ when there exists a user whose mobility has changed from the last update time. Let $\hat{\rho}_k[t,n]$ be the quantized temporal channel correlation at the *n*-th subframe of the current frame, and $\hat{\rho}_k^{(up)}[n]$ be the quantized temporal channel correlation at the time when the resource allocation was updated most recently due to the change of mobility of user *k*. When $\hat{\rho}_k[t,n] \neq \hat{\rho}_k^{(up)}[n]$ is satisfied, which means that mobility of user *k* has changed, we update $S[t,n]$. When there is no user whose CCM or mobility has changed, we maintain the resource allocation as same as the previous frame (*i.e.*, $S[t,n] = S[t-1,n]$).

Assume that only user *k* satisfies one of the conditions above, so that we need to update the resource allocation at the current frame. We may maintain the resource allocation for other users as same as the previous frame, since the channel conditions (*i.e.*, CCM and temporal correlation) of those users are unchanged. We may need to update the resource allocation for users whose transmission channel is correlated with that of user *k*, since such users may be considerably affected by the change of channel conditions of user *k* in a transmission performance manner [32]. We utilize the orthogonality of CCMs to check the variation of transmission performance. For any user $l \neq k$, when $A_{b,l,n_A}[t,n]$ (or $E_{b,l,n_E}[t,n]$) has no overlapped elements with $A_{b,k,n_A}[t,n]$ (or $E_{b,k,n_E}[t,n]$), we may consider that user *k* and *l* have orthogonal channel in an average manner, since their dominant eigenvectors of CCM are orthogonal. In this case, the channel variation of user *k* little affects the transmission performance of user *l* [32]. We maintain the resource allocation for user *l* as same as the previous frame. For example, if $l \in S[t-1,n]$, we schedule the user in $S[t,n]$ so that $l \in S[t,n]$. We update the resource allocation for users not satisfying the orthogonality condition (i.e., newly allocate resource to those

users), by applying the algorithm in Table 5-2. Let $S_{trg-loc}[t,n]$ and $S_{trg-mob}[t,n]$ be sets of users satisfying the update conditions due to the change of CCM and mobility, respectively. We define a set of users whose resource allocation is maintained as same as the previous frame, as

$$S_{init}[t,n]=\left\{ l \in S[t-1,n] \left| \begin{array}{c} A_{b,l,n_A}[t,n] \cap A_{b,k,n_A}[t,n]=\varnothing \\ \text{or } E_{b,l,n_E}[t,n] \cap E_{b,k,n_E}[t,n]=\varnothing \\ \text{for } k \in S_{trg-loc}[t,n] \cup S_{trg-mob}[t,n], 1 \le b \le B \end{array} \right. \right\}. \quad (5.17)$$

By initiating as $S[t,n]=S_{init}[t,n]$ for the algorithm in Table 5-2, we can maintain the resource allocation for users in $S_{init}[t,n]$. By initiating as $S_{rem}[t,n]=\{1,2,...,K\} \setminus S_{init}[t,n]$ for the algorithm, we can update the resource allocation for the remained users (*i.e.*, users not belonging to $S_{init}[t,n]$) in a greedy manner. Since the number of users participating in the greedy algorithm is reduced, the number of iterations in the greedy algorithm is also reduced. The proposed update algorithm is described in Table 5-3, and an example of the scheme with $N_{SF}=1$ is depicted in Fig. 5-3. In the figure, at the $(t-1)$-th frame, we allocate the resource to user 2, 3 and 4. At frame *t*, the CCM of user 1 changes and it triggers the update procedure. Since user 2 and 3 have orthogonal CCMs with user 1, we maintain the resource allocation for those users. Since the CCM of user 4 is similar to that of user 1, we update the resource allocation for user 1 and 4 by applying the algorithm in Table 5-2.

Table 5-3. Proposed resource allocation update algorithm at current frame *t*.

Input: $\mathbf{R}_{b,k}[t], \rho_k[t,n], s_k[t-1,n], A^{(up)}_{b,k,n_A}[n], E^{(up)}_{b,k,n_E}[n], \hat{\rho}^{(up)}_k[n]$

Initialization: $S[t,n]=\varnothing, S_{rem}[t,n]=\{1,2,...,K\}$

In every subframe do:

1. If $S_{trg-loc}[t,n]\neq\varnothing$ or $S_{trg-mob}[t,n]\neq\varnothing$, do:
   - 1.1. Derive $S_{init}[t,n]$ and obtain $S[t,n]$ using the algorithm in Table 5-2 with the initialization of $S[t,n]=S_{init}[t,n]$ and $S_{rem}[t,n]=S_{rem}[t,n]\setminus S_{init}[t,n]$
   - 1.2. Update $A^{(up)}_{b,k,n_A}[n]$ and $E^{(up)}_{b,k,n_E}[n]$ for $k\in S_{trg-loc}[t,n]$
   - 1.3. Update $\hat{\rho}^{up}_k[n]$ for $k\in S_{trg-mob}[t,n]$
2. Otherwise, $S[t,n]=S[t-1,n]$

Output: $S[t,n]$

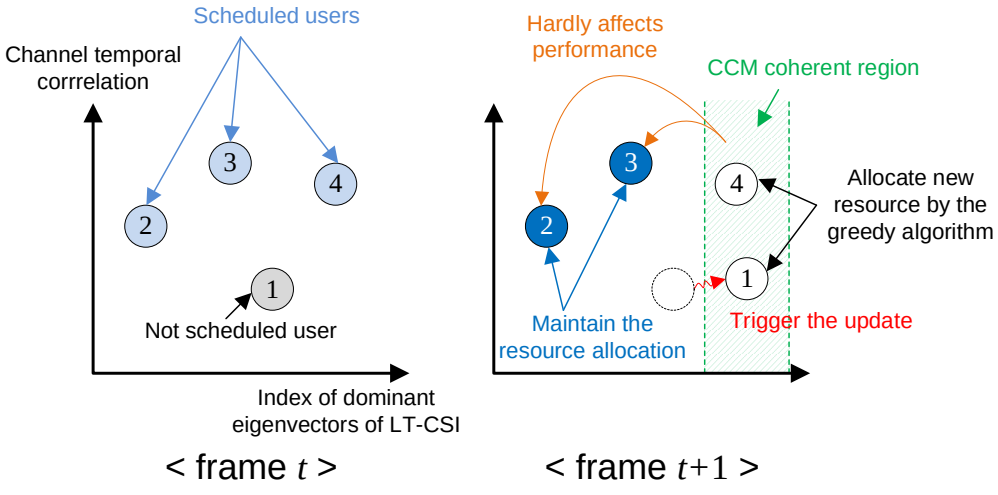

Fig. 5-3. An example of the proposed update algorithm.

Table 5-4. Computational complexity.

	Main loop	CCM approximation
Sum-rate-based	$O\left(BKK_{set}^2N_T^3+KK_{set}^2P_{N_hN_R}^2N_R\right)$	-
CD-based	$O\left(BKN_T^3+BK_{set}^2N_T^3+K_{set}^2P_{N_hN_R}^2N_R\right)$	
SO-based	-	$O\left(BK\max\left(N_{az},N_{el}\right)^3\right)$
Proposed	$O\left(BKK_{set}^2N_T\right)$	

5.2.4. Computational complexity

The computational complexity of the conventional schemes and the proposed scheme is summarized in Table 5-4, where K_{set} denotes the size of a sub-optimal user set obtained by each scheme. The sum-rate-based greedy algorithm calculates the beam weight and the HF to estimate the sum-rate of every candidate user set, requiring high computational complexity. The chordal distance-based (CD-based) algorithm updates a candidate user set using the CD rather than the sum-rate [61], but the computational complexity is still $O\left(N_T^3\right)$ to calculate the CD. Also, the scheme repeatedly checks the termination condition of the algorithm which still involves the estimation of sum-rate [61]. The proposed scheme does not require the calculation of beam weight and HF, requiring much reduced computational complexity which is linear to N_T. However, the proposed scheme requires additional computation for diagonalization of CCMs in (5.4), which costs computational complexity of $O\left(N_T^{1.5}\right)$ when a BS has a square antenna array [22]. In practice, we may not perform the computation in every transmission frame, since the

CCM may have coherence time much longer than a single frame interval even in high mobility environments [11]. The spatial orthogonality-based (SO-based) scheme heuristically schedules users having orthogonal CCMs, without estimating the sum-rate. The scheme requires only the CCM diagonalization process, requiring the lowest computational complexity in the table [32]. However, the performance of the scheme may significantly decrease since K_{set} is determined heuristically, without considering the sum-rate.

5.3. Performance evaluation

We evaluate the performance of the proposed scheme by computer simulation. We consider two adjacent macro cells where each BS is equipped with antennas in a 2-D square ULA, and the spatial channel correlation follows the NLOS ray-based model in moderate AS environments [22]. The BSs transmit data to users by means of the coordinated transmission described in the previous chapter. The main simulation parameters are summarized in Table 5-5.

We compare the proposed scheme with the sum-rate-based greedy algorithm [58] when the achievable sum-rate is perfectly known to the BSs, and is computed as the analysis in (4.37), referred to “perfect sum-rate-based,” and “analysis-based,” in the figures, respectively. We also verify the performance of the CD-based scheme [61], and the SO-based scheme [32], referred to “CD-based,” and “SO-based” in the figures, respectively.

Table 5-5. Evaluation parameters.

Parameters	Values
CCM model	3-D ray-based model [22]
AS	Moderate mode [22]
Carrier frequency $(=1/\lambda)$	2.3 GHz
BS antenna distance	$\lambda/2$
Macro cell radius	200 m
Number of BS antennas (N_T)	64
Number of user antennas (N_R)	4 (if not specified)
Frame length	10 ms
Subframe length	1 ms
Number of downlink subframes per frame (N_{SF})	5
Update period for CCM	10 frames

We first verify the performance of the proposed resource allocation algorithm in Table 5-2. In the simulation, each user is moving at a speed of uniformly randomly distributed in a range of (0, 60) km/h, and $S_\rho = \{0.1, 0.2, ..., 0.9, 1.0\}$. Fig. 5-4 depicts spectral efficiency according to various parameters. It can be seen that the analysis-based greedy algorithm provides performance most similar to the perfect sum-rate-based one, since it accurately estimates the sum-rate exploiting both of CSI and CCM. It can also be

seen that the performance gap between the two cases increases as the subframe index increases due to the analysis error in the presence of channel aging effect. It can be seen that the proposed scheme with or without the calibration by (5.10) outperforms the other low complexity schemes. The calibration little affects the performance, which implies that the estimation error of sum-rate illustrated in Fig. 5-2 may be ignorable. It can be seen that the CD-based scheme provides quite degraded performance because the scheme exploits the CSI only so that it suffers from the channel aging effect. Also, in multi-cell environments, the CD may be not an effective metric to replace the sum-rate since the metric does not have any information about the inter-cell interference [61]. It can be seen that the SO-based scheme provides the worst performance. This is because the scheme heuristically schedules users without the consideration of the sum-rate. It can be seen from sub-figure (d) that the performance gap between the proposed scheme and the analysis-based greedy scheme increases as N_R increases. This is because the proposed scheme is based on the approximation of beam weight by (5.5), which is feasible when $N_T \gg N_R$ holds [30].

To verify the proposed update algorithm in Table 5-3, we observe the average spectral efficiency during 5000 frames where a single frame interval is set to 10 ms. We first verify the performance of the proposed scheme according to variation of CCM. We consider an environment where users are moving in random direction at a fixed speed of 60 km/h, and the average SNR is 20 dB. Fig. 5-5 depicts the average spectral efficiency of the proposed algorithm according to the subframe index. Also, Table 5-6 and 5-7 summarize the average number of updates for resource allocation and iterations in the algorithm in Table 5-2, respectively. All the results are normalized to that of the proposed

resource allocation scheme without the update algorithm. It can be seen that the case of $n_A = n_E = 1$ provides more than 95% of the performance when the update algorithm is not applied, reducing the number of updates more than 10 times. Note that increasing n_A and n_E may degrade the resource allocation performance due to less frequent updates, but may improve the performance defining $S_{init}[t,n]$ more strictly by (5.17). It can be seen from the figure that as n_A and n_E increase, the performance of the proposed scheme usually decreases. This implies that the update period for resource allocation is a main factor in the performance. It can also be seen that the number of updates increases as the number of users increases, since there is more probability that an user exists whose change of CCM is large enough to trigger the update for resource allocation.

We also consider an environment where a speed of each user changes at 10 km/h/s with upper and lower bounds of 60 and 0 km/h, respectively. To evaluate the effect of variation of mobility on the performance of the proposed update algorithm, we assume that CCM of each user remains unchanged while the user is moving. We define d_ρ as a quantization density of the temporal channel correlation, representing difference between two consecutive quantization levels in S_ρ. Smaller d_ρ indicates denser quantization of the temporal channel correlation. Fig. 5-6 depicts the normalized spectral efficiency of the proposed scheme according to the subframe index, and Table 5-8 summarizes the normalized number of updates for resource allocation. It can be seen that the proposed scheme with smaller d_ρ provides higher spectral efficiency due to more frequent updates for resource allocation. It can also be seen that the proposed schemes with $d_\rho = 0.2$ and $d_\rho = 0.5$ provide the same spectral efficiency at the first subframe. Since the channel aging effect is the lowest at the first subframe, the temporal channel

correlation may show little variation. We may not properly detect the variation of user mobility with the rough quantization of $d_\rho = 0.2$ and $d_\rho = 0.5$. It can be seen from Table 5-8 that there was no update for resource allocation when $d_\rho = 0.2$ and $d_\rho = 0.5$ at the first subframe. It can also be seen from Fig. 5-6 that the performance when $d_\rho = 0.5$ is much degraded at subframe 2 and 3, and the performance gap between the cases of $d_\rho = 0.2$ and $d_\rho = 0.5$ is quite significant in those subframes. This implies that the variation of temporal channel correlation is most dynamic in those subframes, so that the rough quantization may yield inaccurate estimation of the sum-rate.

Finally, we verify the performance of the proposed scheme when both of CCM and mobility of users are varying. The edge SNR is set to 0 dB and the calibration by (5.10) is not applied. Also, n_A and n_E are determined as (5.16) and $d_\rho = 0.1$. Fig. 5-7 depicts the spectral efficiency according to the subframe index, and Table 5-9 and 5-10 summarize the average number of updates for resource allocation and iterations in the algorithm in Table 5-2, respectively. All the results are normalized to that of the analysis-based greedy algorithm. It can be seen that the proposed schemes with and without the update algorithm provide similar performance, outperforming the other low complexity schemes. It can also be seen from the tables that the proposed scheme reduces the number of updates and iterations more than 10 and 3 times, respectively, in comparison to the analysis-based greedy algorithm. Note that the proposed update algorithm provides more than 95 % of spectral efficiency of the analysis-based greedy algorithm, significantly reducing the computation complexity.

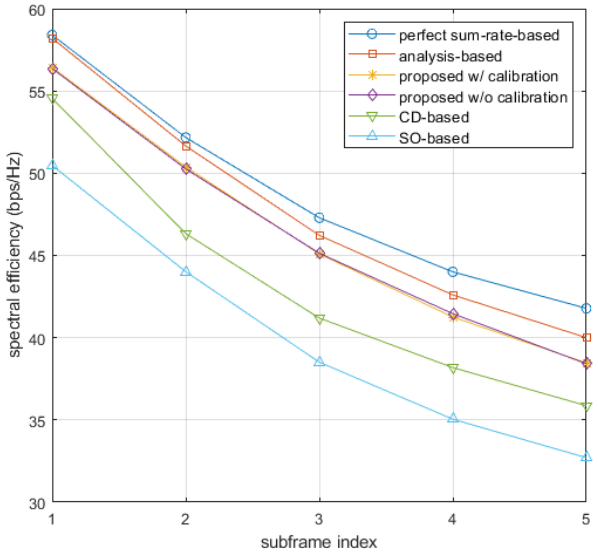

(a) When $N_R = 4$, $K = 8$ and the edge SNR is 0 dB

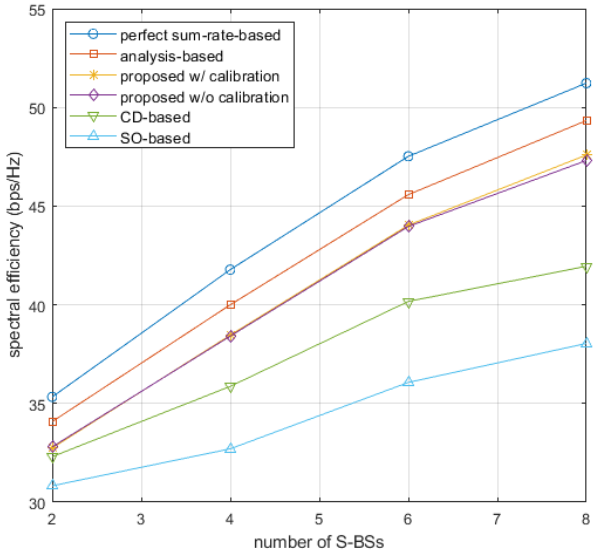

(b) When $N_R = 4$, the edge SNR is 0 dB and the subframe index is 5

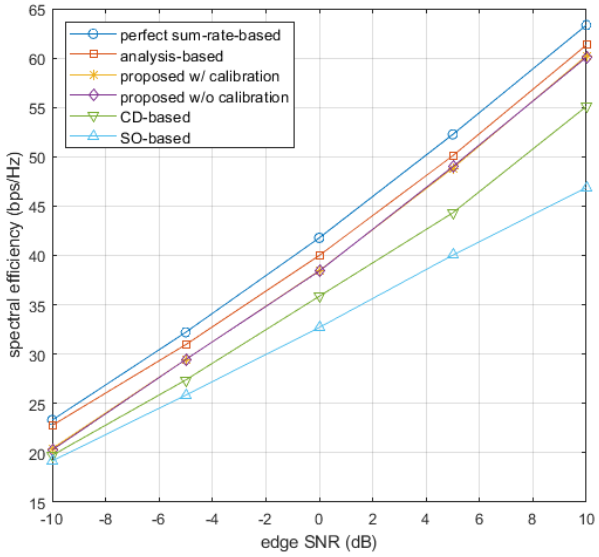

(c) When $N_R = 4$, $K = 8$ and the subframe index is 5

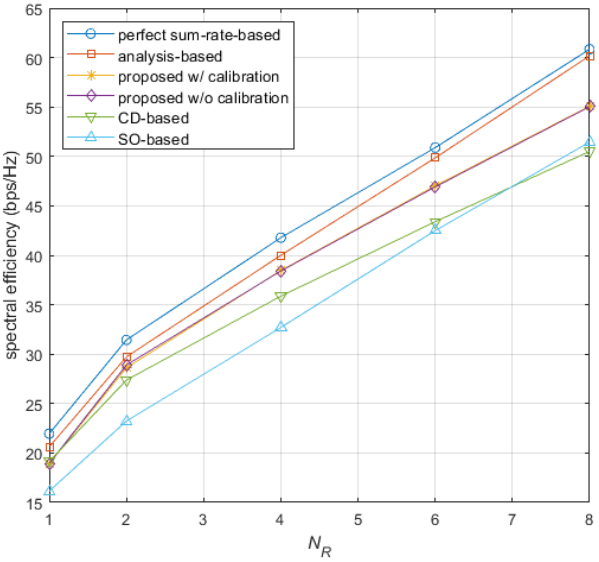

(d) When $K = 8$, the edge SNR is 0 dB and the subframe index is 5.

Fig. 5-4. Spectral efficiency of the proposed and conventional schemes.

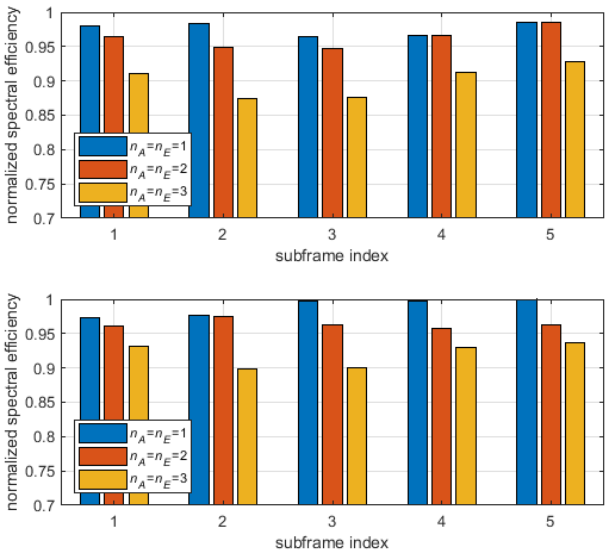

Fig. 5-5. Normalized spectral efficiency according to n_A and n_E.

Table 5-6. Normalized number of updates for resource allocation.

	$n_A = n_E = 1$	$n_A = n_E = 2$	$n_A = n_E = 3$
$K = 8$	0.032	0.011	0.005
$K = 16$	0.058	0.018	0.008

Table 5-7. Normalized number of iterations.

Subframe index		1	2	3	4	5
$K=8$	$n_A=n_E=1$	0.348	0.333	0.369	0.360	0.403
	$n_A=n_E=2$	0.473	0.430	0.490	0.467	0.459
	$n_A=n_E=3$	0.619	0.596	0.643	0.704	0.644
$K=16$	$n_A=n_E=1$	0.307	0.325	0.310	0.323	0.323
	$n_A=n_E=2$	0.470	0.459	0.436	0.467	0.470
	$n_A=n_E=3$	0.634	0.678	0.655	0.628	0.632

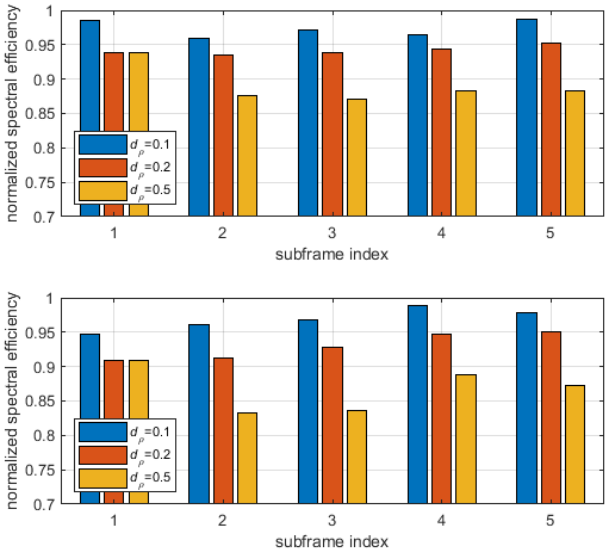

Fig. 5-6. Normalized spectral efficiency according to d_ρ.

Table 5-8. Normalized number of updates for resource allocation.

Subframe index		1	2	3	4	5
$K=8$	$d_\rho = 0.1$	0.013	0.036	0.068	0.087	0.101
	$d_\rho = 0.2$	No update	0.013	0.037	0.049	0.057
	$d_\rho = 0.5$	No update	0.013	0.013	0.025	0.026
$K=16$	$d_\rho = 0.1$	0.025	0.065	0.110	0.132	0.151
	$d_\rho = 0.2$	No update	0.025	0.066	0.083	0.099
	$d_\rho = 0.5$	No update	0.025	0.025	0.047	0.047

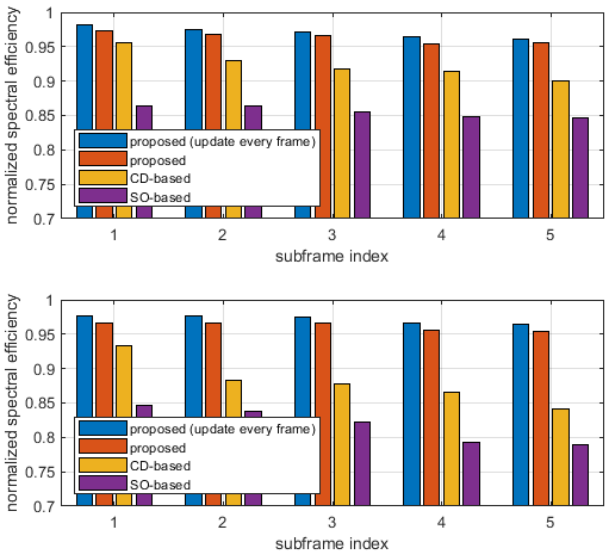

Fig. 5-7. Normalized spectral efficiency of the proposed scheme.

Table 5-9. Normalized number of updates for resource allocation.

Subframe index		1	2	3	4	5
$K=8$	Triggered by CCM	0.017				
	Triggered by mobility	0.013	0.036	0.068	0.081	0.096
	Total	0.028	0.050	0.080	0.091	0.106
$K=16$	Triggered by CCM	0.032				
	Triggered by mobility	0.025	0.068	0.113	0.131	0.149
	Total	0.053	0.088	0.127	0.142	0.157

Table 5-10. Normalized number of iterations.

Subframe index	1	2	3	4	5
$K=8$	0.294	0.260	0.242	0.264	0.277
$K=16$	0.251	0.226	0.230	0.251	0.262

Chapter 6

Conclusions

In this dissertation, we have considered downlink transmission to users in high mobility in m-MIMO environments, particularly in view of channel estimation, signal transmission and resource allocation.

We have designed the CCM estimation scheme lowering the pilot signaling overhead. Exploiting the property that pairs of antennas in an equal distance experience spatial channel correlation similar to each other, we jointly estimate the spatial channel correlation of those antenna pairs by means of the LS estimation. We have analyzed the MSE of elements in the estimated CCM, and designed the refinement scheme which neglects elements of CCM whose estimated MSE is higher than a reference value. The simulation results showed that the proposed scheme affordably estimates the CCM and the CSI in various spatial channel correlation environments.

We also have designed the signal transmission scheme robust to the channel aging effect. We have analyzed the average SLNR for each user in the presence of channel aging effect, and designed the beam weight to maximize the average SLNR. The proposed beam weight comprises the eigen-direction of a linear combination of the CSI

and the CCM with adjustment of temporal channel correlation. We also have analyzed the average SINR obtained by the proposed scheme, and managed the transmit power by using an iterative water-filling technique. The simulation results showed that the proposed scheme improves the transmission performance for users in various mobility conditions, comparing with the conventional schemes

Finally, we have designed the resource allocation scheme for m-MIMO systems in the presence of channel aging effect. We have designed the greedy algorithm that allocates the transmission resource to maximize the sum-rate in the presence of channel aging effect. We can estimate the sum-rate from the beam weight and the HF, which may yield very high computational complexity. To alleviate the problem, we approximately determined the beam weight in the eigen-direction of CCM by means of the AJD, and approximated the HF as a function of the temporal channel correlation. Since we can estimate the sum-rate using spatial and temporal channel correlation, we have designed the update algorithm for resource allocation where the scheduling state of users is updated only when the change of CCM or temporal channel correlation affects the sum-rate. The simulation results showed that the proposed scheme provides performance similar to a greedy algorithm based on accurate sum-rate, significantly reducing computational complexity.

We summarize interesting future research directions below.

- **Ultra-reliable communication**: A cellular system may need to guarantee high reliability in communication for specific applications such as a cellular vehicular-to-everything (C-V2X) [70]. It has been shown that the proposed scheme can significantly improve transmission performance for users in high mobility, which may be applied to

communication between a BS and a vehicle for infotainment services. However, the proposed scheme may not work properly when a BS handles data for the safety applications, which may require ultra-reliable communication [70]. The proposed beamforming scheme may not be helpful for enhancement of reliability, since the use of CCM does not provide a beam weight perfectly matched to short-term channel state (*i.e.*, CSI) between a BS and a vehicle. As a result, the received SINR may fluctuate according to the channel state, although the scheme improves the received SINR in an average manner. To improve the reliability, it may be desirable to develop efficient signal transmission scheme in consideration of the outage probability of received SINR and outdated CSI simultaneously.

- **Low latency communication**: For conventional real-time traffic such as gaming and video streaming, the required latency is about tens of milliseconds which is usually larger than a single transmission frame interval in current cellular systems [71]. For such services, a greedy resource allocation scheme maximizing the sum-rate may provide performance similar to that considering quality of service (QoS) of users, in a QoS manner [58]. This implies that the proposed scheme may be able to support such traffic for users in high mobility. However, it may be required to support ultra-low latency services in the next generation cellular systems, such as remote control and tactile internet. The services may require latency lower than 1 ms [72]. The proposed scheme may not guarantee QoS of such services since the scheme updates the resource allocation only when the CCM or the temporal channel correlation has changed. This means that the update period is at least longer than a single frame interval, which may be also longer than the required latency constraint of the services. It is desirable to

design a QoS-aware resource allocation scheme, which can operate whenever such services are required, regardless of the update period of the resource allocation. The resource allocation schemes for conventional and ultra-low latency services may operate cooperatively in the same available frequency band, regarding the latter as a special operation mode for specific applications [71].

Appendix

Let $\mathbf{U} \in \mathbb{C}^{N \times N}$ be a unitary matrix and $\mathbf{D} \in \mathbb{C}^{N \times N}$ be a diagonal matrix with distinct positive elements. Also, let u_{ij} be an element of $\mathbf{U}$ corresponding to the *i*-th row and *j*-th column, and d_i be the *i*-th diagonal element of $\mathbf{D}$. We assume that the elements of $\mathbf{D}$ are arranged in an ascending order. It can be written that

$$\left[\mathbf{U}\mathbf{D}\mathbf{U}^H\right]_{ii}^{-1} = \frac{1}{\sum_{j=1}^{s} d_i \left|u_{ij}\right|^2} \equiv \frac{1}{\eta_i}. \tag{4.46}$$

Note that u_{ij} satisfies conditions as

$$\begin{cases} 0 \le \left|u_{ij}\right|^2 \le 1 \\ \sum_{i=1}^{N} \left|u_{ij}\right|^2 = 1 \text{ and } \sum_{j=1}^{N} \left|u_{ij}\right|^2 = 1 \end{cases}. \tag{4.47}$$

Let $\hat{\mathbf{U}} = \mathbf{I}_N$ and the corresponding element be $\hat{u}_{ij}$. From the constraints, it can be shown that

$$\begin{cases} \eta_1 - \hat{\eta}_1 \ge 0 \\ \sum_{i=1}^{N} \left(\eta_i - \hat{\eta}_i\right) \ge 0 \end{cases} \tag{4.48}$$

where $\hat{\eta}_i = \sum_{j=1}^{s} d_i \left|\hat{u}_{ij}\right|^2$. By the convexity of (4.46), it can be written as

$$\sum_i^N \frac{1}{\eta_i} \le \sum_i^N \frac{1}{\hat{\eta}_i} = \sum_i^N \frac{1}{d_i} . \tag{4.49}$$

When $\mathbf{D}$ is not a diagonal matrix, we can diagonalize the matrix with the use of $\mathbf{U} = \bar{\mathbf{U}}\mathbf{U}_D^H$ where $\mathbf{U}_D$ is a matrix comprising eigenvectors of $\mathbf{D}$ and $\bar{\mathbf{U}}$ is a unitary matrix. The equality holds when $\mathbf{U} = \mathbf{U}_D^H$.

References

[1] D. Gesbert, *et al*., "Shifting the MIMO paradigm," *IEEE Signal Process. Mag.*, vol. 24, no. 5, pp. 36-46, Sept. 2007.

[2] T. Shim, *et al*., "Traffic convexity aware cellular networks: a vehicular heavy user perspective," *IEEE Wireless Commun.*, vol. 23, no. 1, pp. 88-94, Feb. 2016.

[3] T. Marzetta, "Noncooperative cellular wireless with unlimited numbers of base station antennas," *IEEE Trans. on Wireless Commun.*, vol. 9, no. 11, pp. 3590-3600, Nov. 2010.

[4] F. Rusek, *et al*., "Scaling up MIMO: Opportunities and challenges with very large arrays," *IEEE Signal Process*. Mag., vol. 30, no. 1, pp. 40-60, Jan. 2013.

[5] H. Q. Ngo, E. Larsson and T. Marzetta, "Energy and spectral efficiency of very large multiuser MIMO systems," *IEEE Trans. on Commun.*, vol. 61, no. 4, pp. 1436-1449, April 2013.

[6] N. Jamal and P. Mitran, "Throughput scaling of MIMO channels with imperfect CSIT in the low-SNR regime," *IEEE Commun. Letters*, vol. 18, no. 9, pp. 1563-1566, Sept. 2014.

[7] D. Mi, *et al*., "Massive MIMO performance with imperfect channel reciprocity and channel estimation error," *IEEE Trans. on Commun*., vol. 65, no. 9, pp. 3734-3749, Sept. 2017.

[8] K. T. Truong and R. W. Heath, "Effects of channel aging in massive MIMO systems," *J. of Commun. and Networks*, vol. 15, no. 4, pp. 338-351, Aug. 2013.

[9] A. K. Papazafeiropoulos, "Impact of general channel aging conditions on the downlink performance of massive MIMO," *IEEE Trans. on Veh. Tech.*, vol. 66, no. 2, pp. 1428-1442, Feb. 2017.

[10] R. Chopra, *et al*., "Performance analysis of FDD massive MIMO systems under channel aging," *IEEE Trans. on Wireless Commun.*, vol. 17, no. 2, pp. 1094-1108, Feb. 2018.

[11] I. Viering, H. Hofstetter and W. Utschick, "Spatial long-term variations in urban, rural and indoor environments," in *Proc*. COST273 5th Meeting, 2002.

[12] M. Nicoli, O. Simeone and U. Spagnolini, "Multislot estimation of fast-varying space-time channels in TD-CDMA systems," *IEEE Commun. Letters*, vol. 6, no. 9, pp. 376-378, Sept. 2002.

[13] W. C. Jakes, *Microwave mobile communications*. John Wiley and Sons, 1974.

[14] H. Huh, A. M. Tulino, G. Caire, "Network MIMO with linear zero-forcing beamforming: large system analysis, impact of channel estimation and reduced-complexity scheduling," *IEEE Trans. On Inform. Theory*, vol. 58, no. 5, pp. 2911-2934, May 2012.

[15] J. Choi, D. J. Love and P. Gidigare, "Downlink training techniques for FDD massive MIMO systems: Open-loop and closed-loop training with memory," *IEEE J. of Sel. Topics in Signal Process.*, vol. 8, pp. 802-814, Mar. 2014.

[16] J. H. Kotecha and A. Sayeed, "Transmit signal design for optimal estimation of correlated MIMO channels," *IEEE Trans. on Signal Process.*, vol. 52, pp. 546-557, Jan. 2004.

[17] H. Q. Ngo and E. G. Larsson, "EVD-based channel estimation in multicell multiuser MIMO systems with very large antenna arrays," *in Proc. ICASSP*, pp. 3249-3252, Mar. 2012.

[18] S. Noh, Y. Sung and D. J. Love, "Pilot beam pattern design for channel estimation in massive MIMO systems," *IEEE J. of Sel. Topics in Signal Process.*, vol. 8, pp. 787-801, May 2014.

[19] Z. Jiang, *et al*., "Achievable rates of FDD massive MIMO systems with spatial channel correlation," *IEEE Trans. on Wireless Commun.*, vol. 14, no. 5, pp. 2868-2882, May 2015.

[20] H. Kim, *et al*., "Performance of MIMO channel estimation with imperfect channel correlation information," [Online]. Available: https://www.kics.or.kr/storage/paper/event/2015 summer/publish/14D-23.pdf, 2015.

[21] Y. C. Liang and F. Chin, "Downlink channel covariance (DCCM) estimation and its applications in wireless DS-CDMA systems," *IEEE J. on Sel. Areas in Commun.*, vol. 19, no. 2, pp. 222-232, Feb. 2001.

[22] D. Ying, *et al*., "Kronecker product correlation model and limited feedback codebook design in a 3D channel model," in *Proc*. ICC, pp. 5865-5870, Aug. 2014.

[23] A. van Zelst, and J. S. Hammerschmidt. "A single coefficient spatial correlation model for multiple-input multiple-output (MIMO) radio channels," in *Proc.* URSI General Assembly, 2002.

[24] P. J. Bickel and E. Levina, "Regularized estimation of large covariance matrices," *The Annals of Statistics*, vol. 36, no. 1, pp. 199-227, Feb. 2008.

[25] Y. Chen, A. Wiesel and A. Hero, "Robust shrinkage estimation of high-dimensional covariance matrices," in *Proc.* IEEE Sensor Array and Multichannel Signal Processing Workshop, pp. 189-192, Oct. 2010.

[26] L. Karim, "High-dimensional covariance matrix estimation with missing observations," *Bernoulli*, vol. 20, no. 3, pp. 1029-1058, June. 2014.

[27] T. Tsiligkaridis and A. Hero, "Covariance estimation in high dimensions via Kronecker product expansions," *IEEE Trans. on Signal Process.*, vol. 61, no. 21, pp. 5347-5360, Feb. 2013.

[28] Isserlis L., "On a formula for the product-moment coefficient of any order of a normal frequency distribution in any number of variables," *Biometrika*, vol. 12, no. 1/2, pp. 134–139, Nov. 1918.

[29] P. Harris, *et al*., "Performance characterization of a real-Time massive MIMO system with LOS mobile channels," *IEEE J. on Sel. Areas in Commun.*, vol. 35, no. 6, pp. 1244-1253, June 2017.

[30] V. Stankovic and M. Haardt, "Generalized design of multi-user MIMO precoding matrices," *IEEE Trans. on Wireless Commun.*, vol. 7, no. 3, pp. 953-961, March 2008.

[31] C. Zhang, *et al*., "Statistical beamforming for FDD massive MIMO downlink systems," in *Proc. ICCC*, pp. 1-6, Nov. 2015.

[32] X. Li, S. Jin and R. W. Heath, "3D beamforming for large-scale FD-MIMO systems exploiting statistical channel state information," *IEEE Trans. on Veh. Tech.*, vol. 65, no. 11, pp. 8992-9005, Nov. 2016.

[33] J. Nam, *et al*., "Joint spatial division and multiplexing: Opportunistic beamforming, user grouping and simplified downlink scheduling," *IEEE J. of Sel. Topics in Signal Process.*, vol. 8, no. 5, pp. 876-890, Oct. 2014.

[34] Fan, L., *et al*., "A low-complexity 3D massive MIMO scheme jointly using statistical and instantaneous CSIT," *EURASIP J. on Wireless Commun. And Networking*, vol. 1, p. 235, 2016.

[35] Y. Jeon, *et al*., "New beamforming designs for joint spatial division and multiplexing in large-scale MISO multi-user systems," *IEEE Trans. on Wireless Commun.*, vol. 16, no. 5, pp. 3029-3041, May 2017.

[36] H. Kim, *et al*., "Transmission of wireless backhaul signal in a cellular system with small moving cells," *EURASIP J. on Wireless Commun. and Networking*, vol. 1, p. 238, 2019.

[37] M. Sternad, *et al*., "Using “predictor antennas” for long-range prediction of fast fading for moving relays," in *Proc.* WCNCW, pp. 253-257, April, 2012.

[38] D. Phan-Huy, M. Sternad and T. Svensson, "Making 5G adaptive antennas work for very fast moving vehicles," *IEEE Intell. Transp. Syst. Mag*., vol. 7, no. 2, pp. 71-84, April 2015.

[39] T. Li, *et al*., "Position-aided large-scale MIMO channel estimation for high-speed railway communication systems," *IEEE Trans. on Veh. Tech.*, vol. 66, no. 10, pp. 8964-8978, Oct. 2017.

[40] N. Jamaly, T. Svensson and A. Derneryd, "Effects of coupling and overspeeding on performance of predictor antenna systems in wireless moving relays," *IET Microwaves, Antennas & Propagation*, vol. 13, no. 3, pp. 367-372, Feb. 2019.

[41] M. Sadek, A. Tarighat and A. H. Sayed, "A leakage-based precoding scheme for downlink multi-user MIMO channels," *IEEE Trans. on Wireless Commun.*, vol. 6, no. 5, pp. 1711-1721, May 2007.

[42] E. Björnson, M. Bengtsson and B. E. Ottersten, "Optimal multiuser transmit beamforming: A difficult problem with a simple solution structure [lecture notes]," *IEEE Signal Process. Mag.*, vol. 31, no. 4, pp. 142-148, July 2014.

[43] Wei Yu, G. Ginis and J. M. Cioffi, "Distributed multiuser power control for digital subscriber lines," *IEEE J. of Sel. Areas in Commun.*, vol. 20, no. 5, pp. 1105-1115, June 2002.

[44] Y. Jiang, M. K. Varanasi and J. Li, "Performance analysis of ZF and MMSE equalizers for MIMO systems: An in-depth study of the high SNR regime," *IEEE Trans. on Inform. Theory*, vol. 57, no. 4, pp. 2008-2026, April 2011.

[45] R. D. Cook, "On the mean and variance of the generalized inverse of a singular Wishart matrix," *Electron. J. Statist.*, vol. 5, pp. 146-158, Jan. 2011.

[46] P. Tichavsky and A. Yeredor, "Fast approximate joint diagonalization incorporating weight matrices," *IEEE Trans. on Signal Process.*, vol. 57, no. 3, pp. 878-891, March 2009.

[47] I. T. Jolliffe, *Principal component analysis*. New York: Springer, 2002.

[48] K. K. Wong and Z. Pan, "Array gain and diversity order of multiuser MISO antenna systems," *Int. J. of Wireless Inform. Network*, vol. 15, no. 2, pp. 82–89, May 2008.

[49] R. J. Muirhead, *Aspects of multivariate statistical theory*. John Wiley and Sons, 1982.

[50] D. Lu and D. Li, "A novel precoding method for MIMO systems with multi-cell joint transmission," in *Proc.* VTC, pp. 1–5, May 2010.

[51] Yan Li, *et al*., "An introduction to the computational complexity of matrix multiplication," *J. of Operations Research Society of China*, vol. 1, no. 8, pp. 29-43, Dec. 2019.

[52] Koev, P. and Edelman, A., "The efficient evaluation of the hypergeometric function of a matrix argument," *Mathematics of Computation*, vol. 75, pp. 833-846, Jan. 2002.

[53] Thiele, L., *et al*., "Channel aging effects in comp transmission: Gains from linear channel prediction," in *Proc.* ASILOMAR, pp. 1924-1928, Nov. 2011.

[54] A. Papadogiannis, *et al*., "Efficient selective feedback design for multicell cooperative networks," *IEEE Trans. Veh. Tech.*, vol. 60, no. 1, pp. 196–205, Jan. 2011.

[55] G. Dimic and N. D. Sidiropoulos, "On downlink beamforming with greedy user selection: Performance analysis and a simple new algorithm," *IEEE Trans. Signal Process.*, vol. 53, no. 10, pp. 3857–3868, Oct. 2005.

[56] Zukang Shen, *et al*., "Low complexity user selection algorithms for multiuser MIMO systems with block diagonalization," *IEEE Trans. on Signal Process*., vol. 54, no. 9, pp. 3658-3663, Sept. 2006.

[57] Y. Yang, X. Luo and S. Li, "Low complexity MIMO scheduling with block diagonalization using capacity lower-bound," *IEEE Commun. Letters*, vol. 15, no. 12, pp. 1298-1300, Dec. 2011.

[58] G. Femenias and F. Riera-Palou, "Scheduling and resource allocation in downlink multiuser MIMO-OFDMA systems," *IEEE Trans. on Commun*., vol. 64, no. 5, pp. 2019-2034, May 2016.

[59] S. Jangsher and V. O. K. Li, "Backhaul resource allocation for existing and newly arrived moving small cells," *IEEE Trans. on Veh. Tech*., vol. 66, no. 4, pp. 3211-3219, April 2017.

[60] F. Riera-Palou and G. Femenias, "Cluster-based cooperative MIMO-OFDMA cellular networks: Scheduling and resource allocation," *IEEE Trans. on Veh. Tech.*, vol. 67, no. 2, pp. 1202-1216, Feb. 2018.

[61] B. Zhou, *et al*., "Chordal distance-based user selection algorithm for the multiuser MIMO downlink with perfect or partial CSIT," in *Proc*. IEEE International Conference on Advanced Information Networking and Applications, pp. 77-82, March 2011.

[62] K. Ko and J. Lee, "Multiuser MIMO user selection based on chordal distance," *IEEE Trans. on Commun.*, vol. 60, no. 3, pp. 649-654, March 2012.

[63] W. Song, *et al*., "Frobenius norm based low complexity user selection for multiuser MIMO-OFDM system," in *Proc*. WPMC, pp. 578-582, Nov. 2018.

[64] I. C. Wong and B. L. Evans, "Optimal resource allocation in the OFDMA downlink with imperfect channel knowledge," *IEEE Trans. on Commun.*, vol. 57, no. 1, pp. 232-241, Jan. 2009.

[65] M. K. Awad, *et al*., "A dual-decomposition-based resource allocation for OFDMA networks with imperfect CSI," *IEEE Trans. on Veh. Tech.*, vol. 59, no. 5, pp. 2394-2403, March 2010.

[66] R. Aggarwal, *et al*., "Joint scheduling and resource allocation in the OFDMA downlink: Utility maximization under imperfect channel-state information," *IEEE Trans. on Signal Process.*, vol. 59, no. 11, pp. 5589-5604, Nov. 2011.

[67] G. Femenias, F. Riera-Palou and J. S. Thompson, "Robust scheduling and resource allocation in the downlink of spatially correlated MIMO-OFDMA wireless systems with imperfect CSIT," *IEEE Trans. on Veh. Tech.*, vol. 65, no. 2, pp. 614-629, Feb. 2016.

[68] H. Lee, S. Park and S. Bahk, “An opportunistic scheduling algorithm using aged CSI in massive MIMO systems,” *Computer Networks*, vol. 129, no. 1, pp. 284-296, Dec. 2017.

[69] G. Lee and Y. Sung, "A new approach to user scheduling in massive multi-user MIMO broadcast channels," *IEEE Trans. on Commun.*, vol. 66, no. 4, pp. 1481-1495, April 2018.

[70] W. Anwar, N. Franchi and G. Fettweis, "Physical layer evaluation of V2X communications technologies: 5G NR-V2X, LTE-V2X, IEEE 802.11bd, and IEEE 802.11p," in *Proc*. VTC, pp. 1-7, Sept. 2019.

[71] 3GPP TSG-RAN WG1 Meeting #48, R1-070674, "LTE physical layer framework for performance verification," St. Louis, USA, Feb. 2007.

[72] H. Ji, *et al.*, "Ultra-reliable and low-latency communications in 5G downlink: Physical layer aspects," *IEEE Wireless Commun.*, vol. 25, no. 3, pp. 124-130, June 2018.

Korean Abstract

기지국이 수많은 안테나를 활용하여 높은 전송 이득을 얻을 수 있는 대규모 다중 안테나(massive MIMO) 시스템이 차세대 무선 통신 시스템으로 각광받고 있다. 이를 위해서는 정확한 채널 정보(channel state information)를 기반으로 하는 신호 전송 및 자원 관리 기술이 필수적이다. 하지만 사용자가 고속으로 이동하는 환경에서는 기지국이 추정한 채널 정보와 실제 전송 채널이 크게 달라지는 채널 변화 효과(channel aging effect)가 발생하여, 시스템 전송 성능이 심각하게 하락할 수 있다. 위 문제를 해결하기 위하여, 상대적으로 사용자 이동성에 느리게 변화하는 공간 상관도 행렬(channel correlation matrix)을 활용할 수 있다. 하지만 대규모 다중 안테나 시스템에서는 기지국이 공간 상관도 행렬을 추정하는 과정에서 큰 파일럿(pilot) 신호 부담이 발생할 수 있다. 본 논문은 고속 이동 환경에서의 대규모 다중 안테나 시스템에서 다중 사용자에 대한 신호 전송을 고려한다.

우선, 낮은 파일럿 신호 부담을 갖는 채널 정보 추정 방법을 제안한다. 대규모 다중 안테나 시스템에서 채널 정보 추정은 큰 파일럿 신호 부담을 야기할 수 있다. 이때 공간 상관도 행렬을 활용한 파일럿 신호 설계를 통하여 채널 정보 추정으로 인한 신호 부담을 효과적으로 감소시킬 수 있다. 하지만 이를 위해서는 공간 상관도 행렬을 추정해야 하며, 이 과정에서 큰 신호 부담이 야기될 수 있다. 제안 기법은 기지국이 균일한 선형 안테나 배열(uniform linear array)을 가지고 있는 환경에서, 같은 거리의 안테나

쌍들의 채널 간 공간 상관도가 유사하다는 특징을 활용하여, 상기 안테나 쌍들의 채널 간 공간 상관도를 최소자승추정법(least-square estimation)을 활용하여 추정한다. 그리고 추정된 공간 상관도의 평균제곱오차(mean-square error)를 추정하여, 상기 평균제곱오차가 큰 공간 상관도를 0 으로 치환하여 공간 상관도 행렬의 추정 정확도를 높인다. 또한 상기 추정한 공간 상관도 행렬을 활용하여 낮은 신호 부담으로 채널 정보를 추정할 수 있는 것을 보인다.

둘째로, 사용자 이동성에 의한 채널 변화에 강인한 신호 전송 방법을 제안한다. 사용자들이 서로 다른 속도로 이동하는 환경에서는 채널 변화에 의한 신호 전송 성능 저하 역시 사용자마다 다르게 나타날 수 있다. 위 문제를 해결하기 위하여, 각 사용자에 대한 채널 변화 효과를 개별적으로 고려하면서 평균 신호 대 누수간섭 및 잡음비(signal-to-leakage-plus-noise ratio)를 최대화하는 전송 빔 가중치를 설계한다. 제안 기법은 사용자들의 채널 정보와 공간 상관도 행렬의 선형 결합의 고유방향(eigen-direction)으로 신호를 전송한다. 또한 제안 기법을 사용할 때의 신호 대 간섭 및 잡음비(signal-to-interference-plus-noise ratio)를 분석하고, 이를 기반으로 하는 전송 전력 분배 방법을 제안한다.

끝으로, 사용자 이동성에 따른 채널 변화를 고려하는 자원 할당 방법을 제안한다. 이를 위하여, 상기 채널 변화를 고려하여 시스템 전송 성능(sum-rate)을 최대화하는 탐욕(greedy) 알고리듬 기반의 자원 할당 기술을 설계한다. 고속 이동 환경에서 시스템 전송 성능을 추정하기 위해서는 사용자들에 대한 전송 빔 가중치와 행렬에 대한 초기하 함수(hypergeometric function of a matrix argument)와 관련된 복잡한 연산이 필요하다. 이 문제를

해결하기 위하여, 빔 가중치를 공간 상관도 행렬의 고유방향으로 결정하고, 초기하 함수를 채널 시간 상관도에 대한 함수로 근사한다. 상기 전송 성능 추정 방법이 채널의 공간 및 시간 상관도에만 의존한다는 점을 활용하여, 채널 공간 및 시간 상관도가 크게 변화한 사용자가 존재할 때에 한하여 사용자들에 대한 자원 할당 상태를 갱신하는 방법을 제안한다. 실험을 통하여, 제안 기법이 복잡한 시스템 전송 성능을 기반으로 하는 자원 할당 방법과 유사한 자원 할당 성능을 보이면서도 계산 복잡도를 획기적으로 줄이는 것을 보인다.

주요어: 대규모 다중안테나, 이동성, 채널 변화, 부정확한 채널 정보, 공간 상관도, 낮은 복잡도

학번: 2014-21664

Acknowledgement

7 년에 달하는 박사 과정 동안 정말 많은 것들을 배울 수 있었습니다. 그 긴 여정 동안 소중한 조언들을 아끼지 않고 전해주셨던 이용환 지도교수님께 진심으로 감사드립니다. 특히, 연구뿐만 아니라 연구 외적으로도, 인생을 살아가는데 크나큰 도움이 될 수 있는 주옥 같은 말씀들을 정말 많이 해주셨습니다. 교수님의 충고와 조언들을 항상 마음 깊이 새기며 살아가도록 하겠습니다. 또한 바쁘신 와중에도 제 졸업논문을 지도해주시기 위해 귀한 시간을 할애해주신 박세웅 교수님, 심병효 교수님, 홍대식 교수님, 그리고 신요안 교수님께 감사드립니다. 교수님들의 지도 덕분에, 부족했던 졸업 논문을 완성할 수 있었습니다.

바쁘고 힘든 대학원 생활을 공고동락한 송수신기술연구실 동기 및 선후배님들을 잊지 못할 것입니다. 제가 학부 시절 연구실에서 인턴 생활을 할 때부터 여러가지를 가르쳐주시고 격려해주신 한진석, 변용석, 방재석, 김태훈 선배님께 감사드립니다. 또한 같은 시절 함께 공부하면서 어려운 일들을 헤쳐 나아갔던 정건웅, 박찬식, 윤문형, 김동관 선배님께, 그리고 광희형, 민성이 형, 종일, 현수, 동규에게도 감사의 마음을 전합니다. 또한 연구실 막내 역을 톡톡히 했던 경철, 시헌에게도 감사의 마음을 전합니다. 모든 분들이, 앞으로 뜻하고자 하는 바를 이루시기를 진심으로 기원합니다.

끝으로 긴 시간 동안 저를 지지해주신 부모님 그리고 할머니께 감사의 말씀을 전해드리며, 이 글을 마칩니다.